Mapping the immunological receptors CD14 and macrophage receptor with collagenous structure (MARCO) and their innate recognition potential on trophoblast cells: relevance for human pregnancy

Niwedhie Paluwatta Muhandiramalage

A thesis submitted for the degree of Doctor of Philosophy

School of Biological Sciences

University of Essex

April 2016

Acknowledgement

First of all, I would like to express my deepest gratitude to my supervisor Prof. Nelson Fernandez for his guidance and support throughout the period of the PhD. I am grateful for his encouraging and kind approach of guidance which enabled the successful completion of the study. I'm indebted to him for not only the academic support but for the precious advice for development of transferable skills useful for my future career. I'm truly fortunate to have had the opportunity to complete my final stage of studies under the supervision of such an admirable supervisor.

I am truly grateful to Dr. Asma Jabeen for her unconditional support throughout the past few years. She has been immensely supportive as a senior colleague and an exceptional friend. Her caring nature as a loving sister has provided great personal support at this critical time of my life. I am also thankful to her loving family for not only welcoming me into their family but been understanding and supportive.

Finally, I heartily pay special gratitude to my loving parents Jayakody and Nishanthie Muhandiram and siblings Janith and Jani Muhandiram, for their unconditional love and support throughout the PhD without whom I wouldn't have achieved this goal successfully.

Also I'm grateful to my dear friends Nipun Khanna, Pramod Nayak, Joanne Rajroop, Madushi Fernando and Shavesh Mendis for their continuous encouragement and personal support throughout the study. A special

I'm also thankful to my colleagues in 4.13 of School of Biological Sciences for the great experience and support.

ABSTRACT

The feto-maternal interface is vital to promote growth and development of the placenta while maintaining tolerance and surveillance through the immune system. Pathogens are detected through pattern recognition receptors, which have a key role in the innate recognition by transducing signals from pathogen-associated molecular patterns. Lipopolysaccharide, a PAMP of Gram-negative bacterium, is recognized by the Toll-like receptor. Cluster of differentiation (CD) 14 and macrophage receptor with collagenous structure (MARCO) are key players in innate recognition. The hypothesis derived from the above is that MARCO might be expressed on trophoblast cells and plays a valuable role in association with CD14. The interaction of CD14 and MARCO was explored with the use of confocal microscopy which showed physical associations, most likely contributing to their function at the feto-maternal interface. Trophoblast responses to LPS indicated a significant role in regulating the expression of CD14 and MARCO and NF-κB translocation and activation. It was also hypothesized a correlation between the down-regulation of Myoferlin and vascular endothelial growth factor (VEGF), and the decreased cell proliferation of trophoblast cells upon treatment with LPS. Myoferlin and VEGF quantification estimated by flow cytometry and western blotting showed significant decrease in LPS treated JEG-3 cells in time and dose dependent manner. The cell proliferation assay revealed a significant decrease in trophoblast cell growth of LPS treatment suggesting it is associated with the decrease of Myoferlin of which the expression is reported to be correlated with VEGF. These data suggest that CD14 and MARCO can be modulated and thus might contribute to feto-maternal tolerance and surveillance preventing pregnancy complications such as preeclampsia.

TABLE OF CONTENTS

LIST OF FIGURES

List of Tables

ABBREVIATIONS

3D   Three-dimensional

AU   arbitrary unit

bp   Base pair

CD   cluster of differentiation

CLR   C-type Lectin Receptors

CRP   Complement regulatory protein

CTBs   Villous cyto trophoblast

CTL   Cytotoxic T lymphocyte

DAPI   4',6-diamidino-2-phenylindole

DC   Dendritic cells

DNA   Deoxyribonucleic acid

ER   Endoplasmic Reticulum

EVTs   Extra Villous Trophoblast cells

FBS   Fetal Bovine Serum

hCG   human Chorionic Gonadotropins

HLA   Human Leukocyte Antigen

hPL   human Placental Lactogen

hsp   heat shock protein

ICM   Inner Cell Mass

IDO   indoleamine-2, 3-dioxygenase

IL   Interleukin

ILT 2/4   Immunoglobulin-like transcript 2/4

IVF   In vitro Fertilisation

kDa   kilo Dalton

LPS   Lipopolysaccharide

LUTs   Look up tables

MARCO   Macrophage Receptor with Collagenous Structure

MHC   Major Histocompatibility Class

MMPs   Matrix Metallo Proteinases

mRNA   messenger Ribonucleic acid

MyD88   Myeloid differentiation factor 88

NFκB   Nuclear Factor kappa-light-chain-enhancer of activated B cells

PAGE   Poly Acrylamide Gel Electrophoresis

PAMPs   Pathogen Associated Molecular Patterns

PBS   Phosphate Buffer Saline

PCC   Pearson Correlation Coefficient

PMT   Photomultiplier tube

PRRs   Pattern Recognition Receptors

SDS   Sodium dodecyl sulphate

STB   Syncytiotrophoblast

TLR   Toll Like Receptor

TNF-α   Tumor necrosis factor-α

VEGF   vascular endothelial growth factor

Chapter 1

Introduction

1.1 Immune system

The innate immune system is a subsystem of the overall immune system that implements early host defence against invading pathogens through its ability to differentiate between the self and non-self. At the maternal-fetal interface, innate immunity affords tolerance of the allogenic fetus, whilst simultaneously maintaining host defence against a diverse array of possible pathogens (Koga et al., 2010). Equilibrium must be maintained between both of these elements in order to promote growth and development of the placenta potentially, an imbalance can severely hinder pregnancy progression, by provoking clinical complications, many of which are caused by intrauterine infections. For this reason innate immunity is the dominate form of immune defence at the maternal-fetal interface. Aside from common immune cells, such as the macrophages and natural killer (NT) killer cells, placental cells, particularly trophoblast cells, have a role in the immune response (Abrahams and Mor, 2005).

1.2 Placentation

A healthy human placenta, which is regarded as a vital organ, is the deciding factor of a human pregnancy's success. The success of its development is integral in a human pregnancy. The process of pregnancy begins with the successful fertilization which is then implanted in the fallopian tube at the ovum. The fertilized zygote, which is surrounded by the zona pellucid a, then swiftly splits and divides consequently into 2-cell, 4-cell, 8-cell and 16-cell stages (morula). The morula has 32-cell stage divisions and it also comprises of two layers – inner and outer – of cells, which consequently contribute in forming the blastocyst. Subsequently, there are further intra divisions within the inner layer of cells and growth will eventually form the implanted

embryo which then develops into a fetus. The outer layer of the cells, which are called trophoectoderm, contains cells that have the ability to create extra-embryonic structures, including the human placenta. These cells are known as the trophoblast.
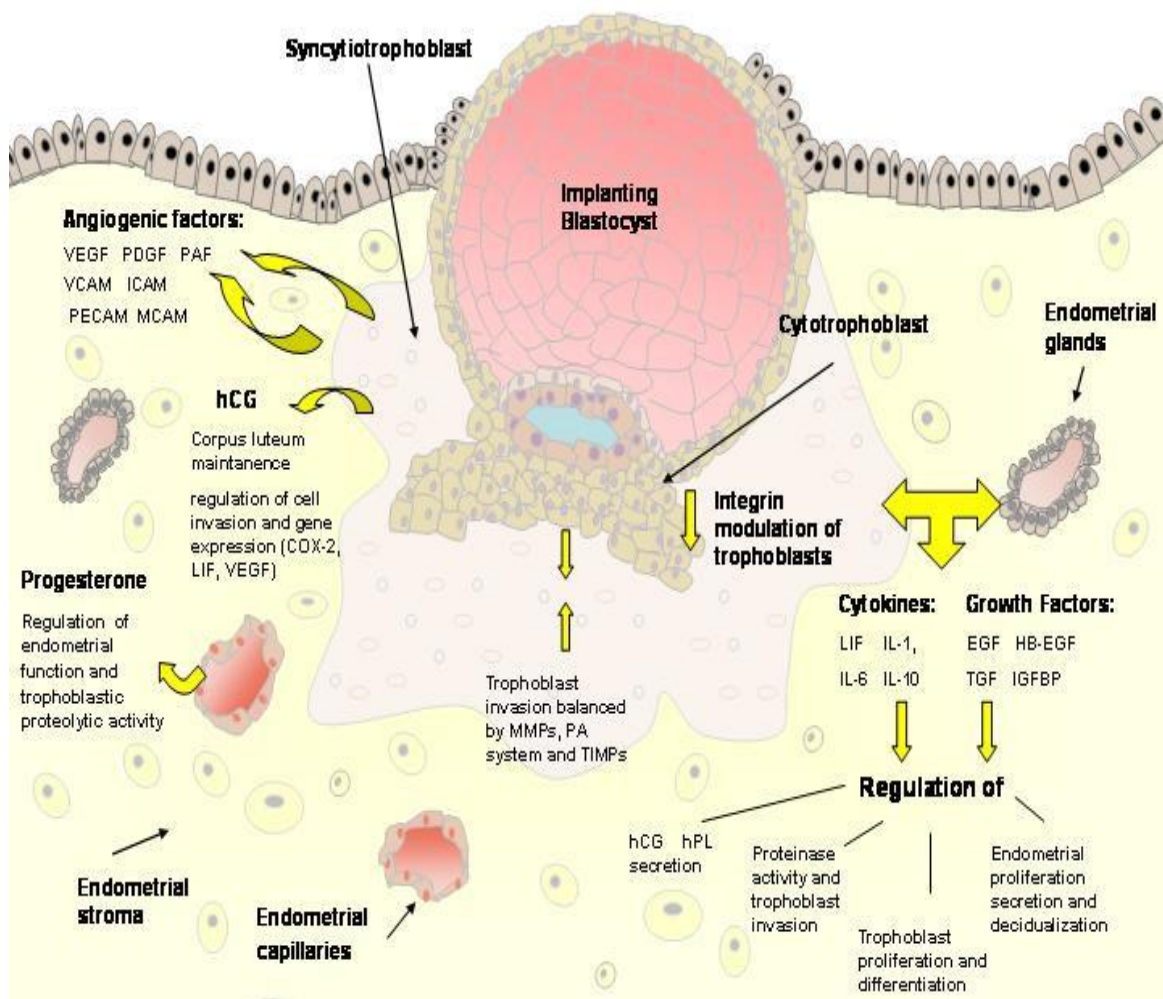
Figure 1.1.Implantation of the blastocyst and invasion of the uterine wall.

An illustration of interactions between trophoblastic and endometrial cells, including angiogenic factors, integrins, cytokines and growth factors.

1.3 Feto-maternal interface

It is postulated that the placental trophoblast cells has a significant role in immune tolerance, since these are the only cells that have contact with maternal tissue (Yie, et. al., 2006). The properties of expressing endogenous retrovirus products, oncofetal proteins, imprinted genes and having relatively unmethylated DNA are the wide range of properties showcased by these cells (Trundley and Moffett, 2004). The presence of negatively charged, sialic acid-rich mucopolysaccharide layer, was originally thought to act as a physical barrier according to Medawar's first hypothesis but this was disproved since due to the fact that it could hinder the immunological cross-talk between the mother and the fetus. The expression of major histocompatiblity complex (MHC) molecules disproves Medawar's second hypothesis where it is stated that there is a lack of immunogenicity in the conceptus (Fernandez et al., 1999). Medawar's third hypothesis was also disproved since pregnancy can stimulate the mother's immune system.

The presence of either two types of helper T cell cytokines can also determine pregnancy outcome, type 2 helper T cells supports a normal pregnancy while type 1 can lead to spontaneous abortions (Raghupathy, 1997). Another vital function of the trophoblast cells is the transportation of maternal antibodies across the placenta and the removal of anti-fetal antibodies. These cells also secrete a plethora of pregnancy factors and hormones which minimises local immunity cementing the importance of immune tolerance (Fernandez et al., 1999).

1.4 Pattern recognition receptors

To detect pathogens, the innate immune system uses a variety of pattern recognition receptors (PRRs). PRRs are mainly expressed by antigen presenting cells and include Toll-like receptors (TLR), cluster of differentiation 14 (CD14) and scavenger receptors (Sankala et al., 2002). PRRs recognize and bind pathogen-associated molecular patterns (PAMP) molecules which result in an immunosurveillance response against invading pathogens (Koga et al., 2010). Pathogen-associated structures, such as lipopolysaccharide (LPS), are recognized by PRRs and have the ability to stimulate the innate immune system. LPS is present in the outer membrane of Gram-negative bacteria and is a very effective activator of immune responses (Sankala et al., 2002). In the present study, emphasis will be placed on CD14 and macrophage receptor with collagenous structure (MARCO) that play a valuable role in immune response through first-hand surveillance of pathogens (Abrahams &Mor, 2005).

Emerging evidence indicates that trophoblast cells have the capacity to recognize and respond to pathogens by expressing TLRs (Abrahams & Mor, 2005). TLRs are a type of extracellular PRR, and have a primary role in the innate immune response in recognition of conserved molecules present on pathogens. Upon recognition of PAMPs which are unique to the pathogens, TLRs transduce signals which facilitate chemical reactions that lead to the synthesis of cytokines. The cytokines attract macrophages to the site of inflammation. Following ligation, the majority of TLRs induce activation of NFκ-B and cytokine production in a myeloid differentiation factor 88 (MyD88)-dependent manner. The mode of expression and regulation of TLRs during pregnancy are unknown, as is their functional activity during pregnancy. Further studies of TLRs at the maternal-fetal interface will aid in understanding the mechanism that maintains the balance between fetal tolerance and pathogen defence (Holmlund et al, 2002).

CD14 is one of the components of the receptor complex which mediates LPS-induced signal transduction (Zanoni et al., 2011). CD14 is a 55 kDa glycoprotein which is initially processed in the endoplasmic reticulum and then expressed on the cell surface (Gegner et al., 1995). CD14 plays a significant role in this potent immune response through the transfer of LPS to the TLR-4-MD2 complex (Gangloff et al., 2005).

MARCO has been suggested to play a role in antimicrobial defence, and the up-regulation of MARCO during bacterial infection in macrophages of the liver and spleen provides evidence for this concept (Arredouani et al., 2004). Thelen et al. (2010) reported that MARCO transcription and cell surface expression increased after bacterial binding ,indicating its significance in phagocytosis .The expression of MARCO is also stimulated upon bacterial infection or LPS injection (Sankala et al., 2002).

In summary, PRR in trophoblast cells are speculated to be significant in innate immune defence, and may play a key role in the maternal innate immune system. Nevertheless, their role in fetal tolerance still remains undetermined. Further studies of TLR at the maternal-fetal interface will aid elucidation of the mechanism that maintains the balance between fetal tolerance and pathogen defence (Holmlund et al, 2002).

1.5 Toll-like Receptors

Toll-like receptors constitute a family of transmembrane innate immunity PRRs that mediate immunity by recognising and responding to microorganisms (Burrough et al., 2011). TLRs are expressed on various immune cells, including macrophages, dendritic cells and neutrophils, as well as non-immune cells such as endothelial cells, epithelial cells and fibroblasts (Burrough et al., 2011). In humans, the TLR family consists of more than 10 transmembrane proteins and each receptor responds to a distinct ligand (Ma et al., 2007).

TLRs bear leucine-rich repeats in the extracellular domain which recognize PAMPs in bacteria, viruses, fungi and parasites. Ligation of TLRs initiates the production of proinflammatory cytokines and immunoregulatory molecules via a common intracellular signalling pathway (Lorne et al., 2010). MyD88, an essential adaptor protein in the IL-1R1 signalling pathway, is recruited by the TLR upon ligand recognition. TLR interaction with MyD88through the toll interleukin 1 domain results in activation of a kinase cascade, activating the NFκB pathway and resulting in an inflammatory response (Abrahams et al., 2005).

TLR-4 are recognized to be significant receptors in immune responses against pathogens. TLR-4 is significant for the recognition of Gram negative bacteria and is effective in responses to LPS (Holmlund et al., 2002). In addition to PAMPs, TLR-4 have the ability to bind damage-associated molecular patterns (DAMPs), such as heat-shock protein (Hsp) 60, Hsp70, Hsp90, high mobility group box protein 1, and fibrinogen (Mor 2008).

TLR-4 induces activation of NFκ-B pathway and cytokine production in a MyD88-dependent manner. However TLR-4 can also signal in a MyD88-independent manner, through another adapter protein, Toll/IL-1 receptor domain-containing adaptor inducing IFN-β (TRIF), which induces the expression of type I interferons (IFN) and IFN-inducible proteins, as shown in figure 1.2 (Koga et al ., 2010).
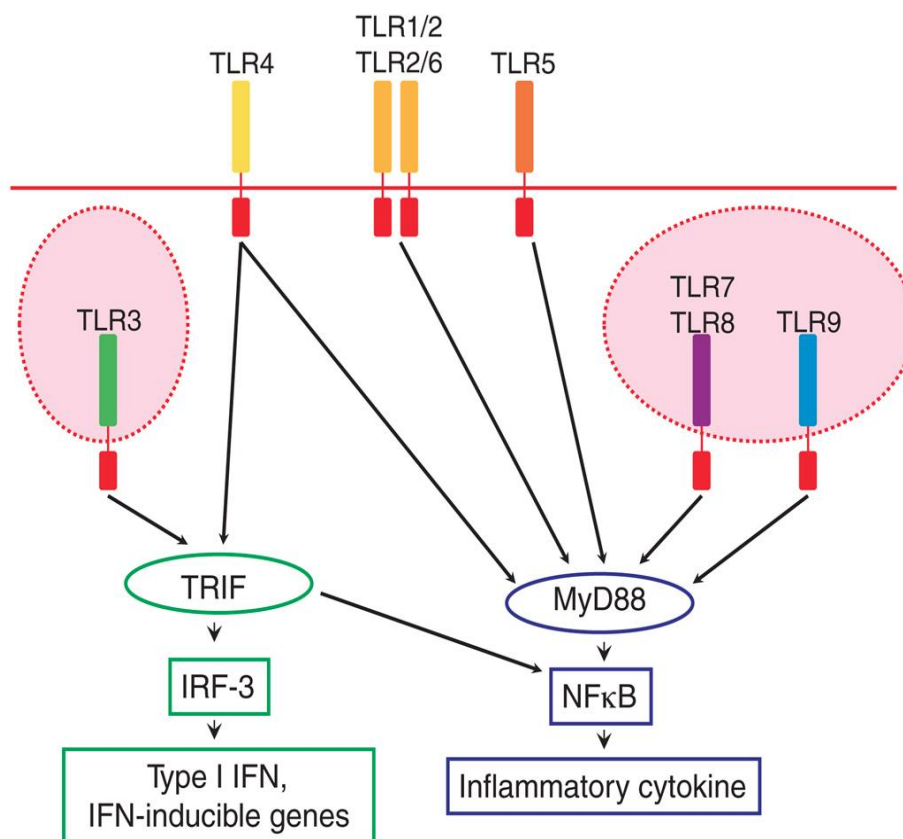
Figure 1.2: Signalling by Toll-like receptors

The MyD88-dependent pathway of TLR-4 induces synthesis of inflammatory cytokines .TLR-4 also induces IFN and IFN-inducible genes in a MyD88-dependent pathway.

1.6 Function of TLRs in the Placenta

In the human placenta, all TLR members have been detected. Most are expressed in trophoblast cells. The expression of TLRs in trophoblast can differ according to gestational and differential stage (Mor 2008). In first trimester placentae, TLR-2 and TLR-4 are expressed by villous cytotrophoblast and extravillous trophoblast cells, but not by syncytiotrophoblasts (Koga et al., 2010). The absence of TLR expression in the syncytiotrophoblast is speculated to restrict the response by placental tissue to microbes that have broken through this layer. Thus, the fetus is only threatened by pathogens if the TLR-negative syncytiotrophoblast layer is ruptured and the pathogen is able to enter through the decidual or placental villous compartments (Koga et al., 2009).

Ma et al., (2007) evaluated the expression of TLR-4 in third-trimester placentae. Most TLR-4 expression is observed in syncytiotrophoblast and endothelial cells (Ma et al., 2007).

First-trimester trophoblasts exhibit a moderate up-regulation of cytokines induced by ligation for TLR-4 with LPS (Koga et al., 2010).

1.7 TLR-4 response and preterm labor

TLR-4 is implicated in susceptibility to preterm delivery, as induced by Gram-negative bacteria. Within the context of TLR-4 signalling associated with preterm delivery,15-hydroxyprostaglandin dehydrogenase expression, a prostaglandin-catabolizing enzyme present in fetal and maternal tissue, is down-regulated subsequent to the ligation of TLR-4 with LPS (Koga et al, 2009). It has therefore been speculated that bacterially induced preterm labor is mediated by TLR-4 through down-regulation of degradation of prostaglandin. Systemic and local inflammatory responses subsequent to LPS regulation may be the cause of preterm labor (Koga et al., 2009).

The fetal death and decidual necrosis has been proven to be reduced by the TLR-4 antagonist. However, bacterial colonization in the placenta was not affected by this antagonist, confirming that TLR-4 antagonized has the ability to control the inflammatory response (Abrahams et al., 2005).

1.8 Fetal Development

TLR-4 activation in the fetus is speculated to be the cause of cerebral white matter damage, a significant problem affecting in preterm neonates. Contrarily, however, the TLR system is involved in protective effects against neonatal allergic diseases such as asthma (Koga et al., 2010).

Immunohistochemistry analysis of skin samples obtained from preterm delivered babies revealed the expression of TLR2 and TLR-4. Given also that following LPS exposure fetal monocytes secrete cytokines and chemokines, it can be stated that fetal cells can contribute to innate immune defence.

1.9 TLR expression at the maternal–fetal interface in pregnancy disorders

The expression of TLR-2 and TLR-4 in chorioamniotic membranes   at term and in preterm parturition has been reported to be associated with chorioamnionitis (CAM), a condition most often associated with prolonged labour. It has been shown that TLR2 and TLR-4 mRNA is significantly greater in chorioamniotic membranes from women at term with spontaneous labor in comparison to women not in labor. The expression of TLR2 in chorioamniotic membranes was significantly higher in CAM patients than in those without CAM. Additionally, in non-CAM preterm labor, TLR-2 expression was limited to the basal surface of amniotic epithelial cells. In contrast, diffuse and strong positive staining of the entire cytoplasm of the epithelium was observed in CAM patients (Koga et al., 2010).

In contrast, high expression of TLR-4 in villous Hofbauer cells was observed in preterm placentae of patients with CAM, compared to expression levels in preterm placentae of patients without CAM, or term placentae of patients with or without CAM. Recently, TLR-4 has been found to be expressed in the basal membrane of the amniotic epithelium in CAM patients (Ref). It was presumed that an infection may induce the translocation of TLR-4 from apical to basal membrane was induced by the infection. This might decrease the signalling of TLR-4 during early infection while maintaining the amniotic epithelium as a hostile environment to invasive bacteria (Kumasaki et al., 2004).

Significantly higher TLR-4 expression in trophoblast was observed in women with preterm delivery associated with pre-eclampsia, in comparison to women with or without CAM-associated preterm delivery. Furthermore, the presence of inflammatory cytokines indicated its ability to induce TLR-4 expression by the co-localization of TLR-4 with activated NF-kB, TNF-α and M30 and it is suggested to enhance the response to TLR ligands (Koga et al., 2010).

There has been recent interest in polymorphisms in TLR genes and their impact on pregnancy disorders. Such polymorphisms have been observed to be associated with impaired function of TLR molecules and an enhanced susceptibility to infections. Recent experimental studies have revealed that susceptibility to early-onset preeclampsia is affected by TLR-4 polymorphisms, which enhanced liver enzymes and low platelets syndrome. Furthermore, the presence of the TLR2 Arg753Gln polymorphism and two TLR-4 SNPs (Asp299Gly and Thr399Ile) was associated with normal pregnancy controls. These observations indicate the significance of TLR in preeclampsia and also its involvement in various pregnancy disorders (Mor 2008).

Despite their independent involvement inimmunoregulatory responses, synergy between TLR-2 and TLR-4 has been proposed, wherein consistent signalling is reliant upon the co-stimulation of both receptors. In the release of TNF from murine macrophage cells, collaboration was observed

between LPS, the ligand for TLR-4, and muramyl dipeptide, a ligand for TLR-2. It has also been reported that responses to endotoxin were altered subsequent to inoculation of muramyl peptides into mice (Holmlund et al., 2002). Koga et al. (2010) have speculated that the co-expression of TLR2 and TLR-4 on both villous trophoblasts and intermediate trophoblasts could therefore play the role of a defence mechanism by stopping participation of these cells in potentially fatal reactions.

In summary, TLRs in trophoblast cells play a key role in placental innate immunity. However the exact function of TLRs in fetal tolerance is unknown. The mechanisms for regulation of the expression pattern and functional activity of TLRs during pregnancy are also still unknown. Further studies of TLRs at the maternal-fetal interface will aid in the elucidation of the mechanism that maintain the balance between fetal tolerance and pathogen defence (Holmlund et al., 2002).

1.10 Lipopolysaccaride (LPS) and Lipopolysaccharide Binding Protein (LBP)

Pathogen-associated structures such as LPS are recognized by PRRs and have the ability to stimulate the innate immune system. LPS is a major component in the outer membrane of Gram-negative bacteria. It is a very effective activator of immune responses as its lipophillic component and the saccharide polymer is covalently linked to the anchor domain of the membrane (Sankala et al., 2002). The primary role of LPS is to stimulate mononuclear phagocytes, which then synthesize and secrete immunoregulatory and inflammatory cytokines such as IL-1, IL-6 and TNF-α (Gangloff et al., 2005). Endotoxin shock can occur due to excessive secretion of these cytokines, and LPS is found to mediate shock caused by Gram-negative bacteria (Haziot et al., 1996).

Cellular recognition of LPS necessitates that LPS binds lipopolysaccharide binding protein (LBP), a soluble acute-phase protein. LBP binds to the lipid A segment of LPS and acts as a

catalyst for the transfer LPS to the cell surface PRR CD14 (Gegner et al., 1995). . Subsequent signal transduction is primarily mediated by CD14 and TLR-4,.Since CD14 lacks a transmembrane domain, TLR-4 is required to transmit signals across the plasma membrane (Anas et al., 2010). TLR-4, associates with LPS-bound CD14 along with myeloid differentiation factor 2 and transfers LPS, resulting in signal transduction (Gangloff et al., 2005). Recent studies have provided evidence that other receptors are involved in the mediation of LPS-induced cell activation, including TLR-2 and MARCO (Bowdish et al., 2009).

Lipopolysaccharide (LPS), PAMP of Gram-negative bacteria, is recognized by the PRR, Toll-like receptor (TLR-4). Cluster of differentiation (CD) 14 and macrophage receptor with collagenous structure (MARCO) are key PRRs. The hypothesis derived from the above is that MARCO is expressed on trophoblast cells and plays a valuable role in association with Cluster of Differentiation (CD14) in immune response through first hand surveillance of invading pathogens. The interaction of CD14 and MARCO was explored with the use of confocal microscopy which confirmed the colocalisation of these receptors in trophoblast cells suggesting they form physical associations contributing to their function at the feto-maternal interface.

1.11 CD14

CD14, the receptor for bacterial LPS, is a 55kDa glycoprotein. CD14 is initially processed in the endoplasmic reticulum and then expressed on the cell surface (Gegner et al., 1995). The protein is composed of 375 amino acids and it contains leucin-rich repeats which are significant in PAMP binding (Anas et al., 2010). CD14 binding of LPS occurs within a pocket of the CD14 structure (Anas et al., 2010). CD14 is designated as an acute phase protein as its expression in liver cells is induced by the inflammatory cytokine IL-6 (Anas et al., 2010).

CD14 exists in membrane bound (mCD14) and soluble (sCD14) forms. There are two different forms of sCD14 with molecular masses of 48 kDa and 56 kDa. An increase in the secretion of

the LPS-induced cytokines TNF-α and IL-6, mediated by purified 48 kDa sCD14, has been observed (Labeta et al., 1993)

1.11.1 Cell surface expression of CD14

CD14 is mostly expressed on myeloid cell surfaces, including on macrophages, monocytes and neutrophils. In non-myeloid cell types, it is expressed on epithelial cells, endothelial cells and fibroblasts at comparatively low levels (Tobias et al., 1994). CD14 exists in two forms: glycosylphosphatidyl (GPI)-anchored membrane protein (mCD14), present on monocytes, and soluble protein (sCD14) in plasma (Heidenreich, 1999).

1.11.2 CD14 cellular function

CD14 serves as the main receptor for LPS (in the presence of LBP) and mediate responses to LPS (Heidenreich 1999). This was confirmed by Wright (1995), who reported that targeted disruption of the murine CD14 gene resulted in animals with at least 100-fold less sensitivity to LPS. The CD14-deficient mice were found to be highly resistant to endotoxin shock. However a minute amount of the inflammatory cytokines TNFα and IL-6 was synthesized at a LPS dose which is highly lethal for mice expressing CD14. This indicated the presence of CD14-independent pathways of cellular activation. Furthermore the CD14-deficent mice unexpectedly survived and exhibited no symptoms of bacterial-induced shock when injected with a dose of Gram-negative bacteria *(Escherichia coli.)* lethal to normal mice. This presented a new role of CD14 in the dissemination of bacteria in of Gram-negative infections (Haziot et al., 1996).

Recent studies have shown that CD14 is only of the components of a receptor complex which mediates the LPS-induced signal transduction. CD14 plays a significant role in this potent immune response through the transfer of LPS to the TLR-4: MD2 complex (Gangloff et al., 2005). However a study with CD14-deficient murine macrophages has shown evidence of a

CD14-independent pathway of signal transduction by different LPS chemotypes (figure 3). The majority of Gram- negative bacteria synthesize 'smooth LPS' (Gangloff et al., 2005). The smooth LPS is composed of the lipid moiety, a core polysaccharide and a variable O-polysaccharide whereas the failure to attach either of the components other than lipid A moiety results in the formation of 'rough LPS'. In both the chemotypes of LPS, the lipid A moiety is the bioactive element which has pathogenic functions in infections caused by Gram-negative bacteria. Subsequent to induction with rough LPS, equal quantities of TNF was secreted by both the CD14-deficient murine macrophages and the CD14-expressed macrophages and no secretion to smooth LPS was observed. This signifies the necessity of CD14 for only the smooth LPS for the activation of TLR-4: MyD88 pathway. Furthermore no IFN-α/β was secreted upon stimulation with smooth or rough LPS which indicates that CD14 is required for TLR-4: TRIF pathway activation by both the LPS chemotypes (Anas et al., 2010).
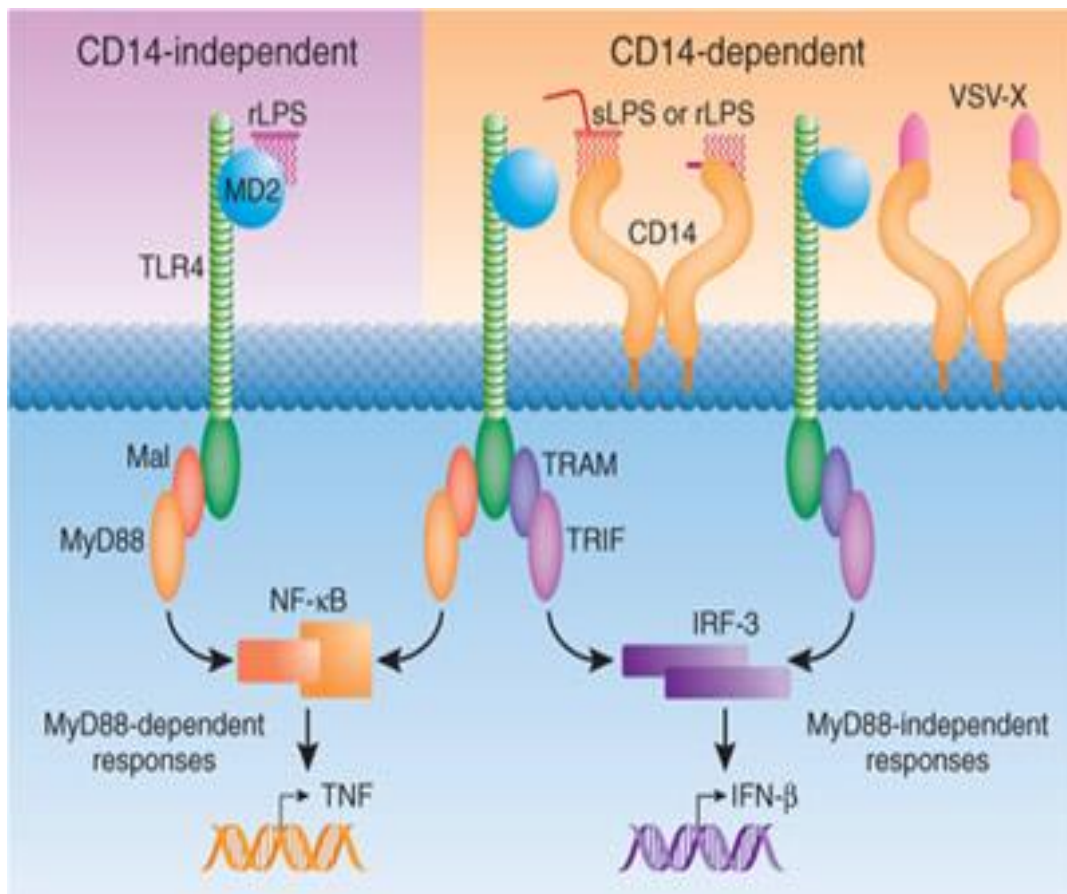
Figure 1.3 Toll-like receptor signalling. (Koga and Mor 2008).

CD14-independent and CD14-dependent signalling by Toll-like receptors. MyD88-dependent

TLR-4 inducted activation of TNF and IFN-β cytokines

LPS-induced activation of myeloid cells is not only dependent on the GPI- anchor of membrane CD14 (Heidenreich 1999). Cellular activation by LPS in cell types that have a low count of surface CD14, for example epithelial and endothelial cells, is also mediated by soluble CD14 (sCD14) (Anas et al., 2010). SCD14 acts as a LPS receptor in cells that express no mCD14 (Labeta et al., 1993).

CD14's multifunctionality is due to its ability to stimulate different PRRs. Yang et al. (1999) discovered that LPS- induced TLR-2 activation in monocytes is enhanced by the presence of mCD14b due its association with the TLR-2, which results in the formation of the LPS receptor complex. CD14 was also identified to facilitate the activation of monocytes by IL-2 Bosco et al., (1997)

CD14 can participate in TLR activation by interacting with non-LPS PAMPs, including viral components. Also, CD14 can enhance cell activation through the TLR-3 ligand poly (I: C), which transfers CD14 to TLR-3 and acts as a vital infection detector due to its ability to recognize viral nucleic acids. This evidently illustrates the role of CD14 in inflammatory responses (Anas et al., 2010). CD14 has been found to be receptive to most bacterial cell wall components as well Gram-negative bacteria including Gram- positive bacteria, fungi and spirochetes. (Heidenreich, 1999).It is responsible for the activation of several other PRRs stimulated by other bacterial PAMP's, including peptidoglycan, lipoarabinomannan, phospholipids and LTA (Heidenreich 1999). Peptidoglican-induced activation of TLR-2 is reported to be mediated by CD14. However activation of mCD14-deficient epithelial and endothelial cells by peptidoglycan:- sCD14 complex is a failure in contrast to LPS induction. Moreover CD14 is found to enhance immune cells activity induced by LTA along with LBP (Anas et al., 2010).

1.11.3 Role of CD14 during pregnancy

The expression of CD14 on trophoblast cells was first reported in 1993 (Guilbert et al. (1993). However, a comprehensive study of CD14 expression and its function in trophoblast cells has not been conducted. However placental infections initiated by Gram-negative bacteria is a clear indication of the presence of CD14 on trophoblast cells as it acts as the receptor of LPS, located on the outer membrane of the bacteria.

The presence of the intracellular Gram-negative bacterium *Chlamydia pneumonia* has been correlated with vascular disease. During pregnancy, dissemination of *C. pneumoniae* into the peripheral blood may lead to infection of the placenta. *C. pneumonia* infection has been demonstrated to affect trophoblast viability and to result in decreased invasion capacity of extravillous trophoblasts via the extracellular matrix. *C. pneumoniae* DNA has been detected in placental tissues, confirming the role of *Chlamydia*in the reduction of uterine wall invasion by infected extravillous trophoblast cells. In addition, a correlation has been noted between *C. pneumoniae* and preeclampsia: antibodies against the bacteria were observed in the circulation of women with severe with preeclampsia (Han et al., 2011). Further studies will be necessary to elucidate the expression of CD14 in trophoblast cells and its role in innate immune responses. Such studies may assist the development of therapeutic strategies against trophoblast dysfunction.

1.12 Macrophage Receptor with Collagenous Structure

Scavenger receptors are immunosurveillance receptors which have been classified into a number of subclasses according to their tertiary structure (Thelen et al., 2010). Class A scavenger receptors (SR-As) are a collection of pattern-recognition receptors which consist of: SR-AI/II, Macrophage Receptor with Collagenous structure (MARCO), Scavenger Receptor with C-type Lectin (SRCL) and SCARA5 (Arredouani et al., 2006). MARCO is a trimer containing a collagenous domain and a C-terminal scavenger receptor cysteine-rich (SRCR) domain (Sankala

et al., 2002). It is encoded by the gene located on chromosome 2 (Thelen et al., 2010). The majority of murine MARCO is expressed on the marginal zone macrophages in the spleen, on macrophages of the medullary cord in lymph nodes and on peritoneal macrophages (Granucci et al., 2003). The expression of human MARCO is detected to be most robust in the liver, lymph nodes, monocytes and alveolar macrophages which is involved in the filtration of blood and lymph fluids (Jozefowski et al., 2005). MARCO has the capability of binding both Gram-positive and Gram-negative bacteria but not yeast (Granucci et al., 2003).

1.12.1 Cell specific functions of MARCO

MARCO may play a significant role in the innate host defence system. This is indicated by up-regulation of MARCO during bacterial infections in the liver and spleen (Arredouani et al., 2004). Thelen et al., (2010) reported that the degree of MARCO transcription and cell surface expression increase after bacterial binding which further supports its significance in phagocytosis. Moreover the expression of MARCO can be stimulated upon bacterial infection or LPS injection as LPS present on the Gram-negative bacteria acts as a ligand of MARCO (Sankala et al., 2002). However due to the ability to bind both Gram-negative bacteria and Gram-positive bacteria, MARCO has at least another bacterial ligand. Furthermore it was reported that MARCO binding to bacterial strains which express "rough LPS" was greater in comparison to strain which express "smooth LPS" (Sankala et al., 2002). Another factor which indicates the importance of MARCO in innate immune defence is its stimulatory effect on IL-12 production in macrophages. The decrease in IL-12 production in peritoneal macrophages in contrast to wild type cells, stimulated by LPS proved MARCO mediation of this regulation. It was further confirmed by the increased IL-12 production due to MARCO ligation with a mAb inhibited (Jozefowski 2005).

It is apparent that MARCO is the major receptor in alveolar macrophages for unopsonized pathogens. Sankala et al. (2002) have demonstrated that genetically modified MARCO-deficient mice show impaired phagocytosis of *Streptococcus pneumoniae* in the lungs. Additionally, the neutrophil count in infected lung tissue from MARCO-deficient mice was significantly higher in comparison to wild type tissue. These data confirmed that MARCO-deficient mice have impaired ability in the capacity to clear of *S. pneumoniae* from the lungs, which leads to increased mortality. Therefore MARCO is a critical receptor in the innate immune response against inhaled particles and airborne pathogens. *S. pneumoniae* is a Gram-positive bacterium which is known as the main cause of community acquired pneumonia, bacteraemia and bacterial meningitis. Further studies of MARCO and its regulation will aid the development of therapeutic measures against pneumococcal infections.

Cell surface expression of MARCO has been proven to be greater in SR-AI/II-deficient peritoneal macrophages than on. Thelen et al. (2010), reported that MARCO is more essential, in comparison to the SR-AI/II receptor in human decidual macrophage, for phagocytosis of *Clostridium sordellii*, a rare firmicute associated with infections of the reproductive tract. It was evident by the inhibition of phagocytosis by sMARCO, a specific MARCO-dependent inhibitor but not by AcLDL, a specific antagonist of SR-AI/II receptors. This was confirmed by observation of SR-AI/II-deficient mice, which display increased MARCO expression. This is hypothesized to cause greater phagocytic activity in SR-AI/II-deficient macrophages in comparison to wild-type cells. In addition, upregulation of MARCO expression in SR-AI/II-deficient mice was confirmed by greater mRNA transcription of MARCO in SR-AI/II-deficient macrophages in comparison to wild-type cells. Moreover, MARCO function in human cells was further evidenced y the impaired ability of MARCO-deficient peritoneal macrophages to phagocytise *C.sordellii*. MARCO-deficient mice displayed enhanced susceptibility to mortality due to *C.sordellii* infection of the uterus, which indicates impaired clearance of the pathogen.

Hence, it was established that MARCO plays a significant role in innate defence against *C.sordelli i*in the uterus (Thelen et al., 2010). Toxic shock syndrome due to *C.sordellii* and *C. perfringens* was reported a mortality of 1 in 200 women of reproductive age. *C.sordellii* is an anaerobic, spore forming gram-positive bacteria related to highly lethal female reproductive tract infections, soft tissue infections and bacteraemia. *C.sordellii* infections of the reproductive tract emerge subsequent to childbirth and abortion. The expression of MARCO in the uterus and its function in defence against *C.sordellii* infection indicate that it might serve an important role in trophoblast cells.

1.13 Myoferlin

At cellular level, myoferlin is found in cell membrane, which is a membrane protein of cytoplasmic vesicles and nuclear membrane. At tissue level, however, it is profoundly communicated in skeletal and cardiovascular muscles while, feebly communicated in kidney, brain and placenta (Bernatchez et al., 2007; Davis et al., 2002). A research found that C2 area of myoferlin and different individuals from its family change the lipid pressing of plasma layers. Besides, myoferlin additionally encourage membrane parting and layer combination (Marty et al., 2013). Another examination uncovered that myoferlin controls the security and function of the vascular endothelial development variable receptor 2, along these lines, loss of myoferlin in endothelial cells created absence of cell multiplication, movement, and nitric oxide discharge (Bernatchez et al., 2007).
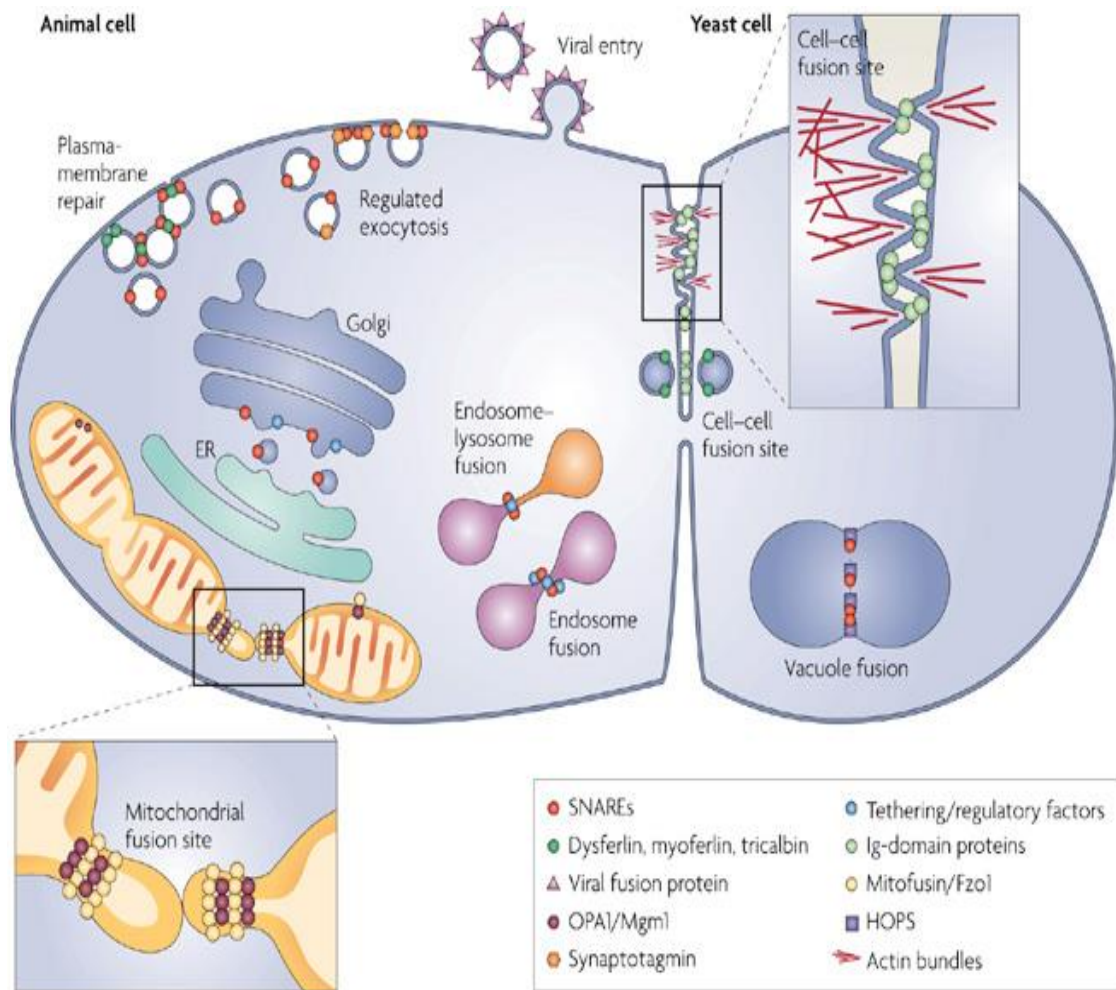
Figure 1.4: Role of myoferlin during membrane fusion. (Martens and McMahon, 2008).

1.13.1 Myoferlin: role in pregnancy

Late studies have described that transformation or hereditary interruption of myoferlin advances strong dystrophy-related phenotypes in mice, which are the significance of debilitated plasma membrane integrity. Be that as it may, no biological functions have been credited to myoferlin in non-muscle tissue. Articulation of myoferlin alongside its family member dysferlin has been accounted for in the trophoblast placenta, where just dysferlin has been discovered to be connected with trophoblast cell combination (Robinson et al., 2009). Diminished appearance of myoferlin in trophoblast cells may prompt diminished cell expansion and as result lacking intrusion upon bacterial and/or viral contamination Myoferlin is connected with the constancy and purpose of the vascular endothelial development component receptor 2 (Bernatchez et al., 2007).

1.14 Vascular Endothelial Growth Factor (VEGF)

A key regulator of angiogenesis is the Vascular Endothelial Growth Factor (VEGF) which has a significant function in conceptive functions, embryogenesis and skeletal development (Ferarra et al., 2003). VEGF also known as VEGF-A, is a member of the platelet-derived growth factor (PDGF) family, which also include VEGF-B, VEGF-C, VEGF-D, VEGF-E, VEGF-F and placental Growth Factor (PlGF) (Hoeben et al., 2004). In addition, different types of VEGF mRNA are generated as result of single 8- exon splicing of VEGF (Tischer et al., 1991). A few distinctive VEGF isoforms: VEGF121, VEGF145, VEGF148, VEGF165, VEGF183, VEGF189, and VEGF206 are formed as result of the VEGF splicing (Hoeben et al., 2004). The isoforms are named taking into account it's quantity of amino acid residues. For instance, VEGF165 contains 165 amino acid residues (Tischer et al., 1991). There are distinctive isoforms of VEGF; VEGF121, VEGF145, VEGF148, VEGF165, VEGF183, VEGF189 and VEGF206 as a result of gene splicing. However, VEGF110 is generated from proteolytic cleavage (Hoeben et al., 2004). The binding of heparin to the VEGF isoforms determines the ability of VEGF isoforms to diffuse

through cells. For example, VEGF121 can diffuse unreservedly inside the cell as does not bind to heparin. Then again, VEGF165 is accepted to have in between characteristics, in this way it can be discharged out of the cell. Although, a distinguishing amount of VEGF165 may remain in the cell surface and extracellular matrix. VEGF189 and VEGF206 proteins are concealed inside the extracellular matrix as a consequence of a high affinity of binding to heparin, (Park et al., 1993; Ferrara et al., 2003). VEGF receptor tyrosine kinases (RTKs); fms-like tyrosine kinase (Flt-1/VEGFR-1) and kinase domain region also known as fetal liver kinase (KDR/Flk-1/VEGFR-2) regulates biological processes of VEGF.(Ortéga et al., 1999).

1.14.1 Vascular Endothelial Growth Factor: role in pregnancy

The expression of the receptors VEGFR-1 and VEGFR-2, VEGF and PlGF, has critical impact in proceeding placental angiogenesis (Pietro et al. 2010). VEGF is expressed by extra villous trophoblasts situated in the anchoring villi, in the placenta, (Ahmed et al., 1995). In addition, due to the significant role VEGF in pregnancy, impaired function of endothelial cells and pregnancy loss as found in the placenta of mice may cause as result of the decrease of VEGF secretion. Also embryonic lethality in mice appears to occur due to VEGF (Ferrara et al., 1996). Lipopolysaccharide is a key segment of the external membrane of Gram-negative bacteria. As most pregnancy complications occur due to maternal or fetal infection, this study is focused on the impact of bacterial LPS on the VEGF proteins inside the trophoblasts. The aim of the research is to study the VEGF proteins present in the cell line will damage and their response tp bacterial LPS in JEG-3 cells.

1.15 Chemokines

Placental development and vasculogenesis are dictated by communication between fetal trophoblast cells and maternal immune cells during pregnancy. Immune privilege, during gestation, is maintained by the release of mediators that enhance cellular communication. Among the soluble factors playing a role in promoting cell growth and development are chemokines; they are critical factors in this process.

Chemokines are a family of structurally-related, small molecular weight, secreted proteins that promote chemoattraction. They are a group of seven transmembrane domain G-protein-coupled receptors. Even though chemokines were originally described as responsible for recruiting immune cells to arbitrate inflammation, they are also regarded as the agents, which control central nervous system development and haematopoiesis (Tran and Miller (2003).

During placental development, cytotrophoblasts release CCL3/MIP-1 alpha and decidual trophoblast cells lining maternal blood vessels secrete CXCL12/SDF-1, attracting CCR5$^+$ and CXCR4$^+$ Natural Killer (NK) cells, respectively, from the maternal circulation (Hanna *et al.* (2003) and Drake *et al.* (2001). NK cells (dNK cells) deployed to the decidua responds to the local environmental prompts (e.g. IL-15) through modifying their phenotypic profile via down-regulating their chemokine receptors. dNK cells lose their cytolytic activity after interacting with HLA-G, a key non-classical MHC Class I molecule expressed on trophoblast cells ((Hanna *et al.*, 2003); Kanellopoulos-Langevin *et al.* (2003) Hunt *et al.* (2006). A positive role for dNK cells were recently suggested by Hanna *et al, which describe them as* source of angiogenic growth factors following activation of the NK-activating receptor NKp44 by ligand-bearing cytotrophoblasts (Hanna *et al.* (2006) dNK cells release CXCL8/IL-8 and CXCL10/IP-10, in addition to PlGF VEGF. These are identified as chemokines that direct CXCR1$^+$ and CXCR3$^+$ trophoblast cells. CXCR1$^+$ and CXCR3$^+$ trophoblast cells are led towards endovascular invasion

and vascular remodelling (Hanna *et al.* (2006) by these chemokines. Hence, the reciprocal attraction between dNK cells and invading trophoblasts, which is influenced by chemokines, appears to be integral for the development of an efficient maternal-fetal interface early in pregnancy.

It has been suggested the regulation of the inflammatory response by chemokines has an influenced on miscarriage. According to a recent epidemiological research which examined chemokine levels in the serum of pregnant women revealed that increased concentrations of CXCL5/ENA-78 and CCL5/RANTES are linked with higher risk of miscarriage (Whitcomb et al., 2007). Even though these two kinds of chemokines have been localized to decidual cells, it is not too clear whether the placental imbalance is accurately represented through these circulating levels.

Martinez de la Torre and colleagues research support a detrimental consequence theory of placental chemokines by reporting a beneficial role of the D6 chemokine receptor decoy in mouse fetal survival (de la Torre *et al.* 2007) D6 is a silent receptor expressed on lymphatic endothelium that scavenges pro-inflammatory chemokines, thus reducing ligand availability to signalling receptors Mantovani *et al.* (2006) After identifying D6 expression in human and mouse placenta, these authors further examined the impact of chemokines and D6 function in foetal immune privilege by administering lipopolysaccharide (LPS) injection, an animal model of inflammation-related fetal loss, on pregnant wild-type (WT) and $D6^{-/-}$ mice. Systemic LPS injection caused an increase in both circulating and placental levels of inflammatory chemokines CCL22/MDC, CCL2/MCP-1/JE and CCL11/Eotaxin in WT mice, with exaggerated levels in $D6^{-/-}$ animals.

Furthermore, an increase in foetal loss is associated with LPS injection, with significantly higher frequency observed in $D6^{-/-}$ mice relative to WT mice. Through the administration of

neutralizing antibodies to inflammatory cytokines, they were able to reduce the fetal losses, which were caused by LPS. Collectively, the integral part of the inflammatory chemokines in pregnancy was highlighted by the results and further recognises D6's protective role in pregnancy as a scavenger receptor (Martinez de la Torre et al., 2007).

It could be assumed that future research will definitely focus on finding out how the fetal development is affect by chemokines, while addressing issues such as time, location, relative concentration, and cellular environment. It is vital to have data of that nature in order to find effective medicine for complications associated with reproduction such as infertility, miscarriage and preeclampsia.

1.16 Infection and human pregnancy

A developing fetus faces numerous risks during pregnancy. Complications such as intrauterine infections, which are generally seen during the early pregnancy, cause a substantial risk to the developing foetus. It is believed that through (i) maternal blood circulation, (ii) ascending into the uterus from the lower reproductive tract, or (iii) descending into the uterus from peritoneal cavity (Espinoza et al., 2006, Mor, 2008), pathogens can enter into the placenta.

Larmont (2003) explains that intrauterine infections have been recorded in up to 40% of cases during the pre-term labour. In addition, Epstein et al., (2000), explain that in 85% of the cases that experienced a pre-term delivery at less than 28 weeks of gestation, have symptoms of infections. Furthermore, it is argued that it is quite possible for intrauterine infections to occur during the early pregnancy prior to any observed pregnancy complications (Gonçalves et al., 2002). It is also said that several types of complications are mainly associated with particular stages of a pregnancy. For instance, a complication such as miscarriage is a common occurrence during the first trimester but complications such as pre-term labour and preeclampsia can occur

during any phase of the pregnancy (Arechavaleta-Velasco et al., 2002, Romero et al., 2003, Gonçalves et al., 2002). When considering the pre-term labour and early miscarriage during the first trimester of pregnancy, bacterial infection has been distinguished as a major cause that triggers those complications (Romero et al., 2010, Kim et al., 2010, Ralph et al., 1999, Hay et al., 1994, Romero et al., 2007).

Toxins, which stimulate cytokine production including interleukin-6 (IL-6), tumour necrosis factor α (TNF-α), chemokines (such as IL-8), interleukin-12 (IL-12) and IFN-γ (Romero et al., 2007, Filisetti and Candolfi, 2004), prostaglandins (Patel and Challis, 2001), proteases and other enzymes (Phillippe et al., 2001, are usually released during a bacterial infection. All of these contribute in forming a coordinated response which is responsible in causing uterine contractions, and placental detachment. Therefore, it is very clear that the role of the human placenta is integral for the protection of the fetus and the comprehension of it is not easy either as it is not very well explained. The phrase 'toll-like receptors' (TLRs) which are members of the pattern recognition receptors (PRRs) family and are expressed at the fetal-maternal interface such as TLR-2 and TLR-4 (Holmlund et al., 2002, Kumazaki et al., 2004, Patni et al., 2009), have been sown in former studies in placenta trophoblasts.

One of the major components of the outer membrane of gram negative bacteria is called Bacterial lipopolysaccharide (Poltorak et al., 1998, Qureshi et al., 1999). It has been identified that around 90% of the surface of the outer bacterial ell is covered by Bacterial lipopolysaccharide. The purpose of this component is to guard the bacteria through serving as physical barricade (Nikaido, 1989; Papo and Shai, 2005). Its constituents both hydrophobic and hydrophilic domains are vital for the survival of the bacterial as well defend it for deprivation of hydrolytic caused by other organs

In summary, it has been assumed that PRRs in trophoblast cells are essential to protect the foetus from pathogens and could be mainly responsible for the maternal innate immune system. However, their purpose with regard to the fetal tolerance by the maternal immune system is yet to be clarified. Hence it is essential to carry out additional studies on CD14 and MARCO in order to clarify the expression of CD14 in trophoblast cells and its role in innate immune responses. The new discoveries might lead to the creation of therapeutic strategies against trophoblast dysfunction which cause complications during pregnancy.

Chapter 2

Materials and Methods

2.1 Materials

2.1.1 General laboratory chemicals

The majority of chemicals used in this study were from Sigma, Poole, England, UK, particularly, Accutase, Dimethyl Sulphoxid (DMSO), Cellytic M Cell Lysis Reagent, Protease Inhibitor Cocktail, Paraformaldehyde (PFA), Tween-20, Saponin and Triton-X 100. Other chemicals such as Sodium Chloride, Acetone, Methanol and Virkon were from Fisons, Leicester, England, UK; Fetal Calf Serum (FCS) was from Imperials Laboratories, England., Germany. Lipopolysaccaride (LPS) from *E. coli* serotype EH100 was purchased from (Sigma Aldrich, UK). Dulbecco's Modified Eagle's Medium (DMEM) and RPMI were from Fisher Scientific, UK.

2.1.2 Cell lines

For the purpose of the present study, we employed human placental cell line JEG-3. Secondly, we included other cell lines in the present study as positive controls such as THP1, and Raji. The human placental choriocarcinoma cell line JEG-3 provided by Prof. I.L. Sargent, Nuffield Department of Obstetrics and Gynaecology, University of Oxford. This cell line is an epithelial adherent monolayer which is highly proliferative, so it was suitable for use as our trophoblastic model system. This cell line was maintained in DMEM/Hams F-12 which was supplemented with 10% (v/v) FCS, and maintained at 37°C and 5% CO_2. Secondary cell lines were used in the present study as a positive control since they express a considerable level of CD14 and MARCO. The secondary cell lines that were used in this study are as follows: THP1, a human monocyte derived from patients with Acute Lymphocytic Leukaemia (ALL) and Raji, a human Burkitt's

lymphoma. All secondary cell lines were kindly provided by Prof. Nelson Fernandez, Department of

Biological Sciences, University of Essex, UK. The cell lines were cultured in RPMI -1640 medium and were maintained at 37°C and 5% CO_2.

2.1.3 Antibodies

The primary and secondary used in this study were obtained from different sources as shown in Table 2.1

Antibodies	Specificity	Isotype/ species	Conjugation	Source
CD14 (MEM-18)	Mouse IgG1	Mouse IgG1/ human	None	Santa Cruz Biotechnologies Inc., Santa Cruz, CA, USA
MARCO (2G12)	Mouse IgG1	Mouse IgG1/ human	None	Sigma-Aldrich UK
Myoferlin (FER1L3)	Mouse IgG1	Mouse IgG1/ human	None	Novus Biologicals, Ltd Cambridge
VEGF (A-20)	Mouse IgG1	Mouse IgG1/ human	None	Santa Cruz Biotechnologies Inc., Santa Cruz, CA, USA
VEGFR-2 (A-3)	Mouse IgG1	Mouse IgG1/ human	None	Santa Cruz Biotechnologies Inc., Santa Cruz, CA, USA
Anti-NFkB P65	NFkB P65	Rabbit polyclonal/ human	None	Novus Biologicals, Ltd Cambridge
Rabbit anti mouse IgG1	Mouse IgG1	Rabbit IgG1/ mouse	FITC	Santa Cruz Biotechnologies Inc., Santa Cruz, CA, USA
Donkey anti-Mouse IgG	Mouse IgG	Donkey IgG/ mouse	IRDye® 800CW	Li-CorBioescieces, Lincoln, NE, U.S.A.
Goat anti-Rabbit IgG	Rabbit IgG	Goat IgG/ rabbit	IRDye® 680LT	Li-CorBioescieces, Lincoln, NE, U.S.A.
TU02	Alpha-subunit Tubulin	Mouse monoclonal IgG/ human	None	Santa Cruz Biotechnologies Inc., Santa Cruz, CA, USA
Rabbit anti-mouse IgG	Mouse IgG	Rabbit IgG/ mouse	Alexa Fluor® 488	Invitrogen, Carlsbad, CA, USA

Rabbit anti-mouse IgG	Mouse IgG	Rabbit IgG/ mouse	Alexa Fluor® 555	Invitrogen, Carlsbad, CA, USA
Goat anti-rabbit IgG	Rabbit IgG	Goat IgG/ rabbit	Alexa Fluor® 488	Invitrogen, Carlsbad, CA, USA
DAPI	AT region of DNA	Dye	N/A	Sigma-Aldrich UK

Table 2.1: List of antibodies used in this study.

2.2 Methods

2.2.1 Cell cultures of cell lines

The JEG-3 cell line was of immense importance for all the experiments of this study as it served as the model with which the placenta could be compared. JEG-3 cells were passaged at 70-80% confluency every 3 to 4 days. The cells were washed with 1X Phosphate buffer saline (PBS) and lifted with 1ml of accutase (Sigma-Aldrich; Dorset, UK) by incubating at 37°C for about 5-10 minutes. The cells were then counted with a hemocytometer and plated out at a density of $1X10^3$ in a new culture flask. THP1 cell lines were expanded differently as they .are suspension cell lines. The cells were centrifuged at 1000 rpm for 5 minutes, supernatant was aspirated and fresh medium was added to the cell pellet. Then cells were seeded at density of $1X10^5$ in a new culture flask.

2.2.1.1Cryopreservation of cells

Cryopreservation of cells was done at 70% confluency. The cells, by means of accutase, were detached, counted and checked for feasibility as mentioned above and then centrifuged. Then the re-suspension of the cells was carried out and as a result they were approximately 1.25 x 106 cells/ ml of freezing mixture (90% FCS and 10% Dimethyl sulfide [DMSO]). Afterwards, 1 ml of the cell suspension was then dispensed into each cryo tube (Fisher Scientific, UK) and placed in -80̊ C freezer for 1-2 days before transferring them to liquid nitrogen at -196̊ C for long-term storage.

2.2.1.2 Growth curve

JEG-3 cell line, which grows in culture, is grown in three separate phases. 'Lag phase' which is the first stage, spans into 1- 2 days. During this period cell numbers increase slightly. It has also been assumed that this is the period where the cells get accustomed to the new media. The next

stage is called the 'log phase' in which an exponential surge in the cell numbers are visible. Then, the final phase is the 'confluent phase'. During this phase, the number of

2.2.1.3 Cell Viability Test

Cell viability was tested to identify whether the cells were dead or living, based on the trypan blue exclusion method. Firstly, the cells were washed with PBS. Then accutase treatment was used to split them and the cell suspension was placed in a conical centrifuge tube. Then a cell suspension of 1:2 dilutions in trypan blue (Sigma, UK) was prepared. Approximately 10µl of diluted cell suspension was loaded into both the haemocytometer chambers, and cells were viewed under the light microscope. The cells were observed as total cells and non-viable (blue) cells. Live cells would have the cell membranes intact and would exclude the trypan blue dye, where dead cells did not.

2.2.2 Cell Stimulation

2.2.2.1 Lipopolysaccharide (LPS)

LPS is unique for gram-negative bacteria presented in the outer membrane, and is made of both hydrophobic and hydrophilic domains and was purchased from (Sigma Aldrich, UK) in freeze-dried powder. LPS was dissolved in 1ml of sterile 1X PBS (1 mg) by swirling gently until the powder dissolved. Solutions were further diluted to the desired working concentration with additional sterile cell culture media, and were stored at -20°C in accordance with the manufacturer's instructions. JEG-3 cells were serum starved with DMEM/Hams F-12 and Ham's F-12 respectively containing 0.1% FCS, for a period of 4 hrs prior to stimulation. Cells were then stimulated with LPS at a concentration of 1, 10 and 20µg/ml, at the following time points; 1 2 , 24 and 48 hours. Cells were counted using a haemocytometer, checked for viability and harvested for sample preparation.

2.2.3 Protein expression analysis using Flow Cytometry

Flow cytometry is a technique used to analyse and measure various properties of cells. The cells are usually labelled with a fluorescent probe, normally a fluorphore conjugated to an antibody. The cells are suspended in fluid; and the cells carrying fluid are passed through a beam of light. This technique uses the principles of light scattering, light excitation, and the emission of fluorochrome molecules to generate specific multi- parameter data from cells. There are three parameters that are measured by photomultiplier tubes; forward scatter (FSC), side scatter (SSC) and fluorescence (FL). One advantage of the flow cytometer is its ability to evaluate a large population of cells accurately and quickly with semi quantitative results. This makes flow cytometry an ideal tool for quantitative analysis of certain cellular properties, especially when the cells of interest are a small fraction of other cell types in a cell population. The results are displayed in many ways, such as in a histogram, dot plot or contour. As standard practice, irrelevant or nonspecific isotype antibody was used as a negative control so that we can evaluate the degree of positivity for other surface proteins in terms of the fluorescence intensity.

2.2.3.1 Cell surface and intracellular staining

For surface staining of specific cell antigens, such as, HLA-ABC or HLA-DR, VEGF, after culturing treated or untreated samples (1×10^6 cells/ sample), cells were washed in PBS. The cells were fixed with a fixation buffer to ensure free access of the antibody to its antigen 4 % PFA (Sigma, UK) and this was followed by a washing step in PBS. The cells were then blocked with blocking buffer (0.1% BSA in PBS) to block non-specific antibody binding sites, then washed again in PBS. Cells were used with either only secondary antibody or neither primary nor secondary antibody as negative controls. For intracellular staining, cells (antigens such as Myoferlin) were permeabilised with 0.25% Triton X-100 in PBS for 10 min. on ice... The staining procedure for intracellular staining was the same as for the surface staining. Samples of

10,000 cells each were analysed using a BDFACS Aria Flow Cytometer using a 488 nm beam for detection of the fluorochrome attached to the secondary antibody (PE, FITC).

2.2.4 Proteomics

2.2.4.1 Protein extraction

Cell lines grown up to 70-80% confluence were washed twice with PBS and frozen down at -80 ℃ until used for cell lysates. To prepare whole cell lysate, CelLyticTM M reagent (Sigma-Aldrich) (contains low percentage of a mild detergent in bicine buffer) and protease inhibitor (Sigma-Aldrich) were mixed at 100:1 ratio respectively and added to frozen cells and scraped with a cell scraper. Cells with reagents were then transferred into a micro-centrifuge tube and incubated on ice for 20 minutes and then vigorously vortexed. Lysed cells were ultra-centrifuged at $20,000 \times g$ for 10 minutes. For further analysis Supernatant was collected and stored at $-80^{o}C$. ProteoJETTM Cytoplasmic and Nuclear Protein Extraction kit (Fermentas, Thermo Fisher Scientific) was used according to instructions provided with the kit to prepare cytoplasmic and nuclear protein fractions. Total protein concentration was determined by the Bio-Rad Protein Assay (Bio-Rad, Hercules, CA, USA) following the manufacturer's instructions.

2.2.4.2 Bradford Assay

This technique is utilized for measuring the protein concertation in the lysate in order to calculate the quantity of protein that ought to be stacked into every well before running the gel. This measure depended on the importance that when the Coomassie Blue Dye is bound to the protein in an acidic medium, a movement in absorbance happens from 465 nm-595 nm bringing about a colour change from chestnut to blue. The measure of complex now appeared in the solution is a measure for the protein concentration by technique for an absorbance analysing. Standard concentration of BSA (Bovine Serum Albumin) 0.015, 0.031, 0.06, 0.125, 0.50, 1, and 2 mg/ml

were readied. A progression of weakening for the example was set up in PBS. 5 µl of the models and tests separately were added to a 96 well-plate. 250 microliters of Bradford reagent was added to every well and the plate was left for incubation at room temperature for 5 minutes. A miniaturized scale titre plate peruse was set up to an absorbance of 595 nm. To minimize test mistake the plate was read three times. A graph for concentration versus absorbance was plotted on Microsoft Excel and the protein fixation was acquired utilizing the y = mx + c condition.

2.2.4.3 One dimensional gel electrophoresis

This method uses the molecular weight of the polypeptide to separate it. The capability of a molecule to move over an electric field is directly proportional to the voltage and the charge of the molecule, while inversely proportional to the molecular friction. Considering that, a semi-solid matrix at a set voltage can separate the proteins electrophoretically taking into account their molecular weight. When the molecules are charged to the same degree and the same sign, the portability of the molecules would be contrarily proportional to their size. In this way, in PAGE, the proteins are negatively charged and are bound to sodium dodecyl sulphate (SDS) and are separated within a matrix of polyacrylamide gel in an electric field based on their molecular weights.

After 12% gels were set up with the BioRad Mini PROTEAN Electrophoresis system, TEMED and APS were added to improve the polymerization process. Once the gels were completely polymerized, they were loaded with electrophoresis buffer into the system. The previously measured protein lysate was used as sample preparation. The mixture of 20µl of protein and 5µl of sample buffer was heated on a dri-block at 95°C for 4 minutes, and then were loaded into the wells of the gels. Then the gel was run at 50V until the samples crossed the stacking gel and then at 80V for about 3 hours. Following separation by SDS-PAGE, the gels were stained with

Coomassie Blue to check the success of the transfer or processed for immunoblotting. Recipes for buffers and solutions are mentioned in the appendix.

2.2.4.4 Coomassie Blue staining

The polyacrylamide gel was prudently expelled from between the plates and afterward put into. Coomassie blue stain, the gel is covered totally, for 2 hrs at room temperature on a shaking table. Taking after that, the gel was put into 100ml of destain arrangement and supplanted with new one until the gel was clear and just the stained protein groups were noticeable. Formulas for buffers and solutions are in the appendix.

2.2.4.5 Western transfer

After protein detachment utilizing electrophoresis, proteins were exchanged to a polyvinylidene fluoride (PVDF) film (Immobilon-FL, Merck Millipore, Merck KGaA, Darmstadt, Germany) the gels is placed in a transfer buffer in the gel framework. Two gel cartridges were lined with a wipe and the gels were situated on channel paper over the wipe. The methanol pre-splashed PVDF membrane was situated over the gel while an extra channel paper and wipe were stacked on the above. A glass pipette was moved over to dispense with air bubbles, and the two cartridges were situated into the BioRad Mini PROTEAN Electrophoresis framework. At that point a cooling unit and exchange cradle were included, and the framework was run overnight at 30 V. Toward the end of the exchange time frame, the framework was separated from a force supply unit and the gel likewise stained with Coomassie blue stain to check the achievement of the exchange.

2.2.4.6 Immunoblotting

To fix the protein on the membrane, they were washed with PBS and air dried then soaked in methanol for one minute. With 5% skimmed milk in PBS, membranes were blocked. To detect the proteins of interest, the following mAb were used: anti-CD14 (clone MEM-18) anti-MARCO (clone 2G12), anti-Myoferlin (clone FER1L3) and anti-VEGF (clone A-20). To probe the cell extracts an alpha-subunit specific tubulin antibody (TU02), beta-subunit specific actin (Poly 6221) and Heat shock protein (Hsp 90) was loaded as a control. Captured proteins were detected by secondary antibodies Infra-Red Dye IRDye® 680LT Goat anti-mouse and IRDye® 800CW Donkey anti-Mouse IgG (Li-CorBioescieces, Lincoln, NE, U.S.A.) at a dilution of 1:10,000 in PBS with 5% milk and 0.025% Tween-20 (Sigma-Aldrich). Using the ODYSSEY infrared imaging system (Li-Cor Bioscience) signals were detected. To estimate the molecular weight of the proteins under study we used PageRulerTMPlusPrestained Protein Ladder from Fermentas (Thermo Fisher Scientific).

2.2.5 Laser scanning confocal microscopy

Confocal laser scanning microscopy is a valuable technique used to obtain three-dimensional and high-resolution images of very small objects. It is far superior in comparison to conventional microscopes due to many factors; firstly to be able to control the depth of the field, secondly minimal interference in background from the focal plane and thirdly: thick specimens can be studied in serial sections.

In order to avoid distortion of image and minimizing blur due to sections above and below the focal plane, Laser scanning confocal microscopy was used in this study to get clear visualization cellular components in contrast to standard fluorescent microscopy.

Confocal microscopy permits the optical sectioning and achieving the three dimensional (3D) images of the specimen. An objective lens helps to focus a laser beam onto the targeted section,

labeled specimen, which emits fluorescent light as a result. The fluorescent light is further passed through dichroic mirror with a pinhole source focused at the detector, which records the data on a computer. Thus light emitted from out of focus points are excluded. A 3D image Is achieved by horizontal and vertical scanning of the cells labeled section using motor driven mirrors.

2.2.5.1 Immunofluorescence staining for microscopy

Cell monolayer culture and twofold staining: JEG-3 cell lines were independently refined in LabTek 8 well chambers (Thermo Fisher Scientific) at a density of 6X103 cells for every well, for two days taking after seeding. However, for the staining technique, every one of the steps was done at room temperature. By using 4% paraformaldehyde the cells were settled (Sigma, UK) for 20 minutes and hindered with 2% (w/v) BSA arranged in 1x PBS (phosphate support saline) for 1 hr at room temperature. The incubation steps were additionally completed at room temperature. For staining, the cells were incubated with a particular monoclonal immune response for 1 hr took after by washing three times with PBS. The optional immune response utilized was hostile to mouse IgG conjugated with Alexa Fluor® 488 or Alexa Fluor® 555 (Invitrogen, Carlsbad, CA, USA), these were incubated for 1h. For twofold staining, cells were blocked again for 1h and afterward stained with particular monoclonal counter acting agent for 1h. After 3 washes, cells were brooded with against mouse IgG TRITC conjugated counter acting agent for 1h. Isotype controls were stained with just optional counter acting agent. Cells were then altogether washed and chambers were expelled from the slide. Slides were washed in a container containing 1X PBS and dried. The cells were then mounted with against blur mounting medium and precisely secured with the spread slip keeping away from any air bubbles. Edges of the spread slip were fixed with straightforward nail clean and dried noticeable all around. Arranged slides were put away at 4°C in the dark for further examination.

2.2.5.2 Microscopy for colocalisation studies

Image acquisition for colocalisation studies was performed as described in Obara et al. (Obara et al., 2013). Using a Nikon A1R confocal microscope with a plan-apochromatic violet corrected (VC) 1.4 numerical aperture (N.A.) 60x magnifying oil-immersion objective cell images were obtained. Images were acquired using one-way sequential line scans in four channels. With a laser power 3.2 arbitrary units (AU), DAPI was excited at 405nm and its emission collected at 450/50nm with a PMT gain of 118 AU. Alexa Fluor 488 was excited at 488nm with a laser power 7.8 AU, its emission collected at 525/50nm with a PMT gain of 140 AU (hereafter called the green channel). Alexa Fluor 555 signal was excited at 561nm with laser power 2.1 AU and collected at 595/50nm with a PMT gain of 117 AU (hereafter called the red channel). Differential interference contrast images were acquired using the transmitted light detector at a gain of 103 AU. In all cases, no offset was used, and the scan speed was 1⁄4 frames/s (galvano scanner). The pinhole size was 34.5μm, approximating 1.2 times the Airy disk size of the 1.4 N.A. objective at 525nm. Scanner zoom was centered on the optical axis and set to a lateral magnification of 55nm/pixel and a Nyquist factor of 2.54 (for Alexa Fluor 488) and 2.79 (for Alexa Fluor 555). Axial step size was 140nm, with 40-60 image planes per z-stack. Both channels were examined of the cells with average to fair signal strength. Cells were in isolated positions with few or no neighboring cells, allowing accurate quantitation of the flat plasma membrane and uncrowded receptor distribution.

In order to reliably determine colocalisation with this method, optimized samples were acquired considering following criteria. First, saturated pixels were avoided, as they are the endpoint of the dynamic range. Values above this were not recorded, and saturated pixels may represent lost information and therefore were not used for quantification. Second, datasets were acquired with the correct sampling parameters. These are determined by the Nyquist-Shannon reconstruction theorem (Nyquist, 1928; Shannon, 1949). Briefly, this means that the smallest structure in an

image, as determined by the microscope's resolution using Abbe's criterion, should be represented by at least two pixels. Higher sampling (three to four pixels) is also acceptable, but under sampling must be avoided. Third, aberrations were minimized in the imaging setup. This was done by using objective corrected for spherical ("plan") and chromatic aberrations (achromatic, apochromatic and apochromatic violet-corrected (VC), depending on the number of colours corrected for). Furthermore, uni-, not bi-directional scanning, zooming in to the center of the field of view, and separating colours in line scanning rather than full-frame mode was done as measures for minimizing aberrations.

2.2.5.3 Colocalisation analysis

An innovation strategy stated in Jabeen et al (2013) and Obara et al (2013) was taken after for this examination. The colocalisation approach utilizes MATLAB programming (variant R2010b with Image Processing Toolbox; MathWorks Inc., Natick, Massachusetts) and depends on a 3D blob-like component recognition calculation presented by Obara and colleagues. All process is depending on examination in 3D. The algorithm is separated into two phases: competitor area recognition, and applicant area pruning. After obtaining of discrete datasets for both atoms particles, the fluorescent force of particles is upgraded while smothering the sound by convolving the image with a 3D Laplacian of Gaussian (LoG) portion. The LoG piece size is controlled by a client characterized sweep r. Local maxima, recognized by morphological opening, are then used to characterize all areas of particles brighter than their prompt environment. This procedure proceeds until a client characterized low power bound T (separate for every channel, to consider datasets where sound levels are notably diverse) is touched. This is the edge beneath which no particles can be securely distinguished in light of image sound. So as to precisely gauge colocalisation of particles in the double shading fluorescence images, their centroid positions were pinpointed at subpixel determination utilizing weighted centroids. A Local coordinating methodology then played out a comprehensive quest for right matches

between the two vectors of meeting positions, utilizing the normal range of the nearby circle of light r. For every position in one channel, we calculated the Euclidean separation for each position in the other channel. On the off chance that the separation of the nearest combine is lesser than the most extreme colocalisation separation d, then the pair is added to the rundown of matches and expelled from the input vectors. All competitor areas are pruned to kill spurious areas because of image noise. The method is rehashed until there are no more matches fulfilling the greatest colocalisation separation condition. Receptor sets were regarded to colocalise on the off chance that they didn't surpass the measurement deciding the estimated size of a solitary molecule's PSF. A tight limit was decided for this PSF, measuring 165nm in x and y, and 412nm in z. Receptor sets with their centroids facilitate separated than 165nm were named non-colocalising. These outstanding positions in both datasets are then named as unmatched

2.2.5.4 Visualisation

Following loading the system's Graphical User Interface (GUI) and a 3D dataset for every channel, the calculation is controlled by pressing the "Colocalisation" button. Outcomes can then be observed in five diverse ways: 1) Stacks: Centroid positions of every distinguished particle are set apart by red dots in the image stacks, and sliders (in the "Stacks" box of the GUI) permit to travel through the distinctive z-planes. A high zoom can be applied to confirm the precise location of a super resolved centroid situated inside a fluorescent blob. 2) Maximum intensity projections: Visualisation of a whole dataset in one image where projections of every image stack are accessible ('Projection 1' and 'Projection 2' in the "Plot" box), with green and red reference marks stamping unmatched (non-colocalising) particles, and green and red asterisks with blue circles showing colocalisation. 3) Scatterplot: Produces an isometric viewpoint perspective of particles appeared as reference asteriks (green and red for every channel), and colocalisations enclosed in blue. The numbers for colocalisations and particles identified in every channel are additionally shown. 4) Distance outline: shading coded 3D separation guide is

utilized to imagine colocalisations. Every colocalisation is appeared as a solitary circle, with a colour code demonstrating the separation between the two colocalising particles

2.2.5.5 Pearson's correlation coefficient for colocalisation

Pearson's correlation coefficient (PCC) for colocalisation was performed by using colocalisation threshold plugin in ImageJ with auto threshold settings. Three dimensional microscopic images were used for the analysis and value of PCC indicates the correlation between CD14 and MARCO receptors. Composites of merged red and green channels and their scatter plots were used. In THP1 cell line PCC value is 0.925, thus indicating strong positive correlation between CD14 and MARCO receptors. In JEG-3 cells, PCC value is 0.737, thus reflecting a strong positive association between the two receptors

2.2.6 MTT Cell proliferation assay

Trophoblast JEG-3 cells were cultured in 96 well flat bottom plate (Nunc) with seeding density 1×10^4 cells per well in 100µl complete culture medium. To synchronize the cell cycle, cells were stressed for 4h with low serum density (0.1% FBS) in culture medium at 60% confluence. Cell cycle synchronization is related to serum starvation of cells (Chen et al., 2012). Cells were subjected to infection, cells were treated with by lipopolysaccharide (LPS) serotype; O5:B55 (Sigma) treatments (1µg/ml, 10µg/ml, or 20µg/ml) or no treatment (low serum medium only). In parallel-untreated cells was continued as a positive control for cell proliferation and for negative control a cell apoptosis inducing agent Camptothecin (Sigma) was used at a concentration of 4mMolar solution in serum free culture medium. CellTiter 96 Aqueous one solution cell proliferation assay kit (Promega) was used to assess cell growth and proliferation. To determine live cells, each well was briefly subjected to 20µl cell proliferation reagent and incubated at $37^{o}C$ with 5% CO_2 in humidified chamber for 1-4 h for colour development. The amount of

colored product produced is directly proportional to the number of live cells, as only live cells react with the cell proliferating reagent. Elisa plate reader was used at a wavelength of 490nm to read the plate for measuring the absorbance. Before analysis background absorbance was corrected and wells without any cells, medium only were measured for background absorbance.

Chapter 3

Analysis of expression of CD14 and MARCO in human choriocarcinoma JEG-3 cells

3.1 Introduction

The aim of this chapter is to analyse the expression of cluster of differentiation (CD_) 14 and the scavenger receptor macrophage receptor with collagenous structure (MARCO) in the human placental choriocarcinoma cell line JEG-3.The maternal–fetal interface represents a unique site that must promote tolerance to the semi-allogenic fetus, whilst maintaining host defence against a diverse array of possible pathogens. CD14 is one of the components of a receptor complex which mediates LPS-induced signal transduction (White and Demchenko, 2014). MARCO can also interact with LPS. It has been suggested that MARCO plays a role in up-regulation of the antimicrobial defence system during bacterial infections in macrophages of the liver and spleen (Arredouani et al., 2004). CD14 is a 55kDa glycoprotein which is initially processed in the endoplasmic reticulum and then expressed on the cell surface (Gegner et al., 1995). CD14 exists in two forms as glycosylphosphatidyl (GPI) -anchored membrane protein (mCD14) on monocytes and as soluble protein (sCD14) in plasma (Heidenreich 1999).

CD14 is a receptor for complexes of bacterial lipopolysaccharide (LPS) and LPS binding protein that mediates responses to LPS (Heidenreich, 1999). CD14 also recognizes other pathogen-associated molecular patterns, such as lipoteichoic acid (Lotz et al., 2004). CD14-deficent mice survive and exhibit no symptoms of bacterial-induced shock when injected with a dose of Gram-negative bacteria *(Escherichia coli.)* lethal to normal mice. This presented a role for CD14 in the dissemination of Gram-negative bacterial infections (Haziot et al., 1996).

Since CD14 is GPI-linked, its role as co-receptor for the detection of LPS requires the protein membrane cofactors toll-like receptor (TLR) 4 and myeloid differentiation factor 2 for LPS-

mediated transmembrane signalling (Akashi et al., 2003).Binding of LPS to cell-surface TLR-4 initiates myeloid differentiation factor 88/IL-1R-associated protein kinase/TNFR-associated factor 6 complex formation inside the cell. Signal transduction events then trigger activation of the IκB kinase-NF-κB pathway, and of Ser/Thr protein kinases that belong to ERK 1 and 2, JNK and p38 MAPK subfamilies (Akira et al., 2004; Zhang et al., 2004)

MARCO is a multifunctional trimeric glycoprotein that contains a collagenous domain and a C-terminal scavenger receptor cysteine-rich (SRCR) domain (Sankala et al., 2002). It is encoded by the gene located on chromosome 2 (Thelen et al., 2010). The expression of human MARCO is detected to be most robust in the liver, lymph nodes, monocytes and alveolar macrophages, which are involved in the filtration of blood and lymph fluids (Jozefowski et al., 2005; Thelen et al. 2010) reported that the degree of MARCO transcription and cell-surface expression increased after bacterial binding. This supports its significance in phagocytosis of bacteria.

Because of the similarity in spatial expression and function (both ligands for LPS) hypothesis of the study was that these receptors might be working in close association. Therefore, one of the aims of the present study was to investigate the biological interaction between CD14 and MARCO by colocalisation analysis.

AIMS OF STUDY:

1. Expression of CD14 and MARCO receptors on trophoblast cells

2. Colocalisation analysis for CD14 and MARCO receptors expressed on the surface of trophoblast JEG-3 cells.

3.2 Results

3.2.1 Viability, granularity and size of the trophoblast cells

Flow cytometry was used to assess the granularity and viability of JEG-3 cells, B lymphocyte cells from a human lymphoblastic cell line (Raji) and THP-1 monocytes. Unstained cells were used for this test. Scatter plots are displayed as forward scatter on x-axis verses side scatter on y-axis, where each dot on the plot area represents a cell (Figure 3.1) .Each plot area is divided into four quadrants, maximum density of the cells in all three cell lines is localised in the lower left quadrant, which revealed that cells were of the same size, granularity and that the majority of the cells are viable. Cells of irregular shape and abnormal size are more scattered in plot area in upper quadrants.
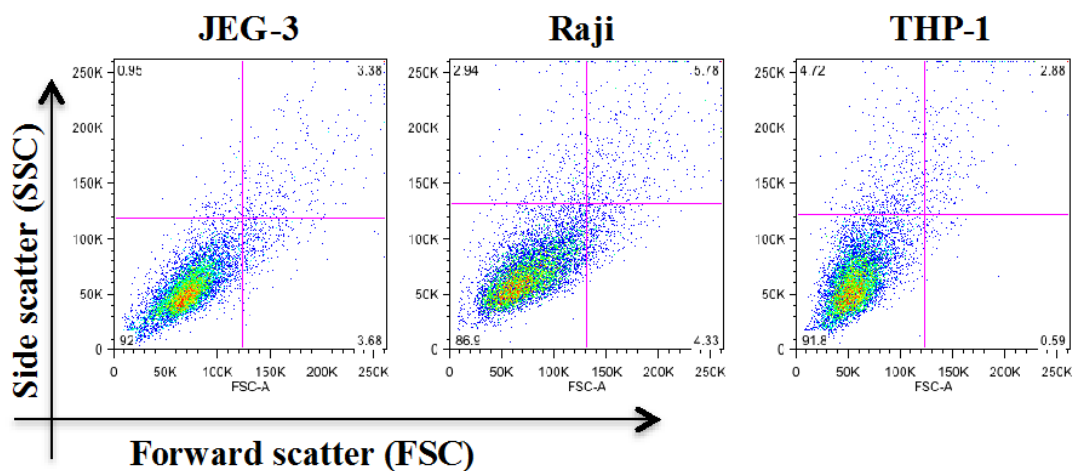
Figure 3.1: Scatter plots displaying forward scatter (FSC) (X-axis) and side scatter (SSC) (Y-axis) of JEG-3, Raji and THP-1 cells.

The FCS scatter data provide information on the relative size of the cells, whereas SSC scatter data estimate their granularity. The units indicate the level of light scatter brightness with 0 being the dullest and 1000 being the brightest. Each dot is a cell ranked by its brightness. The data are representative of three independent experiments.

3.2.2 Cell-surface expression of HLA-A, HLA-B, HLA-C and HLA-DR

The cell-surface expression of HLA-A, HLA-B, HLA-C and HLA-DR molecules in JEG-3 and THP-1 cells was studied in order to examine the immunogenicity of these cell lines and their use as models of trophoblast and monocyte cells.Results are presented as hitogramswhere mean fluorescence intensity (MFI) is along horizontal axis (x-axis) versus total cell count on vertical axis (y-axis) (Figure 3.2). In the flow cytometry analysis, empty histograms show HLA proteins expression while gray filled histograms represent isotype-matched negative control.

It was found that JEG-3 and THP-1 cells express classical HLA class I molecules, HLA-A, HLA-B and HLA-C. However HLA-DR was only expressed on THP-1 cells (Figure 3.2).
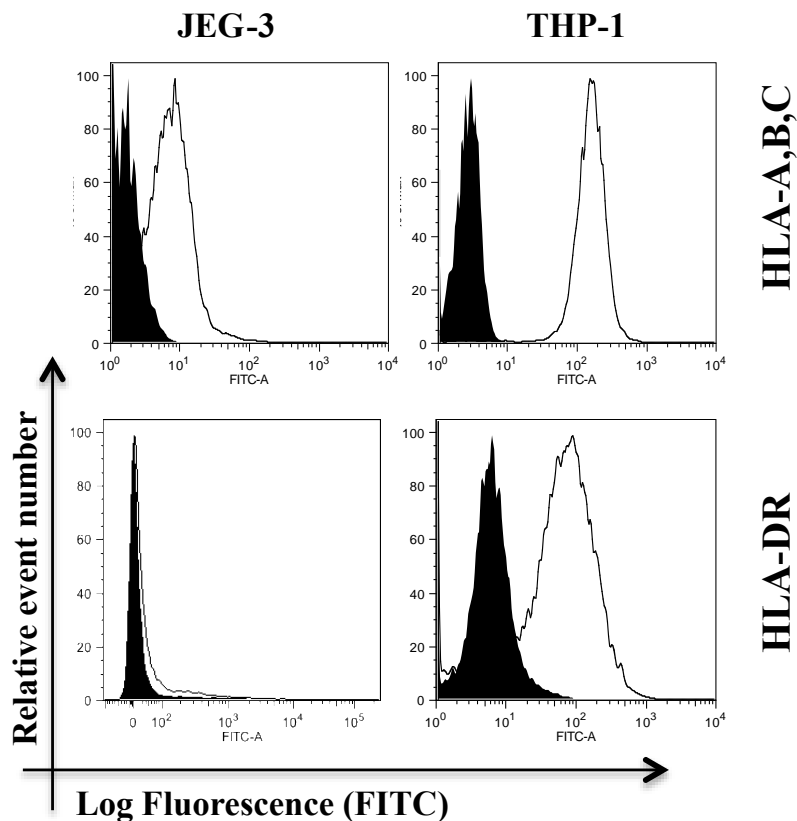
Figure 3.2: Expression of cell-surface HLA-A, HLA-B, HLA-C and HLA-DR in JEG-3 and THP-1 cells.

Flow cytometry analysis of JEG-3 and THP-1 cells showing HLA-A, B, C and HLA-DR expression (empty histograms), displayed as mean fluorescence intensity at the cell-surface . Negative controls were performed by using an isotype-matched control antibody (black-filled histograms). The data are representative of three independent experiments.

3.2.3 Phenotyping of CD14and MARCO in JEG-3 cells

Flow cytometry analysis of cell-surface expressed CD14 was performed on untreated THP-1 and JEG-3 cells. The cells were stained with an appropriate concentration of CD14 monoclonal antibody (MEM-18) followed by fluorescent (FITC) secondary antibody. Cells without staining and isotype cells stained with only the secondary antibody were used as a negative control. Untreated THP-1 cells were used as the positive control.

The analysis revealed a moderate expression of CD14 on the cell surface membrane of untreated JEG-3 cells, whereas, positive control THP1 cells showed strong expression (Figure 3.3A). The geometric means values obtained from flow cytometry analysis are presented as bar graphs (Fig. 3.3B) which show mean fluorescence intensity (MFI) of each cell line in comparison to isotype control.

Flow cytometry analysis of cell surface MARCO receptor expression on test cell line JEG-3and positive control cell line THP1 is shown in figure 3.4 A, where filled histograms are isotype controls and line histograms represent MFI indicating level of expression. JEG-3 cell line had reasonable expression of MARCO whereas, THP1 showed good expression for the same receptor. Geometric means of MFI are further presented graphically (Fig. 3.4B) showing significant expression in comparison to isotype control.

A

JEG-3 | THP-1

Relative event number

Log Fluorescence (FITC)

Cell Surface

B

Relative expression of CD14

■ JEG-3
■ THP-1

Mean Fluorescence Intensity (MFI)

Isotype | Cell Surface
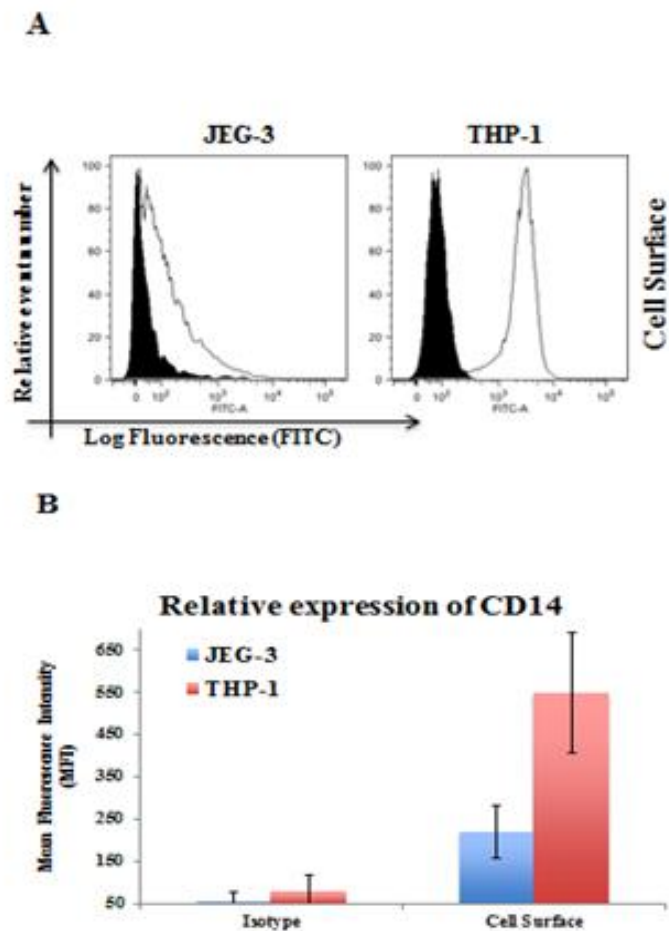
Figure 3.3: Analysis of the expression of cell-surface CD14 in JEG-3 cells.

Flow cytometry analysis showing CD14 expression (empty histograms), displayed as mean fluorescence intensity, on the cell-surface of JEG-3 and THP-1 cells. Surface expression of CD14 in THP-1 cells is shown as a positive control. Negative controls were performed by using an isotype-matched control antibody (black filled histograms). (B) Graphical representation of CD14 surface protein expression in JEG-3 and THP-1 cells. Bar graphs represent level of each protein in mean values ± SD in each cell line. Data are representative of three independent experiments.
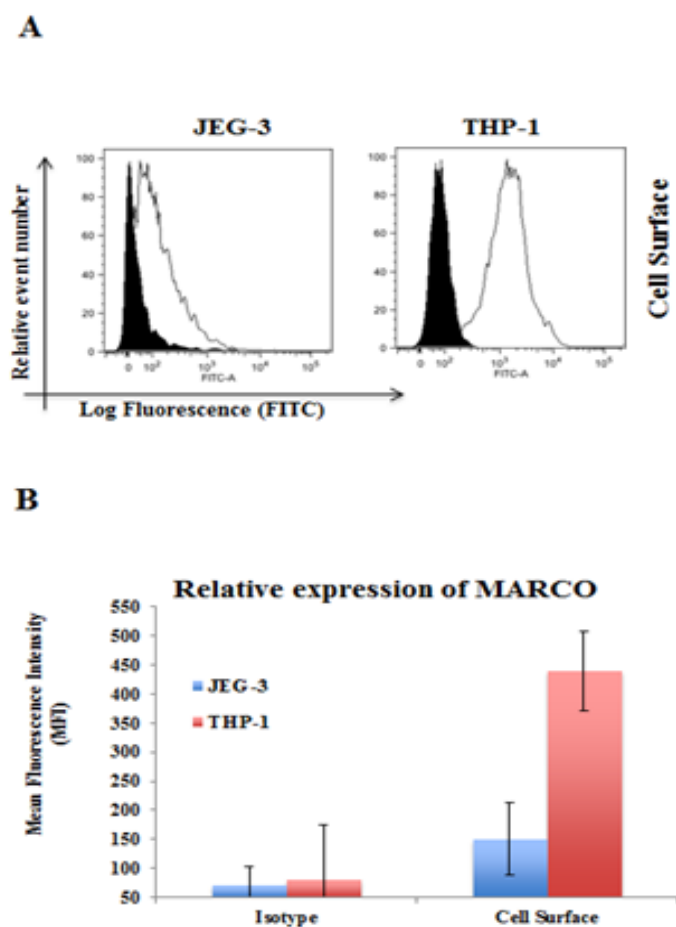
Figure 3.4: Analysis of the expression of cell-surface MARCO in JEG-3 cells.

(A) Flow cytometry analysis showing MARCO expression (empty histograms), displayed as mean fluorescence intensity, on the cell-surface ofJEG-3 and THP-1 cells. Surface expression of MARCO in THP-1 cells, which served as a positive control. Negative controls were performed by using an isotype-matched control antibody (black filled histograms). (B) Graphical representation of MARCO surface protein expression in JEG-3 and THP-1 cells. Bar graphs represent the level of each protein in mean values ± SD in each cell line. Data are representative of three independent experiments.

3.2.4 Immunoblot analysis of CD14 and MARCO

Western blotting was performed in order to investigate expression of CD14 and MARCO in whole cell lysates of JEG-3 and THP1 cells. THP-1 cells were used as a positive control, whereas, α-tubulin and β-actin were used as a loading control to normalize the levels of protein detected by confirming that protein loading is the same across the gel. The expression of CD14 and MARCO were confirmed based on the presence of a protein band corresponding to the expected molecular weight. CD14 was detected at 55kDa, and MARCO was detected at 68kDa, as expected (Figure 3.5).
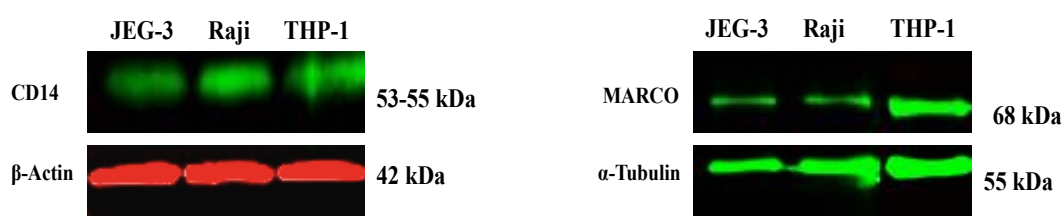
Figure 3.5: Semi-quantitative analysis of the expression of total CD14 and MARCO in JEG-3 cells.

Western blot of JEG-3cells using MEM-18 (anti-CD14), 2G12 (anti-MARCO), and TU-02 (anti-alpha-subunit tubulin) monoclonal antibodies (mAb).MEM-18 is specific for CD14 53-55 kDa, 2G12 is specific for MARCO 68 kDa,Poly6221 detects β-actin, which was detected at a molecular weight of 42 kDa, and TU-02 detects full length α-tubulin. Anti β-actin and antiα-tubulin were used as loading control. A protein band for MARCO was expected to be detected at 68 kDa, and was detected in JEG-3 cells, using the Raji and THP-1 cell line as a positive control. The presence of bands corresponding to the expected molecular weight of CD14 confirmed that JEG-3 cells express CD14, compared to the Raji and THP-1cell line used as a positive control. CD14 was expected to be detected between 53-55 kDa.

3.2.5 Confocal microscopy

Confocal immunofleorescence microscopy was performed in order to obtain graphical evidence of the expression of CD14 and MARCO receptors on JEG-3 cells. To the author's knowledge, the expression of CD14 and MARCO on JEG-3 cells has not been previously studied. THP-I cells were used as a positive control for CD14 and MARCO cell-surface expression, since the two molecules in these cells have been widely studied.

The negative control cells stained with IgG isotype conjugated with either green AF488 or red AF555 secondary antibody, where the blue colour is DAPI stained nucleus (Fig. 3.6). In the images, no signals above background fluorescence were observed thus indicating no false positive signals were detected, furthermore, the morphology of the nucleus indicates that the cells observed are in a healthy state.

Cell surface expression of CD14 receptors on JEG-3 and THP1 cells was visualised by laser scanning confocal microscope (Fig. 3.7). Green fluorescence on both cell lines represents the CD14 receptor expression, where these receptors are uniformly distributed all over the cells. Blue coloured nucleus and differential interference (DIC) images represent the cell health morphology.

Microscopic analysis of MARCO receptor expression in test cell line JEG-3 and in positive control THP1 cell line is shown in figure 3.8. Micrograph of THP1 cell indicates that MARCO receptors are uniformly distribute all over the cell surface, whereas, on JEG-3 cells MARCO receptors are mostly concentrated on Polar Regions. Nucleus and DIC images confirm good cell health and morphology.

THP-1   JEG-3

DIC

DAPI

Secondary
Antibody
AF488

Secondary
Antibody
AF555
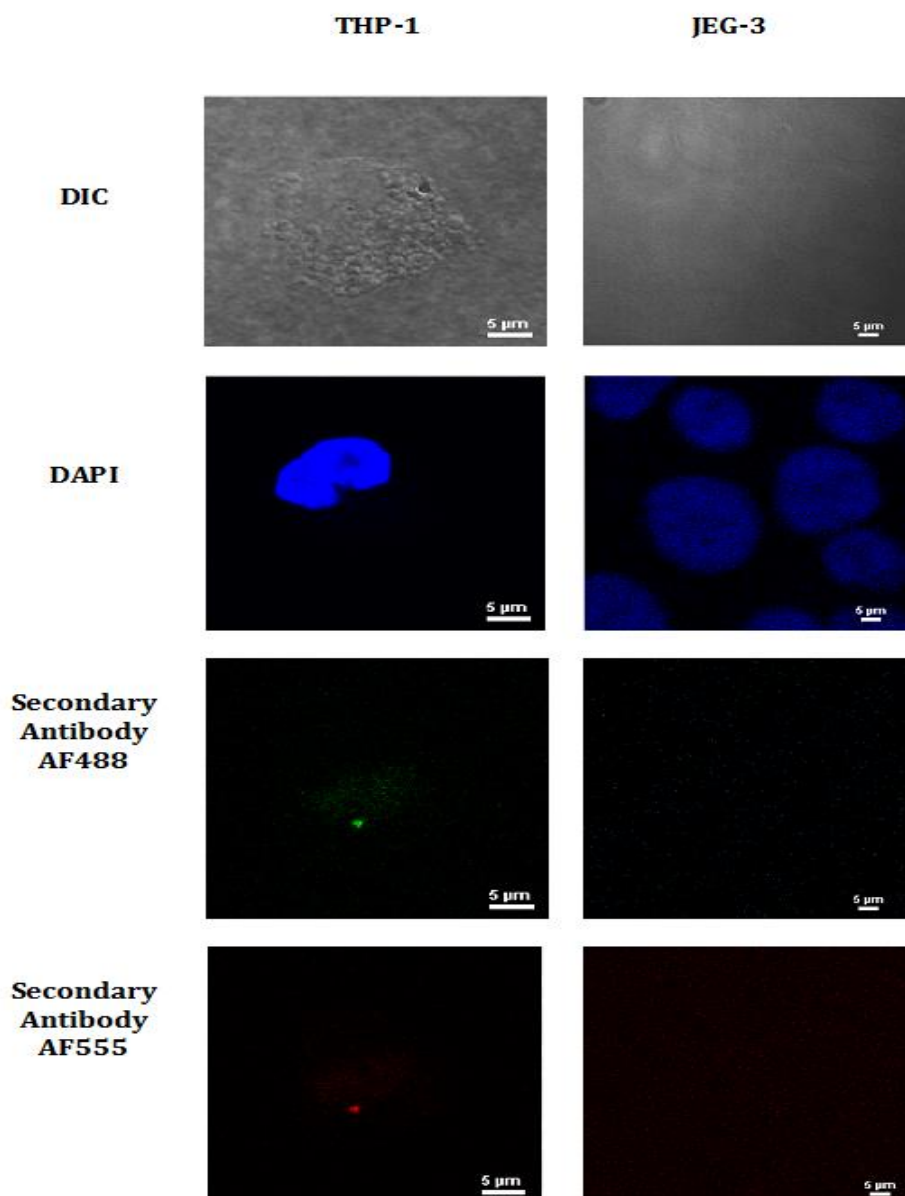
Figure 3.6 Confocal microscopy images of JEG-3 and THP-1 cells as isotype-negative controls.

The isotype control comprised cells stained with isotype control IgG primary and Alexa Fluor® 488 and Alexa Fluor® 555 secondary antibodies. Fluorophores were excited using green 488 nm and red 555 nm wavelength lasers and used to measure non-specific antibody binding. Blue colour shows DAPI stained cell nuclei, red and green show the merged image, whereas DIC is the differential interference contrast image of corresponding cells. Scale bar 5 μm.
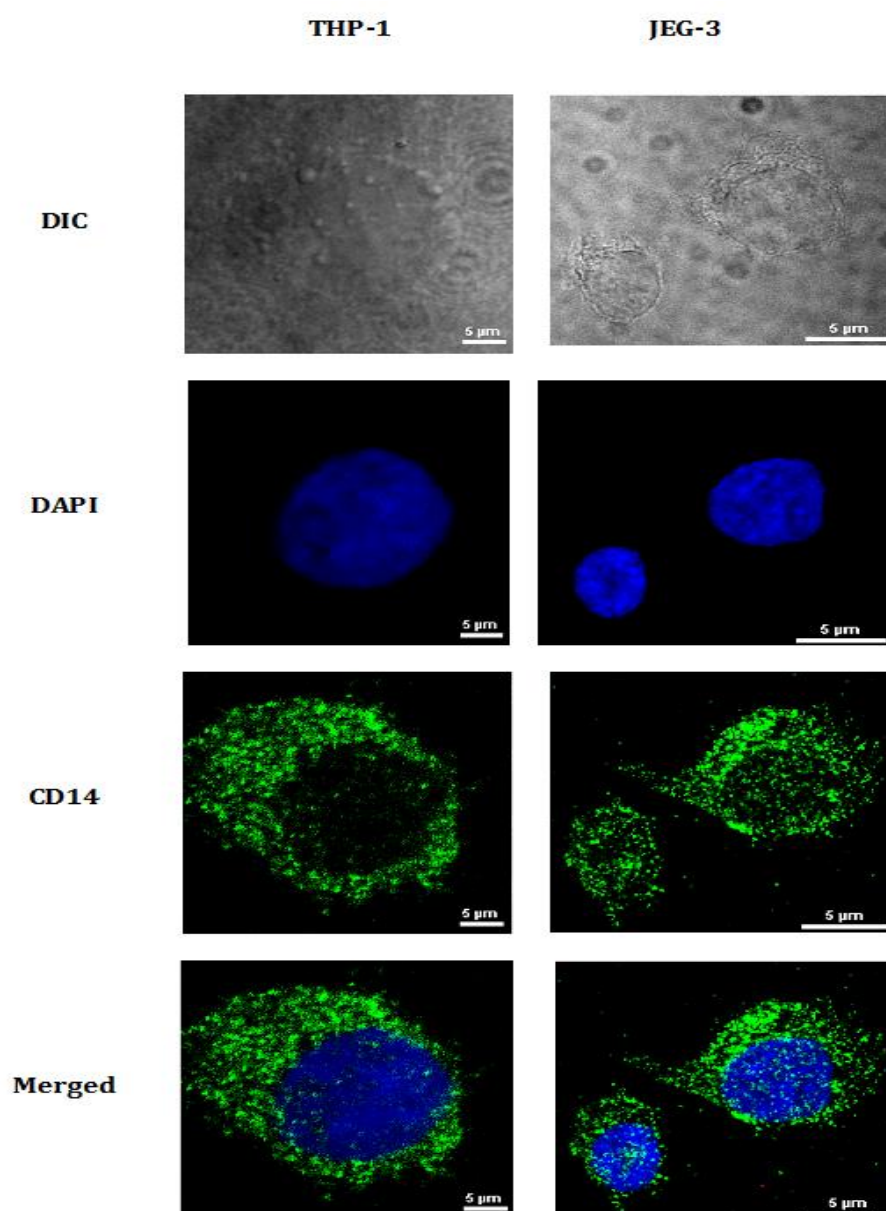
Figure 3.7: Cell-surface staining of CD14 onJEG-3 and THP-1 cells as visualised by confocal laser scanning microscopy.

JEG-3and THP-1 cells were cultured in LabTek 8-well chambers at a density of 3x 10^3 cells per well overnight. Cells were stained with CD14 labelled with Alexa Fluor® 488 (green). Cell nuclei were stained with 4', 6-diamidino-2-phenylindole (DAPI), which is shown in blue. Photomicrographs are representative of three independent experiments. Scale bar 5µm.
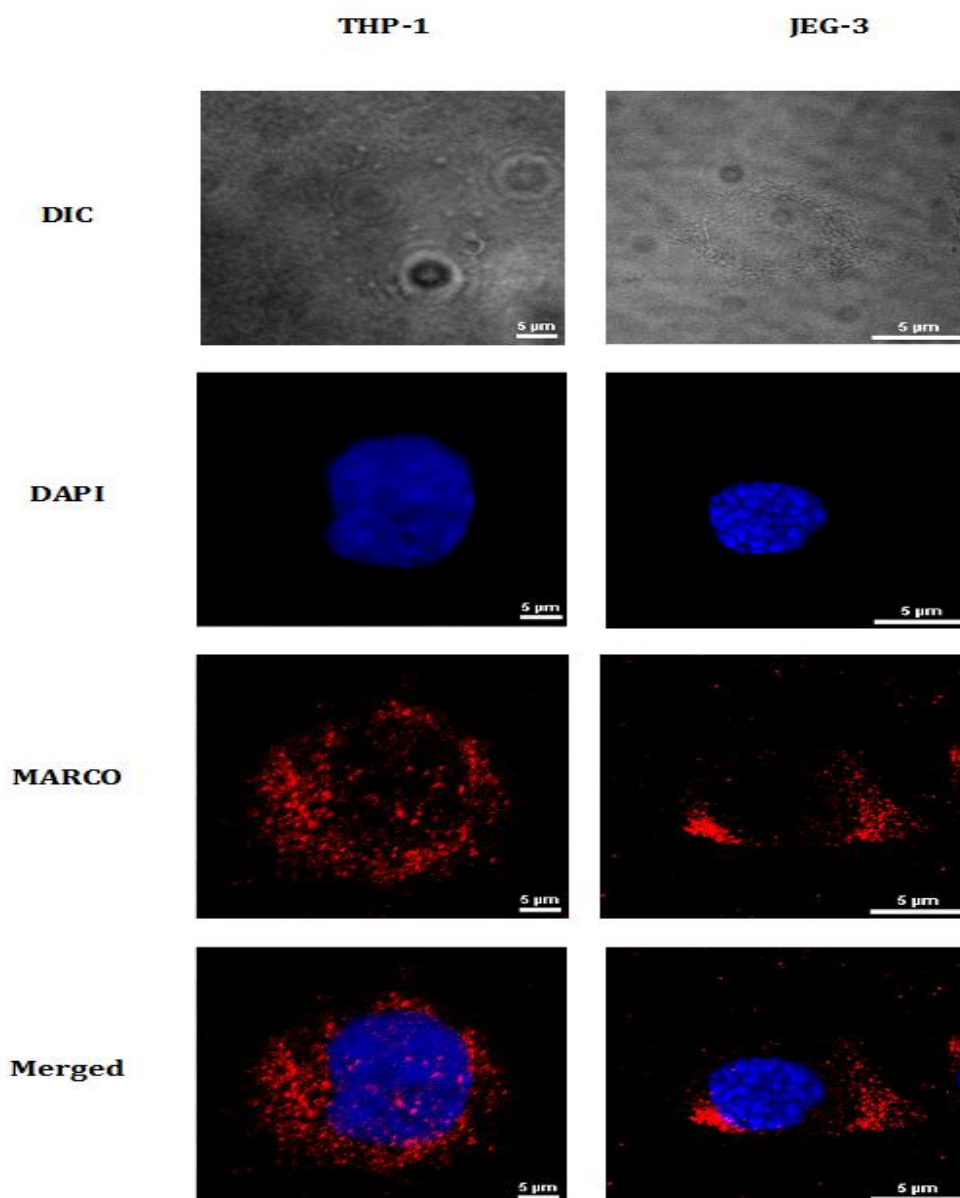
Figure 3.8: Cell-surface staining of MARCO expressed in JEG-3 and THP-1 cells as visualised by confocal laser scanning microscopy.

JEG-3 and THP-1 cells were cultured in LabTek 8-well chambers at a density of $3x\ 10^3$ cells per well overnight. Cells were stained with Alexa Fluor® 555 (red), cell nuclei were stained with 4', 6-diamidino-2-phenylindole (DAPI), which is shown in blue. Photomicrographs are representative of three independent experiments. Scale bar 5µm.

3.2.6 Colocalisation analysis

Colocalisation analysis has been performed to estimate that whether CD14 and Marco receptors are closely associated and interacting each other. For this purpose, firstly, JEG-3 and THP1 cells were double stained for MARCO and CD14 receptors. Cells were then imaged by laser scanning confocal microscope at single cell level using sequential scanning for each wavelength, which avoids bleed through between red and green channels. In the micrograph, green colour represents CD14; red colour represents MARCO, whereas yellow colour in merged images indicates close association of MARCO and CD14 receptors (Fig. 3.9).

 In this study, two different methods to measure the colocalisation have been employed.

    a) Pearson's correlation coefficient for colocalisation

    b) Sparse colocalisation

3.2.6a. Pearson's correlation coefficient for colocalisation

Pearson's correlation coefficient (PCC) for colocalisation was performed by using Colocalisation threshold plugin in ImageJ with auto threshold settings. Three dimensional microscopic images were used for the analysis and value of PCC indicates the correlation between CD14 and MARCO receptors. Composites of merged red and green channels and their scatter plots are shown in figure 3.10. In THP1 cell line PCC value is 0.925, thus indicating strong positive correlation between CD14 and MARCO receptors. In JEG-3 cells, PCC value is 0.737, thus reflecting a strong positive association between the two receptors.
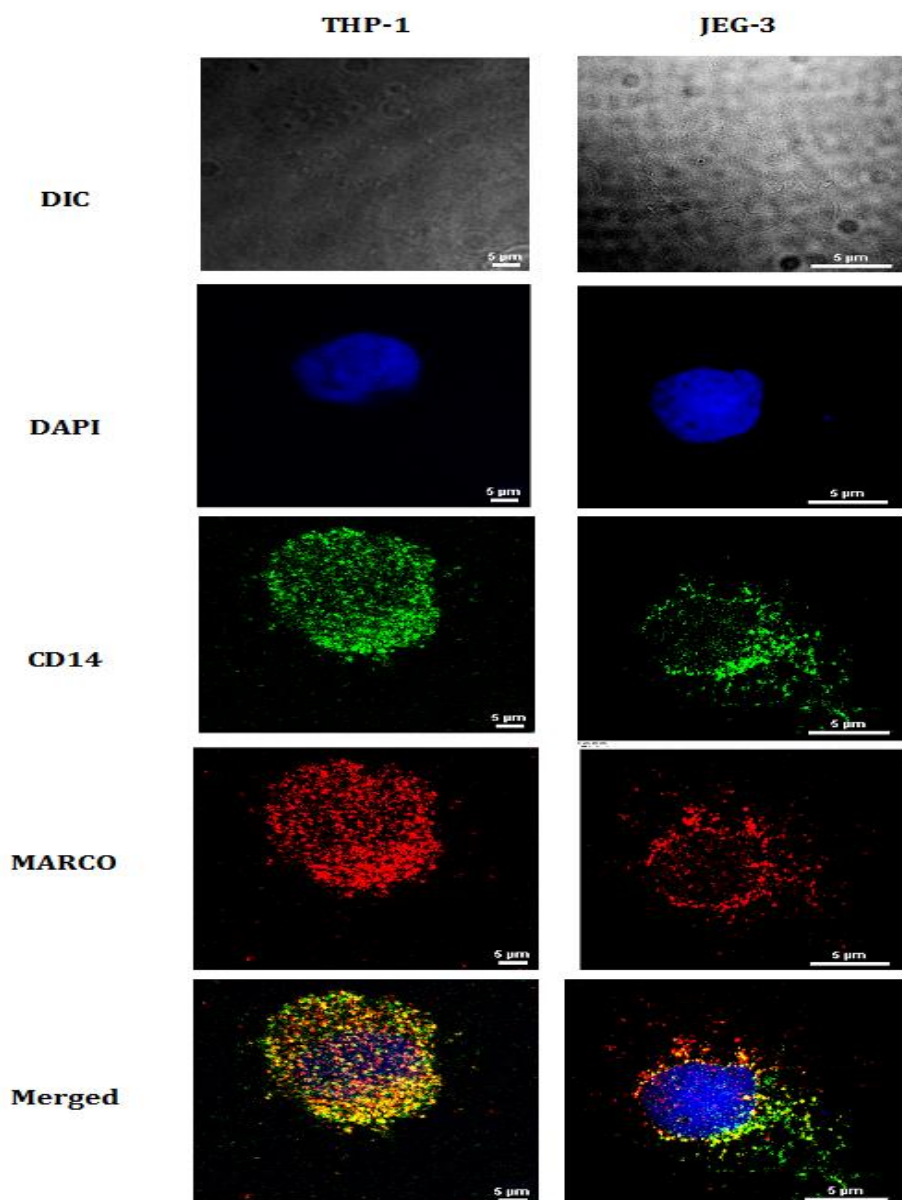
Figure 3.9: Colocalisation of CD14 and MARCO on the cell-surface of JEG-3 cells.

Colocalisation of CD14 and MARCO on the cell-surface of JEG-3 cells and THP-1 is shown. JEG-3 cells and THP-1 were double stained with CD14 primary antibody labelled with (FITC) Alexa Fluor® 488 (green) or with MARCO primary antibody labelled with (TRITC) Alexa Fluor® 555 (red). Yellow fluorescence in the merged green and red channels indicates the close association of the two receptors.

Cell lines	Composite of Green (CD14) and red (MARCO)	2D Colocalisation Scatter Plot	PCC
THP1			0.925
JEG-3			0.737
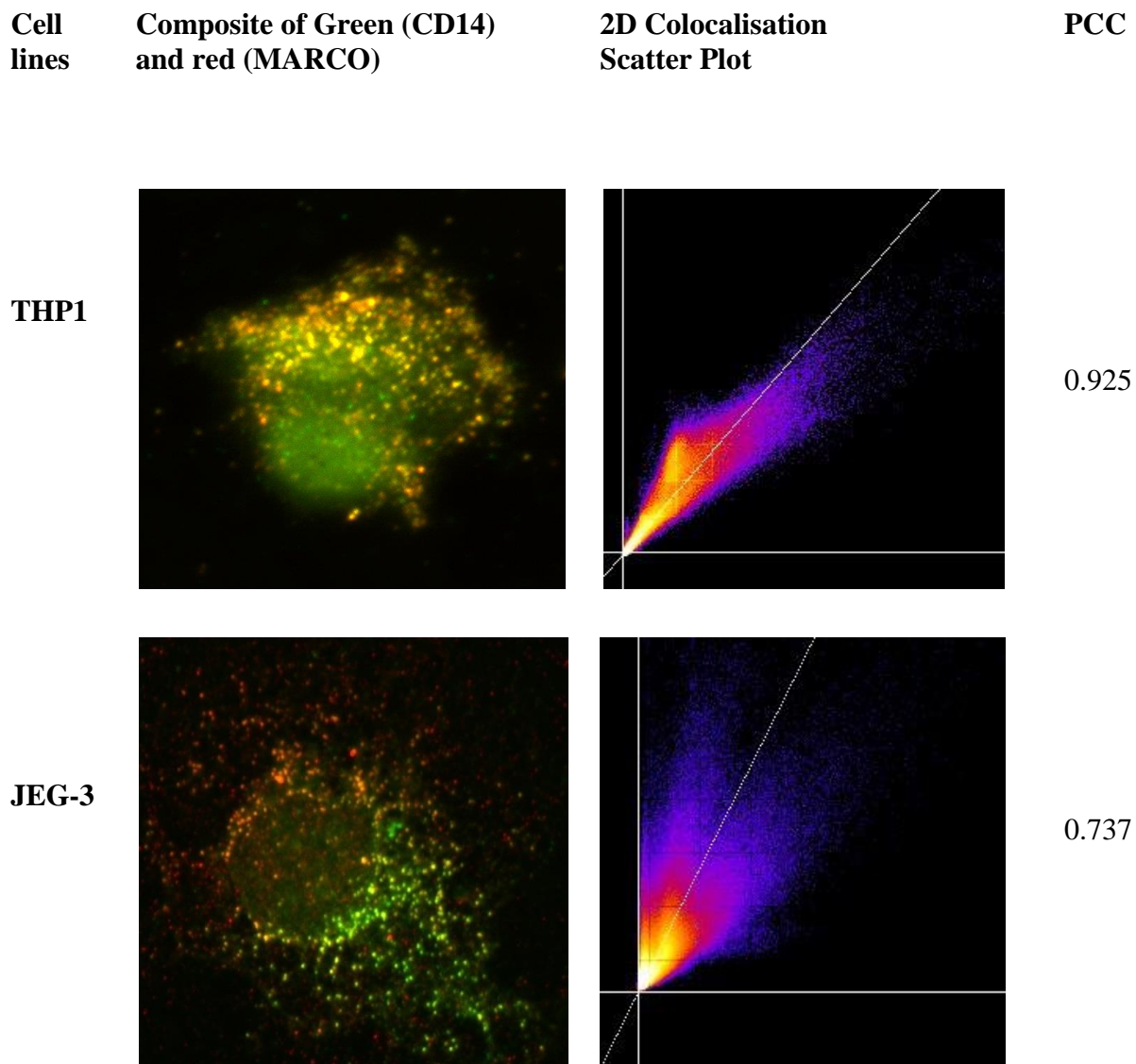
Figure 3.10: Pearson's correlation coefficient (PCC) for colocalisation.

Left column represents composites for red and green merged images. Right column shows 2D scatter plot for colocalised red and green receptors, white diagonal line is best fit for the regression.

3.2.6b. Sparse colocalisation

Sparse colocalisation is an object based quantitative method to estimate the colocalisation of proteins understudy. The cells were immunofluorescent double stained for CD14 and MARCO receptors and three dimensional sequentially scanned images were taken for each wavelength at single-cell level. Cell surface receptors appear as green and red spots in the image (Figure 3.11). Confocal microscopic images of immune receptors tagged with antibodies appeared as masses of spherical blurred spots distributed all over the cell surface. In this study, antibody-labelled surface receptors were imaged separately at different wavelengths, resulting as diffraction-limited isotropic spots of uniform size in each channel. As the resolution is poorer in axial (z) direction than laterally (xy), the three dimensional (3D) receptors appear as cigar-shaped (Figure 3.11). In this study, CD14 receptors are seen as green spots and MARCO receptors as red spots, while yellow spots represent co-expressed CD14 and Marco receptors. In each cell image, the blue colour represents DAPI stained nucleus (Figure 3.11).

For colocalisation analysis, 3D single cell images were first separated for each channel, represented as channel 1 (CD14 receptors) and channel 2 (Marco receptors). Receptors from each channel with varying fluorescent intensity and high background noise were robustly identified by the algorithm. Receptors in channel 1 and channel 2 are identified as green spots and quantified as number of receptors expressed on one cell (Figure 3.12A & B). Identified and quantified green spots in the figure 3.12A represent 229 CD14 receptors, while in figure 3.12B are 83 MARCO receptors.

For identified receptor in each channel, the colocalisation algorithm determines the centre of each ellipsoid, even if they vary considerably in fluorescent intensity and background noise. The radius of each identified spot and level of background noise is determined by the algorithm. Two molecules (one from each channel green and red) are then classified as colocalising if they do

not exceed the user-defined parameter d which is 200nm, the maximum colocalisation distance between the centres. A 3D colocalisation scatter plot is shown in figure 3.13, where green asterisks represent CD14 receptors, red asterisks reflect MARCO receptors, and blue encircled red green asterisks are colocalised MARCO and CD14 receptors.

Sparse colocalisation provided quantitative data for number of colocalised receptors along with distances between centres of two colocalised receptors which are represented in a 3D distance plot (Fig. 3.14). Colour coded distance bar ranging from 20-200nm corresponds to the distance between colocalised receptors (Fig. 3.14 A), and histogram shows frequency of colocalised receptors against the distances between their centres (Fig. 3.14 B).
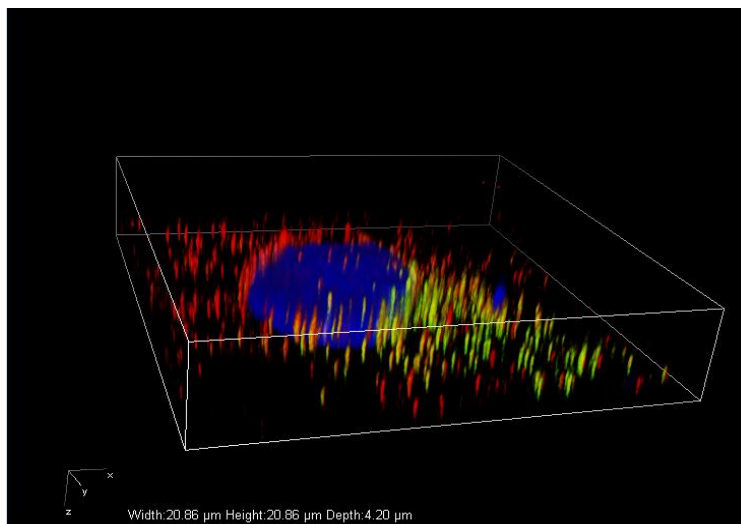
Figure 3.11: Colocalisation of CD14 and MARCO on the cell-surface of JEG-3 cells.

JEG-3 cells and THP-1 cells were cultured in LabTek 8-well chambers at a density of 6x 10^3cells per well overnight. Colocalisation of CD14 and MARCO on the cell-surface of JEG-3 cells is shown. JEG-3 cells were double stained with CD14 primary antibody labelled with (FITC) Alexa Fluor® 488 (green) or with MARCO primary antibody labelled with (TRITC) Alexa Fluor® 555 (red). Colocalisation is shown as yellow fluorescence, the result of merging green and red channels; highly colocalised area of CD14 and MARCO is shown. 3D image was used to analyse the degree of colocalisation. The image is representative of five independent experiments.

A — Particles channel 1 (green): 229
Colocalised (blue): 46

B — Particles channel 2 (green): 83
Colocalised (blue): 46
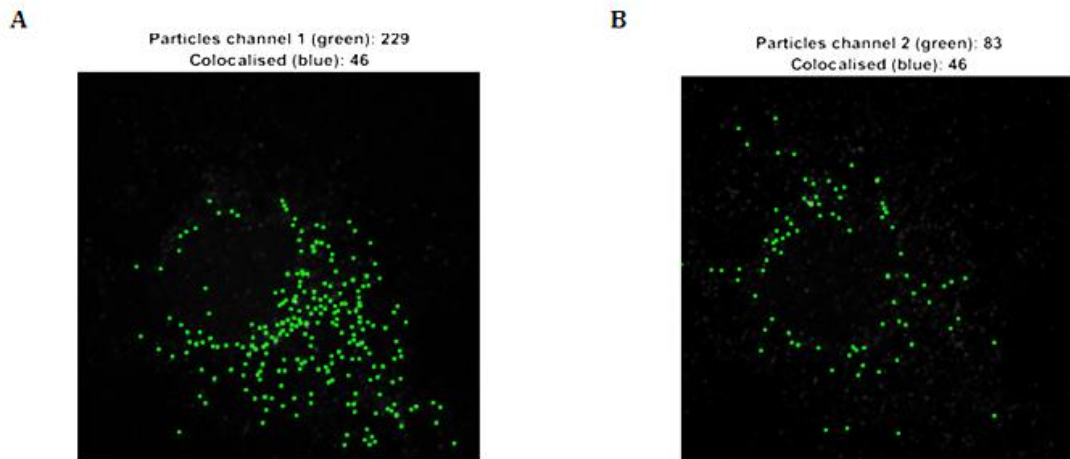
Figure 3.12: Projection images from each channel for sparse colocalisation.

A- Channel 1 represents CD 14 where green spots represent identified and quantified CD14 receptors. B- Channel 2 represents MARCO where green spots represent identified and quantified MARCO receptors.
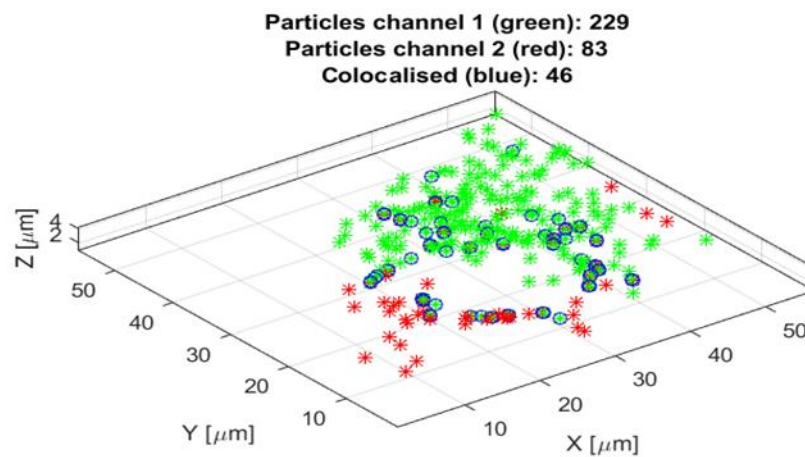
Figure 3.13: Colocalisation 3D scatter plot.

Green asterisks represent CD14 receptors, red asterisks show MARCO receptors, and blue encircled asterisks are colocalised receptors.

A
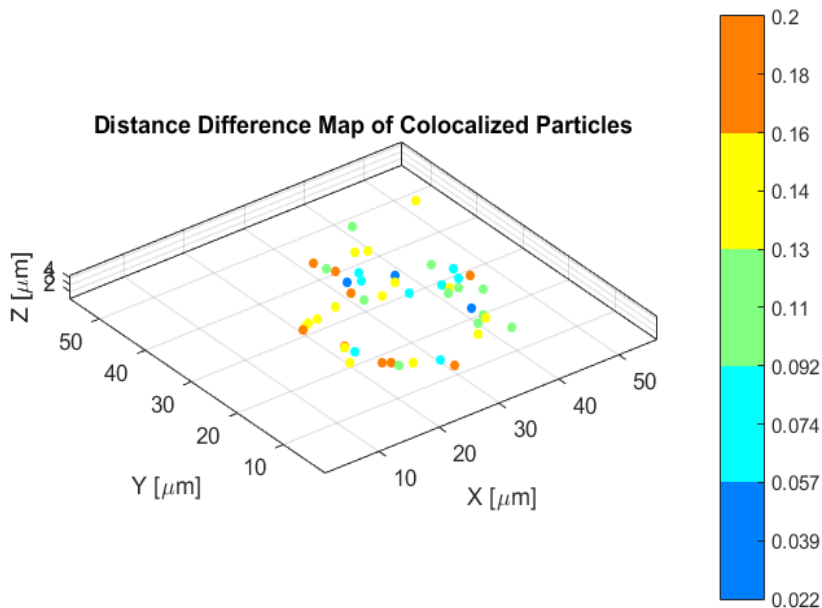
B
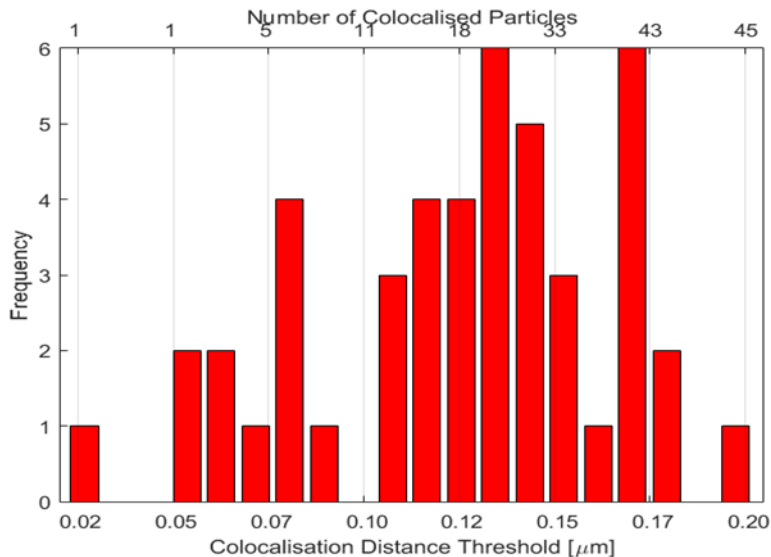
Figure 3.14: Colocalisation distance plot and distance histogram

A. 3D distance plot for colocalised CD14 and MARCO receptors, where coloured bar code represents distance between colocalised receptors. **B.** A histogram graph for intermolecular distance (μm) between colocalised receptors verses number of colocalised receptors.

3.4 Conclusion

Firstly, this study has identified the phenotyping of CD14 and MARCO receptors in JEG-3 choriocarcinoma first trimester trophoblast cells by using flow cytometry, immunoblot analysis and microscopy imaging. CD14 expression has previously been confirmed in monocytes and macrophages (Daigneault, et al., 2010).

MARCO has also not been previously reported to be expressed on trophoblast cells. Human MARCO expression is most robust in the liver, lymph nodes, monocytes and alveolar macrophage, and is mainly involved in the filtration of blood and lymph fluids (Jozefowski et al., 2005).

Secondly, the study detected and quantified the biological interaction of CD14 and MARCO receptors on JEG-3 cells by colocalisation analysis. Further investigation is required to confirm the expression of these receptors on human placental tissues.

Chapter 4

Cell surfaceCD14 and macrophage scavenger receptor MARCO expression on cytotrophoblastic JEG-3 cells after LPS exposure

4.1. Introduction

The feto-maternal interface system has two major roles: promoting the growth and development of the placenta and the maintenance of immunological tolerance and surveillance. Equilibrium must be maintained between them; an imbalance can result in clinical complications such as preeclampsia and pre term labour. Placental cells, particularly trophoblast cells, and classical immune cells (macrophages, natural killer cells, etc.) all have a role in immune surveillance at the maternal-fetal interface.

Foreign pathogens are detected through receptors present on macrophages, known as pattern-recognition-receptors (PRRs). PRRs include Toll-like receptors (TLR), cluster of differentiation (CD) 14 and scavenger receptors (Sankala et al., 2002). PRRs recognize and bind to pathogen-associated molecular pattern (PAMP) molecules that are associated with groups of pathogens, which results in an immunosurveillance response against invading pathogens (Koga et al., 2010). Lipopolysaccharide (LPS), a prototypical PAMP present on the outer membrane of Gram-negative bacteria, is recognized by TLR-4. LPS is a very effective activator of innate immunity, as its lipophillic component and polysaccharide polymer are covalently linked to the membrane-anchor domain in the bacterial outer membrane (Sankala et al., 2002).

CD14, together with TLR-4 and lymphocyte antigen 96 (LY96, or MD-2) acts as a co-receptor for the detection of LPS. CD14 is a 55kDa glycoprotein which is initially processed in the endoplasmic reticulum and then expressed on the cell surface (Gegner et al., 1995). The protein is composed of 375 amino acids and it contains leucin-rich repeats which are significant in PAMP binding (Anas et al., 2010). CD14 exists in two forms: glycosylphosphatidyl-inositol

(GPI)-anchored membrane protein (mCD14) on monocytes and solubleCD14 (sCD14) in plasma (Heidenreich 1999).

Scavenger receptors constitute a family of immunosurveillance receptors. They have been categorised into different subclasses according to their tertiary structure (Thelen et al., 2010). Class A scavenger receptors (SR-As) are a collection of pattern-recognition receptors, and include SR-AI/II, macrophage receptor with collagenous structure (MARCO), scavenger receptor with C-type lectin, and scavenger receptor class A, member 5 (Arredouani et al., 2006). MARCO is suggested to play a role in antimicrobial defence, as indicated by its up-regulation in macrophages during bacterial infections in the liver and spleen (Arredouani et al., 2004). The majority of murine MARCO is expressed by marginal zone macrophages in the spleen, by macrophages of the medullary cord in lymph nodes and by peritoneal macrophages (Granucci et al., 2003). The expression of human MARCO is detected to be most robust in the liver, lymph nodes, and monocytes which are involved in the filtration of blood and lymph fluids (Jozefowski et al., 2005).

This part of in-vitro study is focused on the regulation of CD14 and MARCO receptors upon LPS treatment and also to further study the effect of LPS on their biological association in JEG-3 cells.

AIM OF STUDY

- To investigate the regulation of CD14 and MARCO receptors upon LPS treatment in time and dose dependent manner.
- To study the effect of LPS on colocalisation of CD14 and MARCO receptors.

4.2 Results

4.2.1 Surface CD14 expression on JEG-3 cells following LPS exposure

Flow cytometry analysis of cell surface CD14 was performed on THP-1leukemia cells, and untreated and LPS-treated JEG-3 cells. Cells were treated with LPS in a time and dose-dependent manner. The cells were stained with an appropriate concentration of the primary antibody CD14 (MEM-18) followed by secondary antibody anti-mouse IgG FITC. Unstained cells and isotype cells stained with only the secondary antibody were used as a negative control. Untreated THP-1 cells were used as the positive control.

Flow cytometric analysis of CD14 expression upon time and dose dependent LPS treatment is presented in figure 4.1, where expression of CD14 increased with increasing LPS concentrations and increasing incubation times. This effect can be observed by shifting of empty histogram on log scale x-axis from left to right, as compared to dark filled histogram representing isotype control. The highest expression of CD14 was detected in JEG-3 cells treated with 20 µg/ml of LPS for 12 hours.

Graphical representation of MFI values for CD14 expression is plotted against LPS dose and incubation times in figure 4.2. The graph reflects that CD14 receptors were up regulated with the effect of LPS in both dose and time dependent manner.
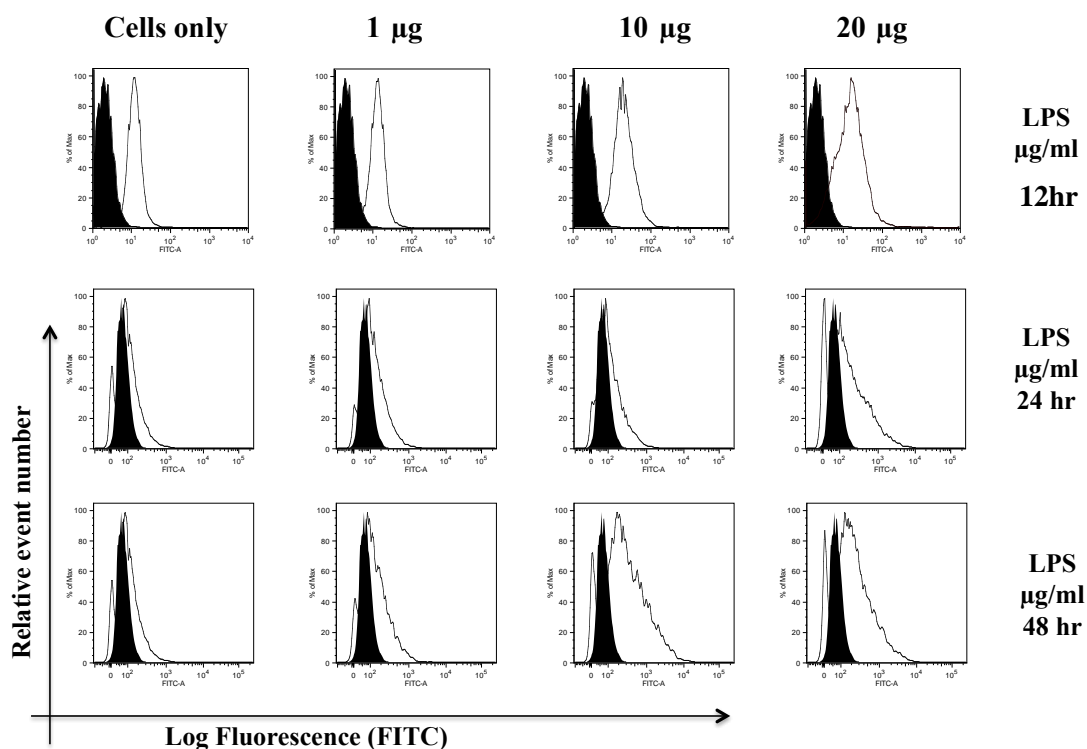
Figure 4.1: Flow cytometric analysis of surface expression of CD14 by JEG-3 cells following time and dose dependent LPS exposure.

JEG-3 cells were cultured in the presence of LPS (1, 10 and 20 ug/ml) for 12 hrs, 24 hrs and 48 hrs. Empty histograms represent the expression of CD14 whereas black-filled histograms show isotype control. Data are representative of three independent experiments.
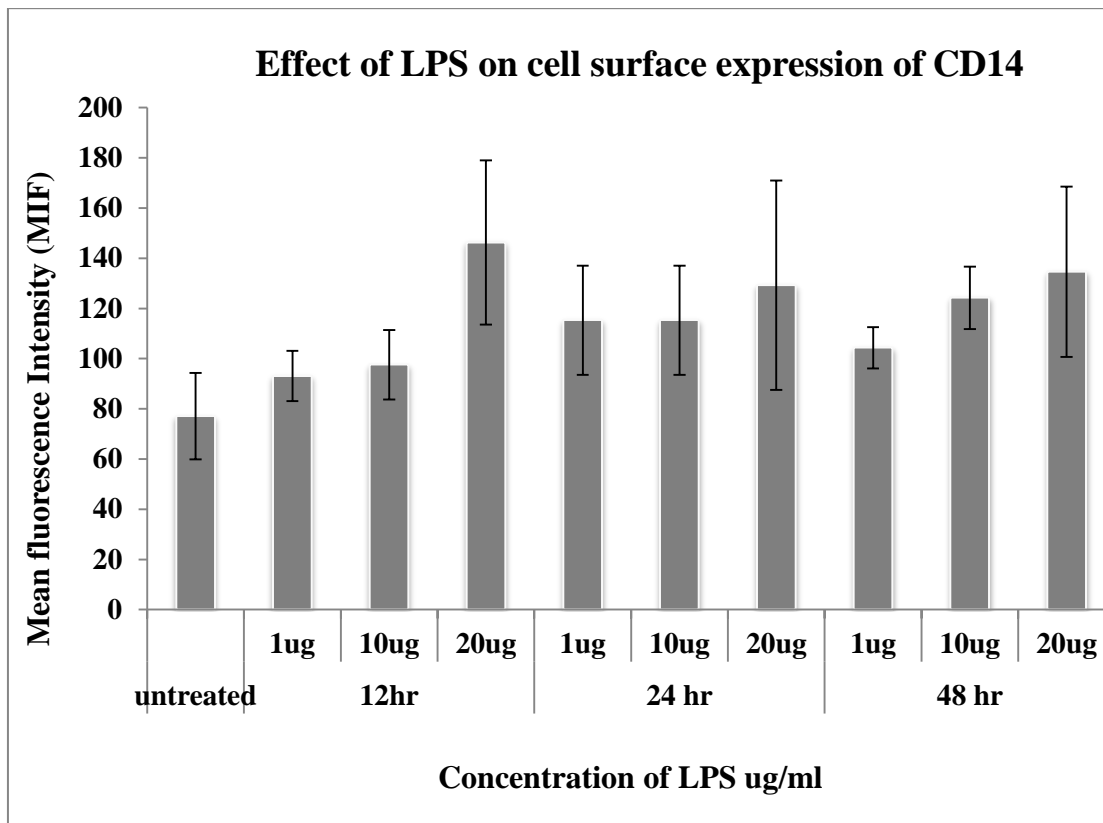
Figure 4.2: Graphical representation of CD14 surface expression in untreated JEG-3 and LPS-treated JEG-3 cells.

Mean fluorescence intensity values were measured based on geometric means. Grey bars represent cell-surface expression of CD14 in untreated and LPS treated JEG-3 cells. ± SD in each treatment group data are representative of three independent experiments.

4.2.2 Cell surface expression of MARCO on JEG-3 cells after LPS exposure

Flow cytometry analysis of cell surface MARCO was performed on untreated and LPS-treated JEG-3 cells. Cells were treated with LPS in a time and dose-dependent manner. The cells were stained with an appropriate concentration of anti-MARCO antibody (clone 2G12), followed by FITC-conjugated secondary antibody. Unstained cells and isotype cells stained with only the secondary antibody were used as a negative control

The results show that the expression of MARCO decreased significantly when JEG-3 cells were treated with LPS in the range of 1, 10, and 20 µg/ml of LPS for a period of 12, 24 and 48 hours (Figure 4.3). The highest expression of MARCO was detected in untreated JEG-3 cells whereas, MARCO receptor expression significantly declined upon LPS treatment in both time and dose dependent manner.

The geometric mean values of MFI for MARCO expression are graphically presented against each treatment group in figure 4.4, which indicates continuous down regulation of this receptor with increasing time LPS doses.

Figure 4.3: Flow cytometric analysis of surface expression of MARCO byJEG-3 cells after LPS exposure.

JEG-3 cells were cultured in the presence of LPS (1, 10 and 20 ug/ml) for 12 hrs, 24 hrs and 48 hrs. Empty histograms represent the expression of MARCO on untreated JEG-3and LPS treated JEG-3 cells, whereas black filled histograms show negative controls. Data are representative of three independent experiments.
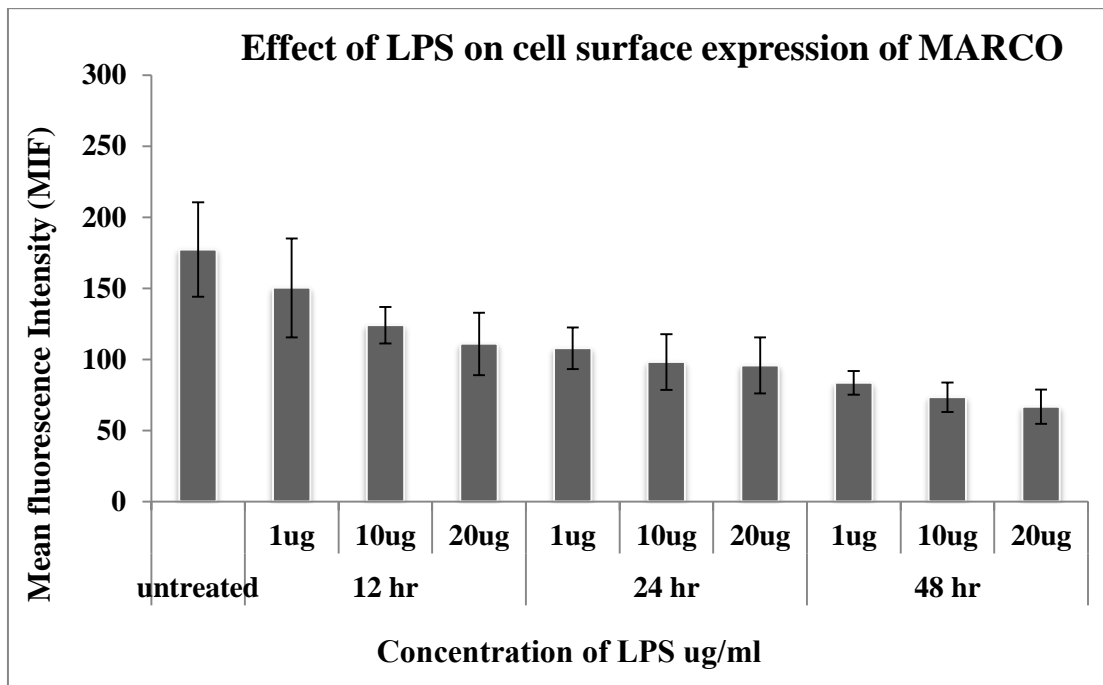
Figure 4.4: Graphical representation of MARCO surface expression in untreated JEG-3 and LPS treated JEG-3 cells.
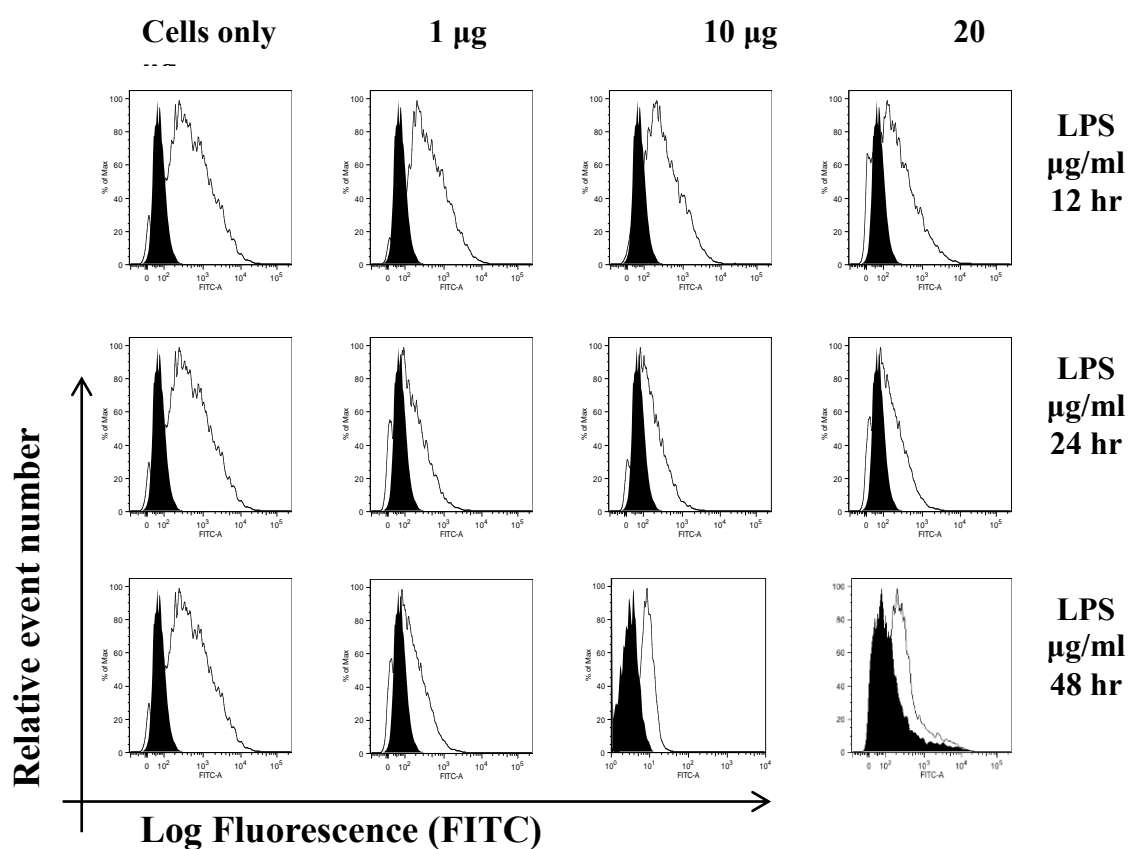
Bar graphs represent the level of MARCO expression in mean values ± SD in each cell line. Data are representative of three independent experiments.

4.2.3 Immunoblot analysis of the effect of LPS on CD14 expression in JEG-3 cells

Western blot analysis was performed in order to investigate CD14 protein expression in   JEG-3 cells after LPS exposure. Cell lysates were prepared from JEG-3 cells cultured in the presence of different concentrations of LPS: 1, 10, 20 μg/ml for 12, 24 and 48 hours. β-actin was used as a loading control to normalise the amount of total protein loaded across the gel. The presence of a 55kDa protein band confirmed the expression of CD14 in JEG-3 cells (Fig. 4.5A). Differential expression of CD14 was observed with increased CD14 expression upon increasing time and LPS doses. The graphical representation of densitometry analysis (Fig. 4.5B) also confirmed the similar pattern of CD14 expression.

A

B

Effect of LPS on the expression of CD14 on JEG-3 cell line
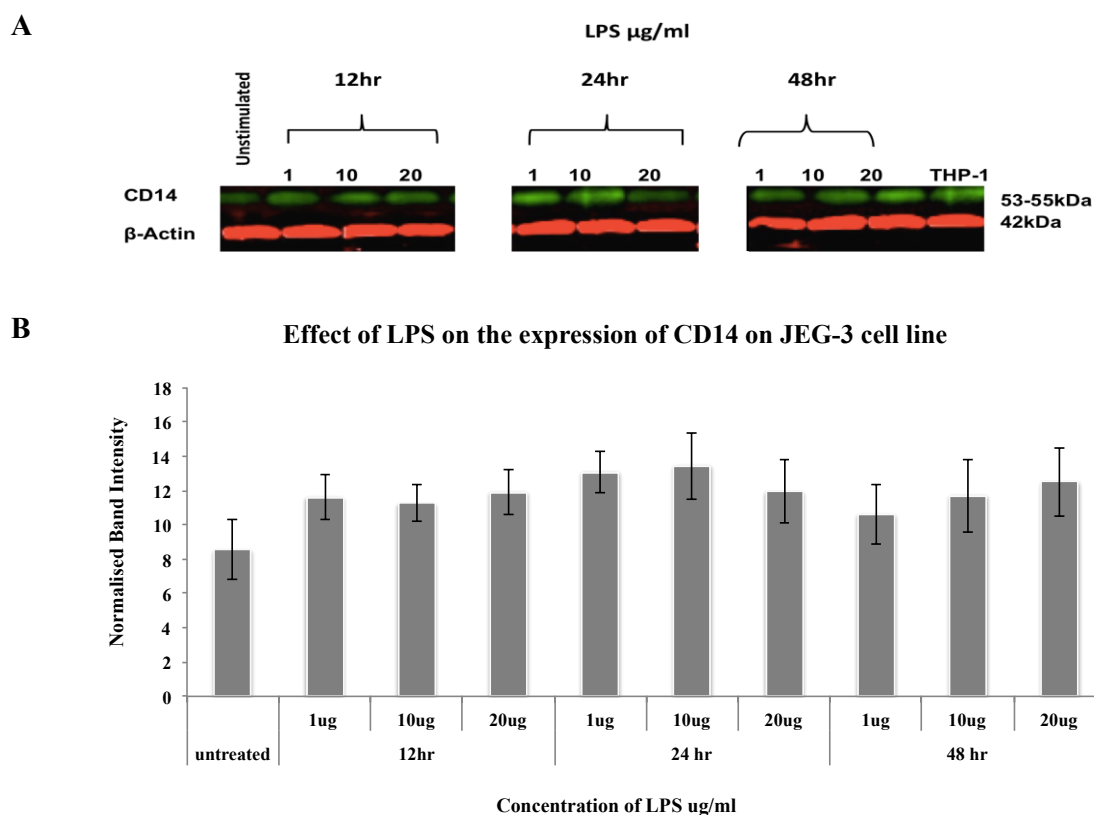
Figure 4.5: CD14 expression by western blot analysis in LPS-treated JEG-3 cell line.

(A) SDS-PAGE (12%) was performed under reducing conditions, followed by Western blotting with primary monoclonal antibodies Poly6221(anti β-actin as loading control) and anti-CD14. β-actin was detected at a molecular weight of 42kDa. The 53-55kDa band that corresponds to CD14 was observed. (B) Relative levels of MARCO in LPS-treated JEG-3 cells. CD14 levels are normalized against β-actin to account for the difference in protein loading during the experiment. The percentage of regulation was calculated after the intensity of each band was adjusted according to its respective β-actin band intensity using Image Studio Lite software (LI-COR Biosciences). A representative immunoblot of three independent experiments is shown.

4.2.4 Immunoblot analysis of the effect of LPS on MARCO expression in JEG-3 cells

Western blot analysis was performed in order to investigate MARCO protein expression in JEG-3 cells after LPS exposure. Whole cell lysates were prepared from JEG-3 cells cultured in the presence of different concentrations of LPS: 1, 10, and 20 μg/ml for 12, 24 and 48 hours. α-tubulin was used as a loading control to normalise the amount of total protein loaded across the gel. The presence of a 68 kDa protein band confirmed the expression of MARCO in JEG-3 cells (Fig. 4.6A). Differential expression of MARCO was observed with decreased MARCO expression upon increasing incubation times and LPS doses. The graphical representation of densitometry analysis (Fig. 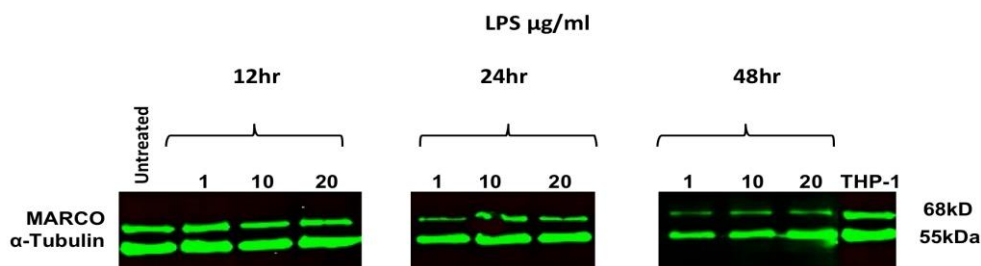4.6B) also confirmed the similar pattern of CD14 expression. Thus, MARCO expression was down regulated upon time and dose dependent LPS treatments.

A

B
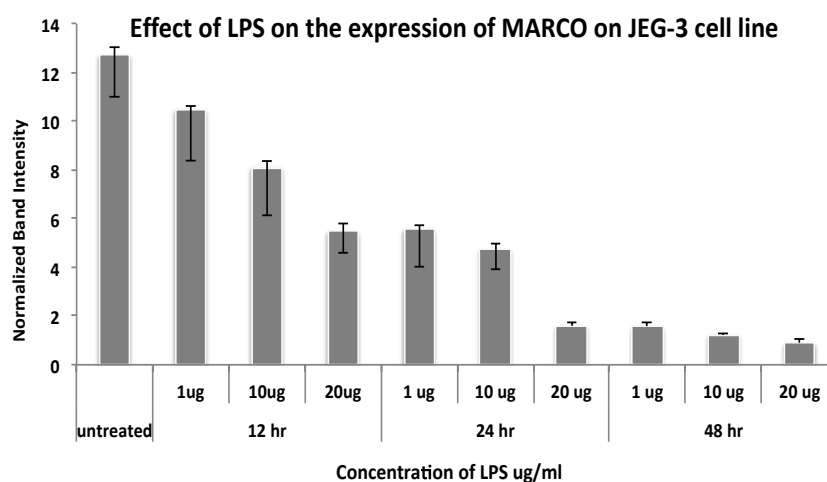
Figure 4.6: MARCO expression by western blot analysis in LPS-treated JEG-3 cell line.

 (A) SDS-PAGE (12%) was performed under reducing conditions, followed by Western blotting with primary monoclonal antibodies TU-02 (anti α-Tubulin as loading control) and anti-MARCO. α-tubulin was detected at a molecular weight of 55 kDa. The 68 kDa band corresponds to MARCO protein. **(B)** Relative levels of MARCO in LPS-treated JEG-3 cells. MARCO levels are normalized against α-tubulin to account for the difference in protein loading during the experiment. The percentage of regulation was calculated after the intensity of each band was adjusted according to its respective α-tubulin band intensity using Image Studio Lite software (LI-COR Biosciences). Comparison of MARCO expression in untreated and LPS-treated JEG-3 cells was assessed using densitometry analysis. A representative immunoblot of three independent experiments is shown.

4.2.5 Confocal microscopy analysis of CD14 and MARCO

Confocal immunofluroscence microscopy was performed to obtain graphical evidence for the expression of CD14 and MARCO receptors on JEG-3 cells incubated with 1, 10 and 20 µg/ml LPS concentrations at 12 hours (Fig. 4.7), 24 hours (Fig. 4.8) and 48 hours (Fig 4.9) time points.. In each micrograph, green colour indicates CD14, and red colour represents MARCO receptors. Colocalisation of MARCO and CD14 receptors in each treatment condition was calculated by measuring Pearson correlation coefficient, where PCC values are provided under PCC column next to each micrograph. The general trend observed in this data was, MARCO and CD14 receptor colocalisation was decreased with increasing LPS doses and increased incubation times. At 12 and 24 hour time points, there is no significant difference in PCC values between different LPS concentrations, whereas, at 48 hour time point PCC values decreased with increasing LPS concentration. Thus considering aforementioned trends in CD14 and MARCO expression in response to LPS, the decreased colocalisation could be due to decreased MARCO expression and lower MARCO to CD14 ratios in 48 hours treatment group.
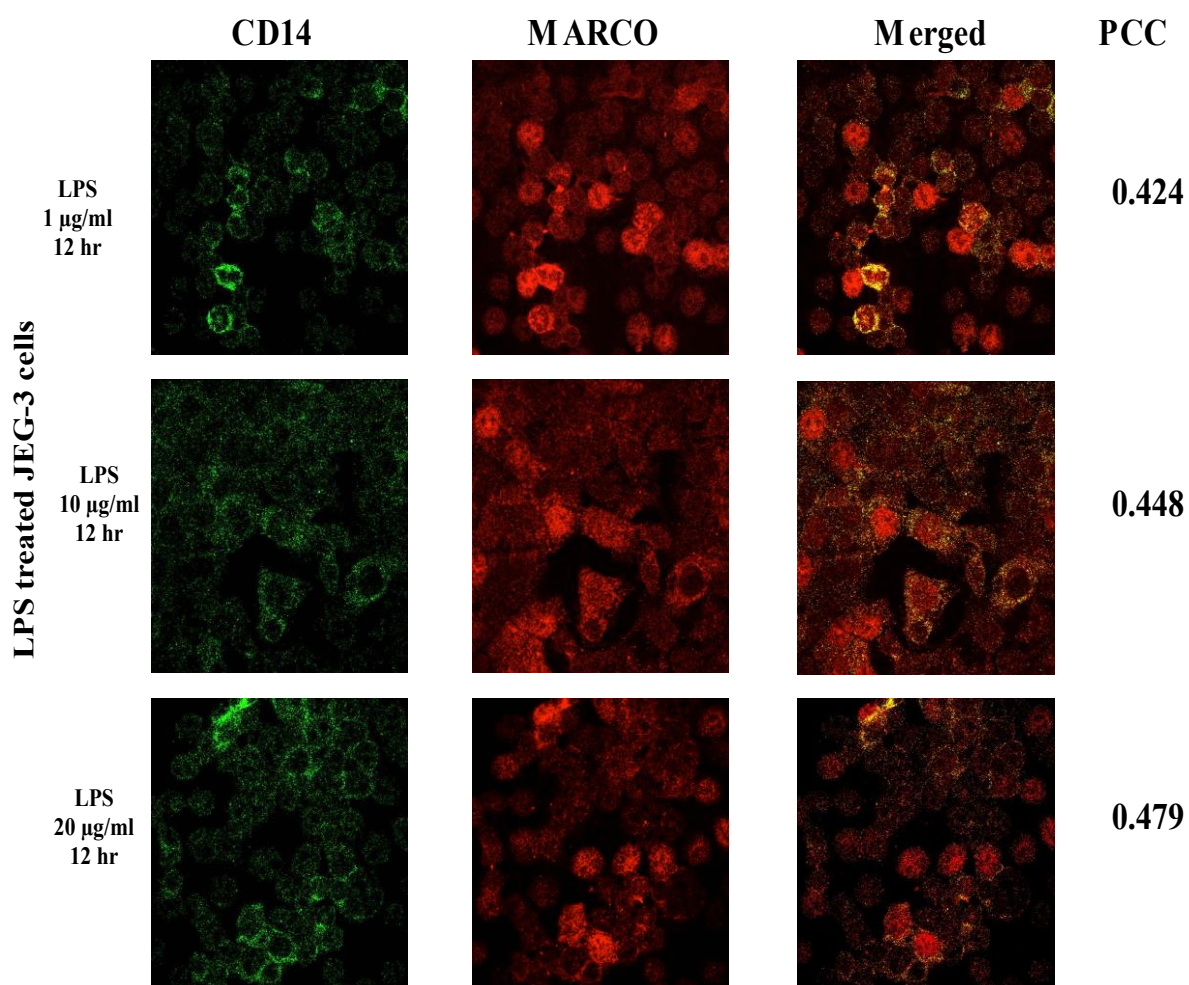
Figure 4.7: Colocalisation of CD14 and MARCO receptors on JEG-3 cells at 12 hours. (Objective x60).

JEG-3 cells were cultured in LabTek 8-well chambers at a density of 8×10^3 cells per well. JEG-3 cells were treated with LPS (1µg/ml, 10µg/ml, 20µg/ml,) for 12 hours. The area of colocalisation is indicated by merged images of the individual receptors. Highly colocalised areas between CD14 and MARCO are indicated in yellow. Pearson correlation coefficient (PCC) was used to analyse the percent of colocalisation.
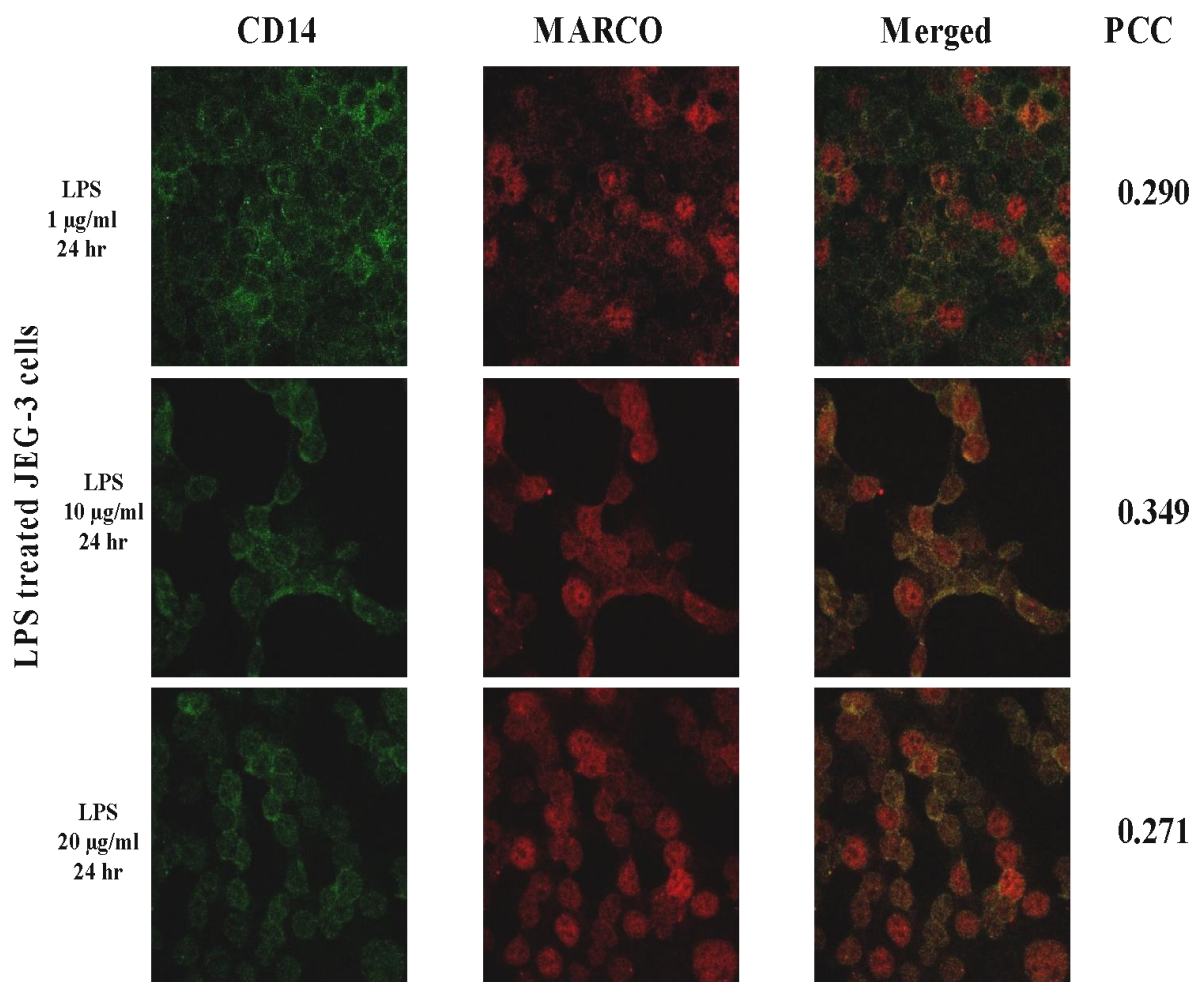
Figure 4.8: Colocalisation of CD14 and MARCO receptors on JEG-3 cells at 24 hours. (Objective x60).

JEG-3 cells were cultured in LabTek 8-well chambers at a density of 8 x 10^3 cells per well. JEG-3 cells were treated with LPS (1µg/ml, 10µg/ml, 20µg/ml,) for 24 hours. The area of colocalisation is indicated by merged images of the individual receptors. Highly colocalised areas between CD14 and MARCO are indicated in yellow. Pearson correlation coefficient (PCC) was used to analyse the percent of colocalisation.
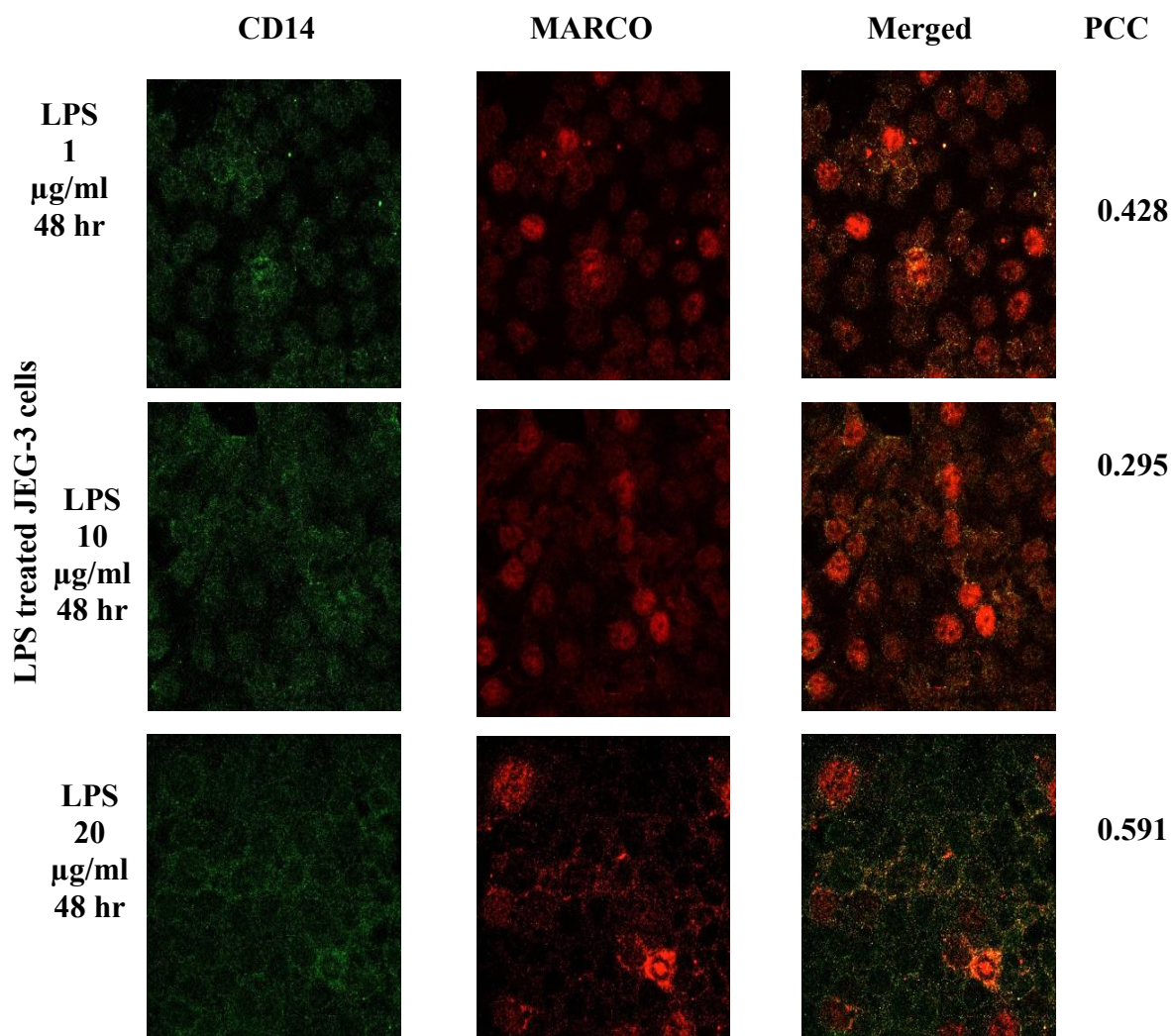
Figure 4.9: Colocalisation of CD14 and MARCO receptors on JEG-3 cells at 48 hours. (Objective x60).

JEG-3 cells were cultured in LabTek 8-well chambers at a density of 8 x 10^3 cells per well. JEG-3 cells were treated with LPS (1µg/ml, 10µg/ml, 20µg/ml,) for 48 hours. The area of colocalisation is indicated by merged images of the individual receptors. Highly colocalised areas between CD14 and MARCO are indicated in yellow. Pearson correlation coefficient (PCC) was used to analyse the percent of colocalisation.

4.3 Conclusion

This part of study has investigated surface CD14 and MARCO expression on JEG-3 cells following their exposure to LPS in time and dose dependent manner. The results of the flow cytometric and immunoblot analyses showed that surface expression of CD14 is increased upon treatment with different concentrations of LPS for different periods of time. In contrast to CD14, MARCO expression was down regulated upon increasing LPS doses and treatment times.

Biological interaction of MARCO and CD14 receptors was unaffected at 12 and 24 hours for all three concentrations, but was decreased at 48 hours with increasing LPS concentration. This phenomenon could be due to decreased MARCO to CD14 receptors ratio. Further investigations and validation studies for these findings are needed in trophoblast tissues.

Chapter 5

 Analysis of cell proliferation, Myoferlin and VEGF expression and NF-κB on the human choriocarcinoma cell line JEG-3 in response to Lipopolysaccharide

5.1 Introduction

In an attempt to investigate the molecular effects resulting from trophoblast infections, a part of this study was focused on trophoblast cell proliferation and activation of the nuclear factor kappa-light-chain-enhancer of activated B cells (NF-κB) activation. Cell proliferation is a crucial factor for the immune system. It is also essential for extravillous trophoblast (EVT) cells, contributing to embryo implantation, invasion into the maternal uterine wall and a successful pregnancy.

Myoferlin is a protein associated with the stability and function of the vascular endothelial growth factor (VEGF) receptor 2 (Bernatchez et al., 2007). Its reduced expression can be a reason for reduced cell proliferation. The effect of LPS on Myoferlin on trophoblast cells has not been elucidated.

NF-κB is a protein complex that regulates DNA transcription. NF-κB is involved in several cellular responses against a range of stimuli including LPS stimulation from bacterial infection, cytokines and viral antigens (Gilmore, 2006). NF-κB is therefore a crucial factor in regulating the immune response to infection. The role of NF-κB in regulating transcription on trophoblast cells has not been addressed. It is reasonable to assume that incorrect regulation of NF-κB would influence the function of trophoblast cells during pregnancy. In non-pregnant settings NF-κB has been linked to inflammatory and autoimmune diseases, septic shock, viral infection, and improper immune development (Perkins, 2007).

With regard to the role of LPS during pregnancy, it is known that LPS ligation to TLR-4 can

signal via both MyD88-dependent and -independent pathways (Akira and Hoshino, 2003) and provoke first trimester trophoblast cells to produce high levels of cytokines, includingIL-2, IL-6, TNF-α and IFN-γ (Abrahams et al., 2004). These studies highlight the sensitivity of trophoblast cells multiple cytokines. Interestingly, placental expression of IFN-γ and TNF-α has been associated with trophoblast cell apoptosis (Aschkenazi et al., 2002; Yui et al., 1994). Thus, regulation of the cytokine repertoire during pregnancy is of pivotal importance.

In this section of the project the expression profile of Myoferlin and VEGF antigens on JEG-3 cells and their role in cell proliferation was examined in response to LPS. Furthermore, cell proliferation and NF-κB activation assays were performed to investigate the effect of LPS on trophoblast cell physiology.

5.2 Results

5.2.1 Myoferlin analysis in JEG-3 cells

Flow cytometry analysis of Myoferlin expression was performed on untreated and LPS-treated JEG-3 cells as explained in section 2.2.2. Cells were treated with LPS in a time and dose-dependent manner. The cells were stained with an appropriate concentration of the primary antibody (FER1L3) specific for Myoferlin followed by secondary antibody (RAM-FITC). JEG-3 cells were incubated with 1, 10 and 20 µg/ml of LPS for 12, 24 and 48 hours. Unstained cells and cells stained with only the secondary antibody were used as a negative control.

Moderate level of expression of Myoferlin on the plasma membrane was observed, in the untreated JEG-3 cells (Fig 5.1 A). Myoferlin expression was down-regulated following treatment with LPS in both the dose 1, 10, 20, µg/ml and time 12, 24 and 48 hours, dependent manner (Figure 5.1 B). The decrease in the flow cytometry histogram can be observed by shift of dotted line histogram towards left, more towards negative control isotype solid line histogram, thus indicating decrease in the mean fluorescent intensity of myoferlin. The lowest expression of myoferlin was detected in JEG-3 cells treated with 20 µg/ml of LPS at all time points. JEG-3 cells treated with 20 µg/ml of LPS for 48 hours showed the least expression of Myoferlin (Fig. 5.1 B).

Myoferlin expression levels are also presented quantitatively in the bar graph (Fig. 5.2), where MFI is plotted against LPS treatment conditions. The decrease in MFI (grey bars) indicates that the expression of Myoferlin was down-regulated after exposing the cells to LPS. Down regulation of myoferlin in response to LPS is highly significant as compared to untreated group.

Figure 5.1. Flow cytometry analysis of surface expression of Myoferlin (FER1L3)

JEG-3 cells were cultured in the presence of different concentrations of LPS (1, 10 and 20 µg/ml) for 12, 24and 48 hrs. Dotted outlined histograms represent the expression of Myoferlin on untreated and LPS treated JEG-3 cells, whereas straight outlined histograms show negative controls. Cells were labelled with a FITC-conjugated secondary anti-mouse antibody. Data is representative of three independent experiments.

A
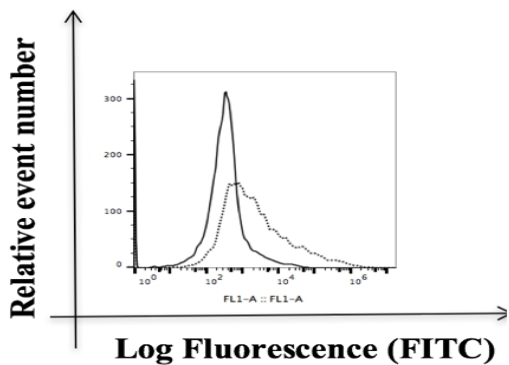
B
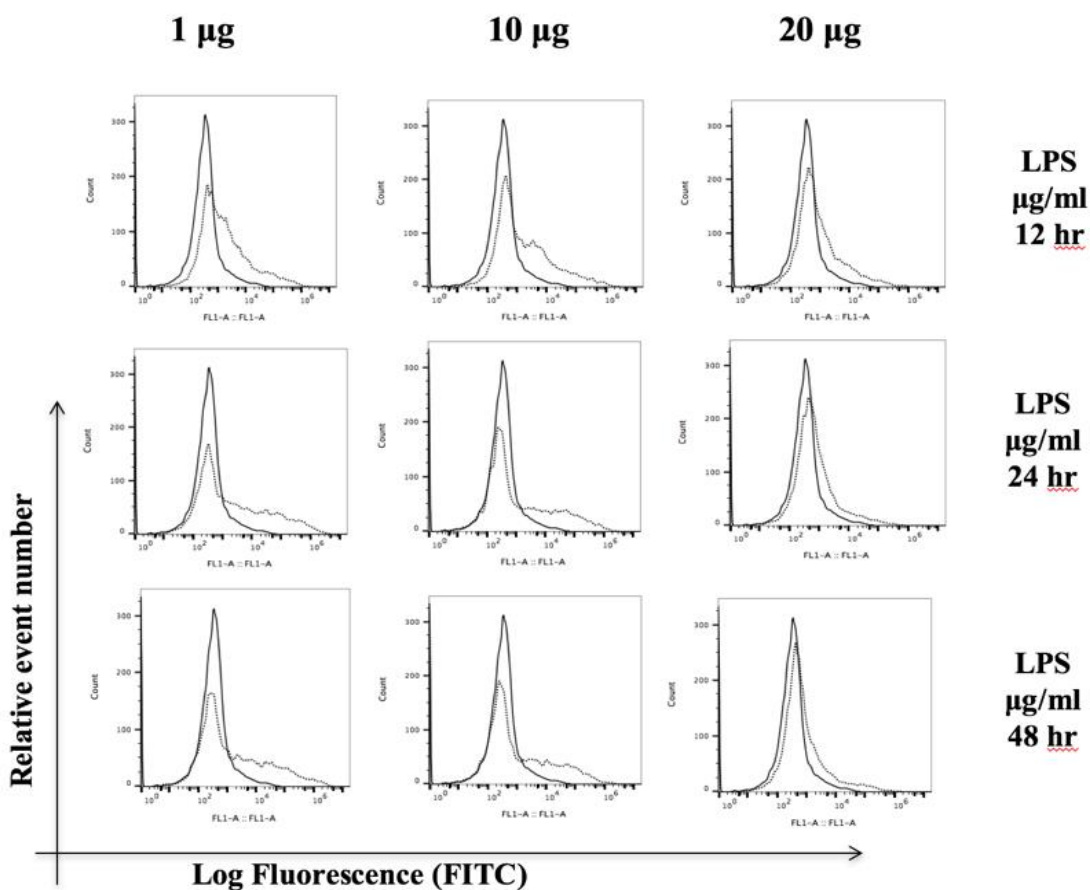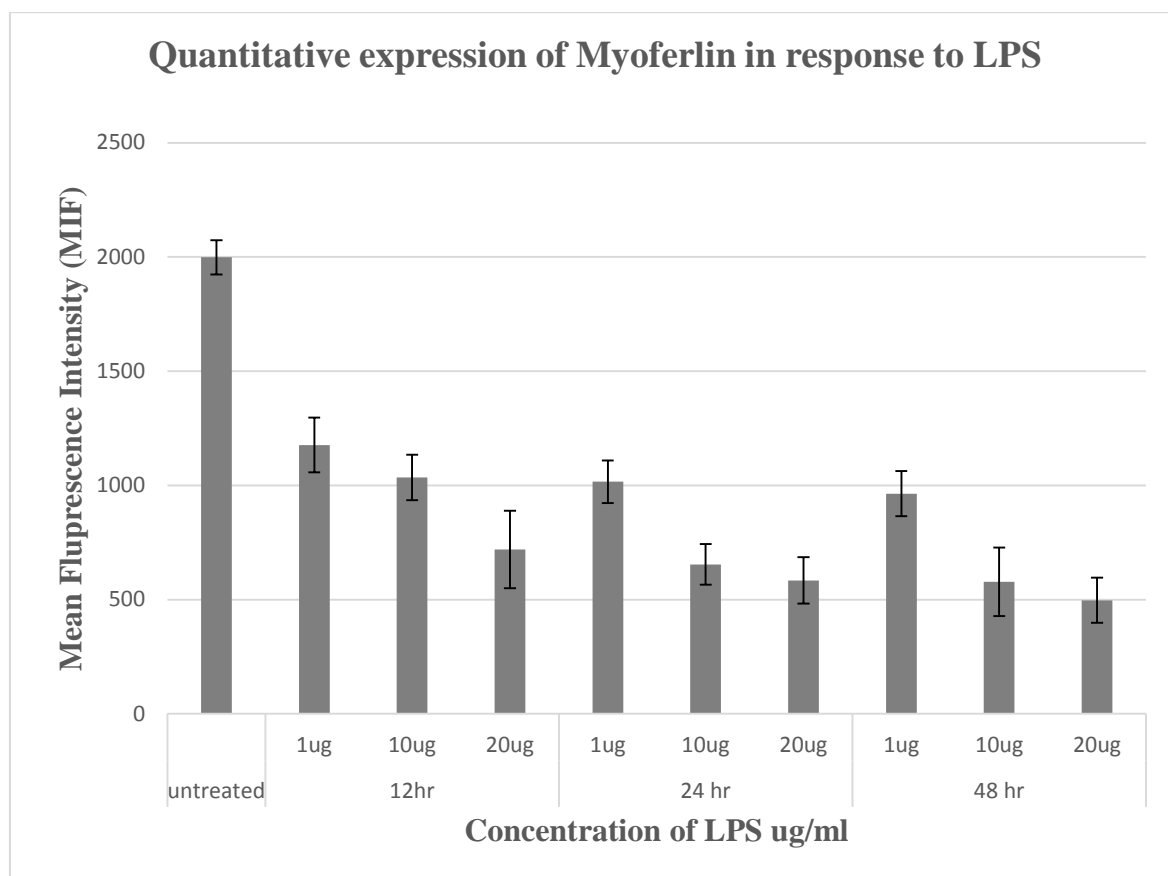
Figure 5.2. Quantitative representation of Myoferlin surface expression in untreated JEG-3 and LPS treated JEG-3 cells.

Myoferlin expression levels on JEG-3 cells were analysed on a BD Accuri flow cytometer and FlowJo 8.8.6 software. Mean fluorescence intensity values were measured based on geometric means. Grey bars represent cell-surface expression of Myoferlin in untreated and LPS treated JEG-3 cells. Bar graphs represent the level of Myoferlin expression in mean values ± SD. Data are representative of three independent experiments.

5.2.2 VEGFR-2analysis in JEG-3 cells

Flow cytometry analysis of VEGFR-2 expression was performed on untreated and LPS-treated JEG-3 cells in a time and dose-dependent manner. The cells were stained with an appropriate concentration of the primary antibody VEGFR-2 followed by secondary antibody anti-mouse IgG FITC. Unstained cells and cells stained with only the secondary antibody were used as a negative control. Untreated JEG-3 cells were used as the positive control or reference group.

Analysis of the data revealed moderate to weak level of expression of VEGFR-2 receptors on JEG-3 cells in comparison to the isotype negative control (Fig. 5.3 A). The expression of VEGFR-2 decreased when treated with LPS in a dose and time dependent manner (Fig 5.3 B). The decrease in the flow cytometry histogram can be observed by shift of dotted line histogram towards left, more towards negative control isotype grey filled histogram, thus indicating decrease in the mean fluorescent intensity of VEGFR-2. Like aforementioned myoferlin data in section 5.2.1, the lowest expression of VEGFR-2 was noticed in JEG-3 cells treated with 20 µg/ml of LPS for all time points. JEG-3 cells treated with 20 µg/ml of LPS for 48 hours showed the least expression of VEGFR-2 (Fig. 5.3 B).

VEGFR-2 expression levels are also presented quantitatively in the bar graph (Fig. 5.4), where MFI is plotted against LPS treatment conditions. The decrease in MFI (grey bars) indicates that the expression of VEGFR-2 was down-regulated after exposing the cells to LPS. Down regulation of VEGFR-2 in response to LPS is highly significant as compared to untreated group.

Figure 5.3. Flow cytometry analysis of surface expression of VEGFR-2 by JEG-3 cells following LPS exposure.

JEG-3 cells were cultured in the presence of the indicated concentrations of LPS (1, 10 and 20 ug/ml) for 12, 24 and 48 hrs. Empty histograms represent the expression of VEGFR-2on untreated JEG-3 and LPS treated JEG-3 cells, whereas grey histograms show negative controls. Data is representative of three independent experiments.

A

B
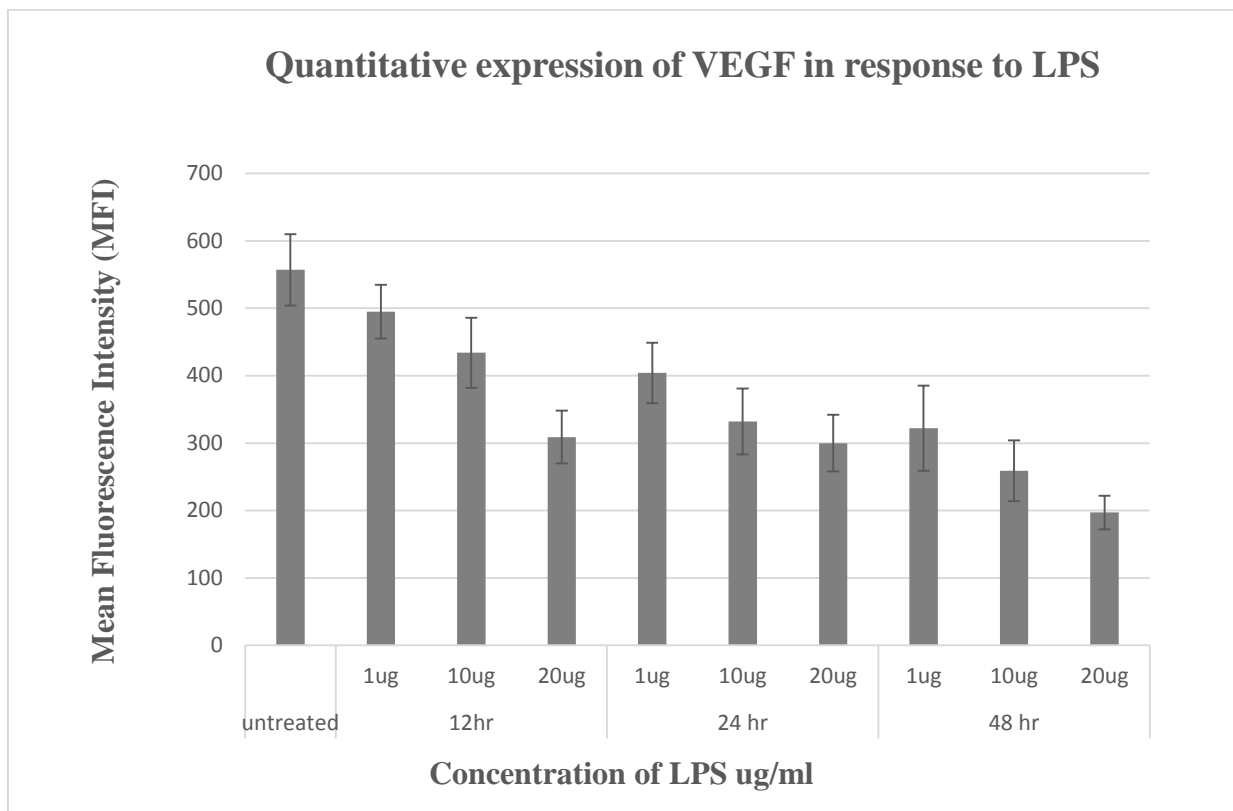
Figure 5.4. Quantitative representation of VEGFR-2 surface expression in untreated JEG-3 and LPS treated JEG-3 cells.

VEGFR-2 expression levels on JEG-3 cells were analyzed on a BD Accuri flow cytometer and FlowJo 8.8.6 software. Mean fluorescence intensity values were measured based on geometric means. Grey bars represent cell-surface expression of VEGFR-2 in untreated and LPS treated JEG-3 cells. Bar graphs represent the level of VEGFR-2 expression in mean values ± SD. Data are representative of three independent experiments.

5.2.3 Immunoblot analysis of Myoferlin and VEGF

Western blot analysis was performed to investigate Myoferlin and VEGF expression in JEG-3 cells following LPS stimulation. Cell lysate were prepared from JEG-3 cells cultured in the presence of LPS of different concentrations: 1, 10, 20 µg/ml for 12, 24 and 48 hours, and untreated control group for each time point, used as reference. Heat Shock Protein 90 (Hsp 90) was used as a loading control to access the equal loading of total protein across the gel.

The presence of a 210 kDa band confirmed expression of myoferlin in JEG-3 cells (Fig. 5.5 A). The results show slight but steady decrease in the expression of myoferlin in the whole cell lysate, with increasing LPS concentrations and incubation times, and in comparison to untreated reference group. Thus, these results indicate that LPS down-regulates the expression of myofelin in JEG-3 trophoblast cells.

In case of VEGF, three isoforms have been detected at molecular weights 40, 46 and 55 kDa (Fig. 5.5 B). No significant difference in the VEGF isoform bands has been detected across LPS concentrations at 12 hour time, but at 24 and 48 hour time points a very noticeable difference in the VEGF bands are observed across the LPS doses, where VEGF bands are weaker with increasing LPS doses as compared to untreated reference group. At 48 hours incubation times, VEGF bands are very faint along with increasing LPS concentrations, and in comparison to untreated reference group. Thus, these results identified that VEGF and myofelin expression in total protein of JEG-3 trophoblast cells is down regulated by LPS.

A
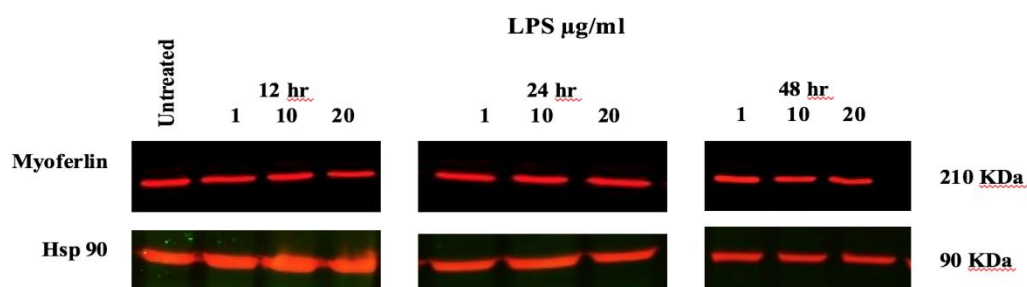
B
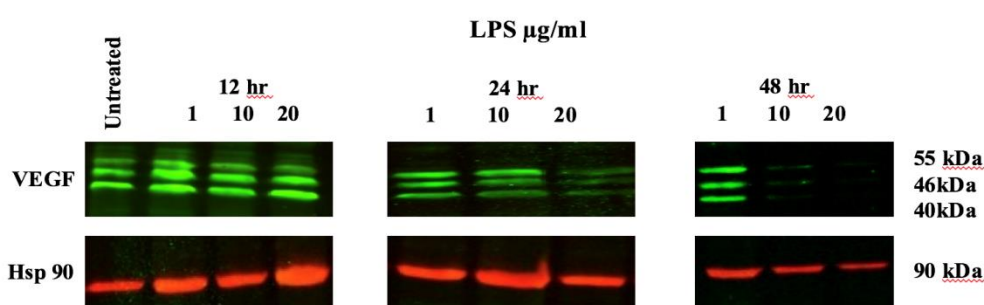
Figure 5.5: Characterization of the expression of Myoferlin and VEGF in untreated and LPS-treated JEG-3 cells.

Western blot analysis of Myoferlin (FER1L3) and VEGF (A-20) in JEG-3 cells whole lysates from untreated and LPS treated JEG-3 cells in time and dose dependent manner. **A**: Myoferlin (FER1L3) was detected at a molecular weight of 210 kDa. **B**: Levels of VEGF (A-20) were detected for VEGF isoforms at a molecular weights 55, 46, 40 kDa. Hsp 90 (Heat Shock Protein 90) was used as loading control in both A and B. The figures are representative of three independent immunoblot experiments.

5.2.4 Analysis of Myoferlin by Confocal microscopy

Confocal immunofluroscence microscopy was performed to further examine the expression of Myoferlin receptors on JEG-3 cells and visualize their topographical distribution. Cells without staining and isotype cells, stained with only secondary antibody, were used as a negative control, which did not show cell autofluorescence or non-specific binding to the cells (data not shown here). The DAPI stained blue nucleus indicates the cells observed are in a healthy state. Confocal microscopic images of LPS treated JEG-3 cells in time and dose dependent manner have been presented as 1, 10, and 20 µg/ml LPS at 12 hours (Fig. 5.6), at 24 hours (Fig. 5.7), and at 48 hours (Fig. 5.8). The expression of Myoferlin decreased over time in response to LPS. This indicates that LPS has a regulatory effect on the expression of Myoferlin on trophoblast cells and hence can lead to a possible effect on pregnancy.
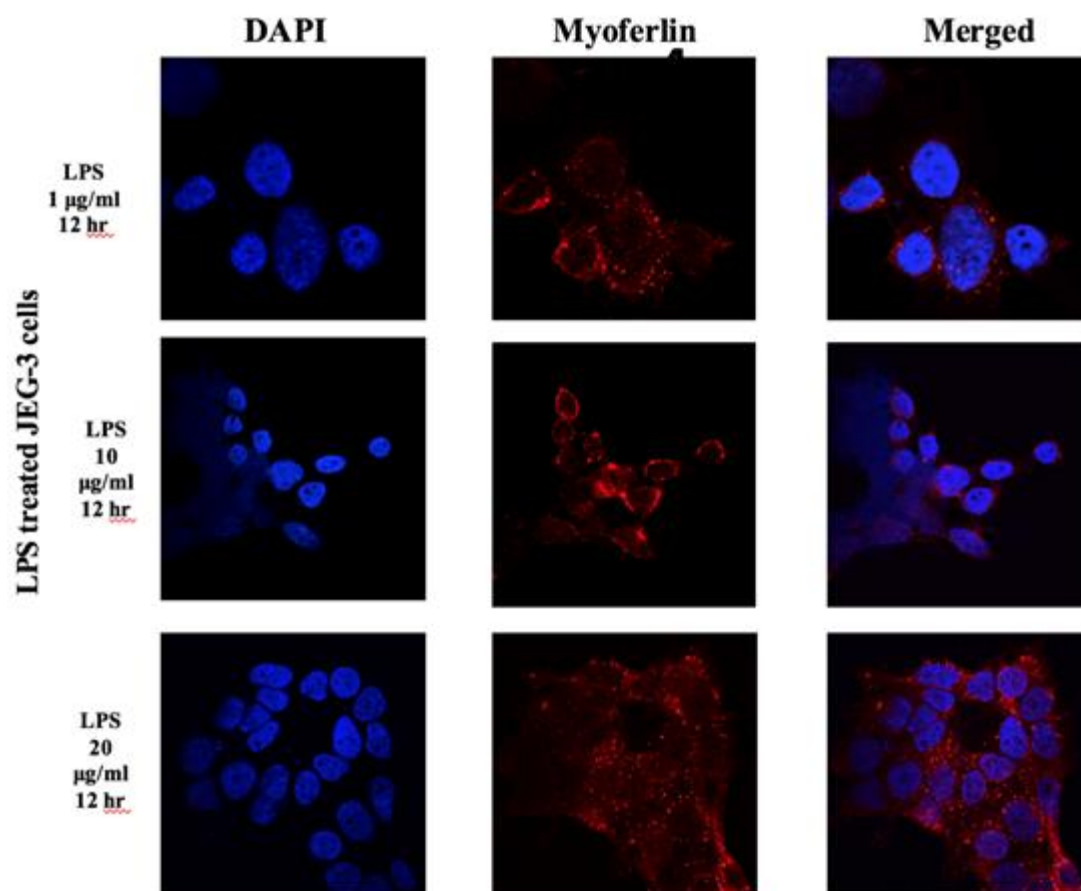
Figure 5.6: Time-dependent modulation of Myoferlin on JEG-3 cells in response to 12 hr treatment with LPS as visualised by confocal laser scanning microscopy.

Cells were stained with the Myoferlin specific antibody (FER1L3) labelled with Alexa Fluor® 555 (red), cell nuclei were stained with 4', 6-diamidino-2-phenylindole (DAPI), which is shown in blue. Photomicrographs are representative of three independent experiments. Scale bar 5 µm.
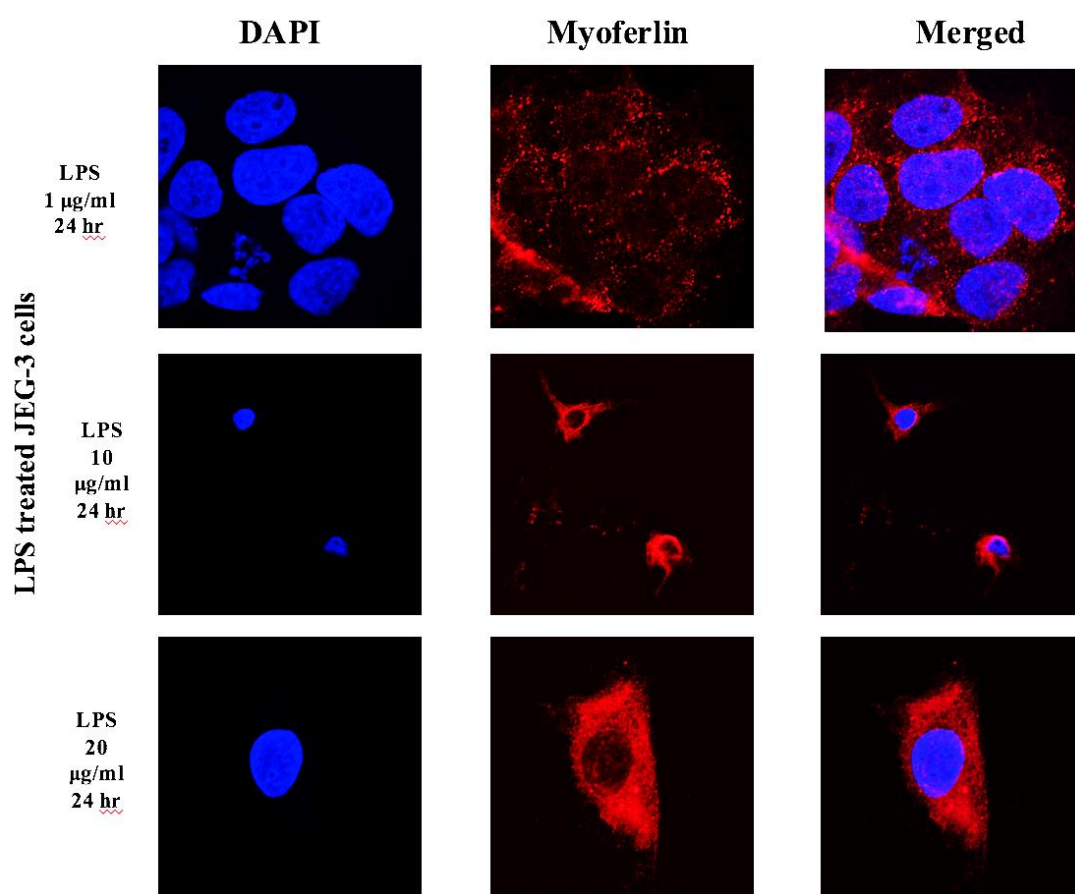
Figure 5.7: Time-dependent modulation of Myoferlin on JEG-3 cells in response to 24 hr treatment with LPS as visualised by confocal laser scanning microscopy.

Cells were stained with the Myoferlin specific antibody (FER1L3) labelled with Alexa Fluor® 555 (red), cell nuclei were stained with 4', 6-diamidino-2-phenylindole (DAPI), which is shown in blue. Photomicrographs are representative of three independent experiments. Scale bar 5 μm.
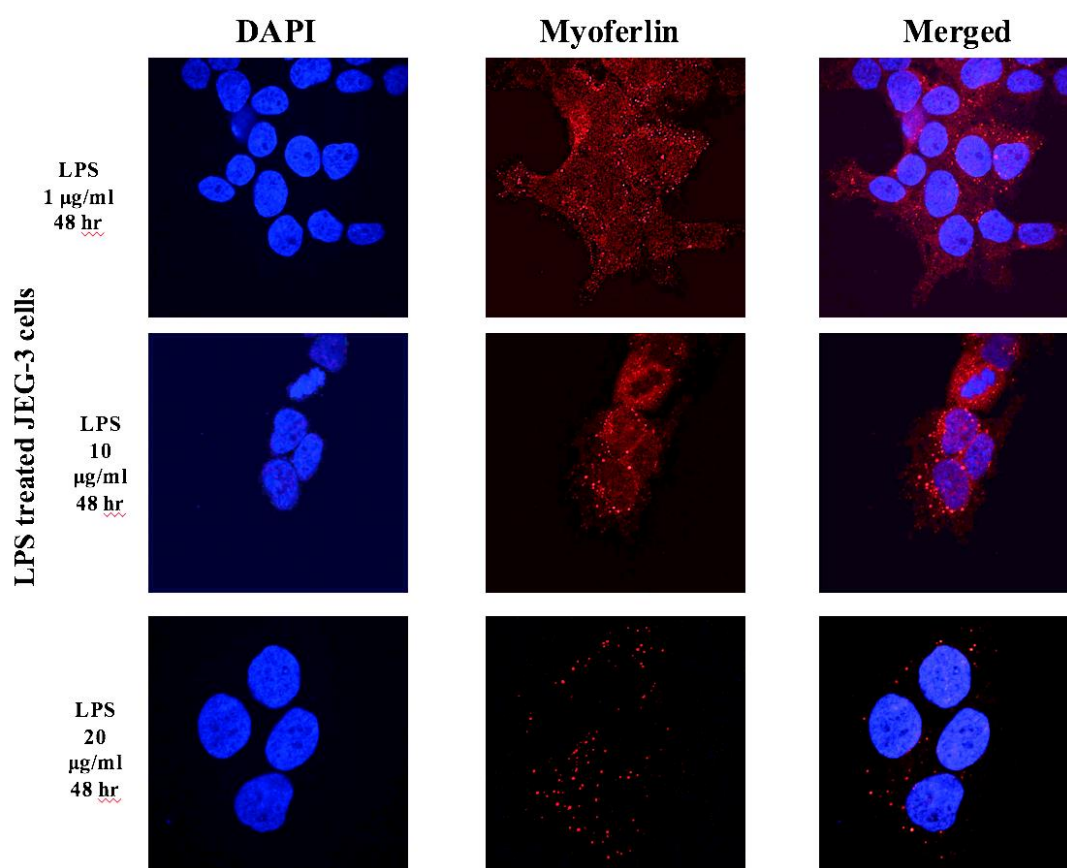
Figure 5.8: Time-dependent modulation of Myoferlin on JEG-3 cells in response to 48 hr with LPS as visualised by confocal laser scanning microscopy.

Cells were stained with the Myoferlin specific antibody (FER1L3) labelled with Alexa Fluor® 555 (red), cell nuclei were stained with 4', 6-diamidino-2-phenylindole (DAPI), which is shown in blue. Photomicrographs are representative of three independent experiments. Scale bar 5 µm.

5.2.5 Analysis of VEGF by Confocal microscopy

The VEGF receptor expression was studied through confocal immunofluroscence microscopy to further examine the expression of on JEG-3 cells and visualized their topographical distribution. Cells without staining and isotype cells, stained with only secondary antibody, were used as a negative control where no cell autofluorescence or non-specific antibody binding was observed (data not shown here).

Confocal microscopic images of untreated and LPS (20 µg/ml) treated JEG-3 cells are shown in figure and cells treated with LPS for a period of 12, 24 and 48 hours. The expression of VEGF decreased over time in response to LPS in both time and dose-dependent manner (Figure 5.2.9). This indicates that LPS has a regulatory effect on the expression of VEGF on trophoblast cells and hence a possible effect on pregnancy.

Figure 5.9: Time-dependent modulation of VEGF on JEG-3 cells in response to LPS as visualised by confocal laser scanning microscopy.

Cells were stained with the VEGF specific antibody (FER1L3) labelled with Alexa Fluor® 555 (red), cell nuclei were stained with 4', 6-diamidino-2-phenylindole (DAPI), which is shown in blue. Photomicrographs are representative of three independent experiments. Scale bar 10 μm.
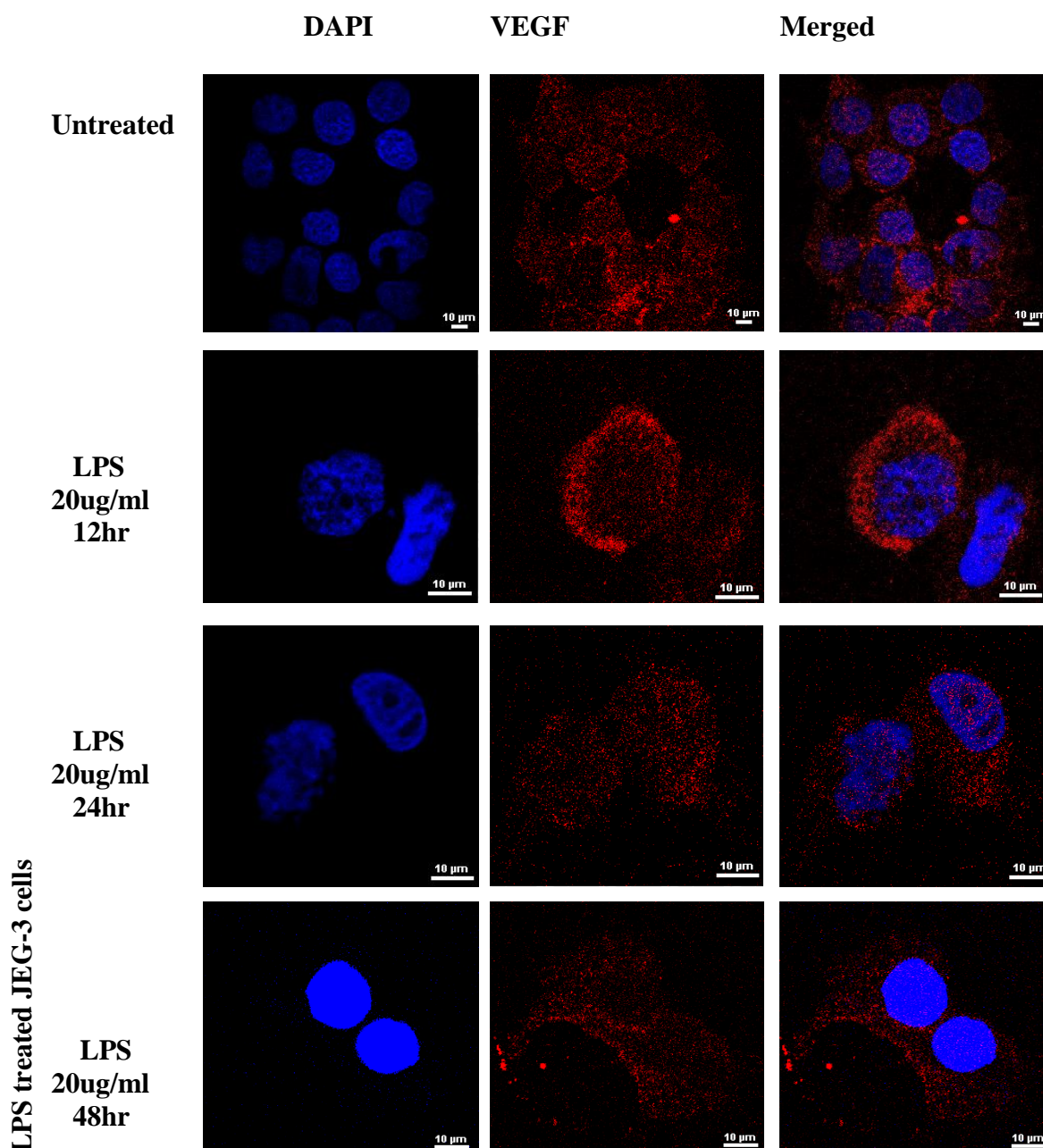
5.2.6 Trophoblast Cell Proliferation Assay in response to LPS

Proliferation of trophoblast cells upon exposure to LPS was studied in dose and time dependent manner. JEG-3 cells were treated with varying concentrations of LPS (1, 10 and 20 μg/ml) for 12, 24 and 48 hours. Untreated cells were used as a positive control and Camptothecin (CPT) a cytotoxin served as a negative control. Results from time dependent effect of LPS treatments on JEG-3 cells are presented in figure 5.10, where cells were incubated with 20 μg/ml LPS for 12, 24 and 48 hours.

The results indicate that at 12 hours of treatment, JEG-3 cells showed ~70% viable cells in response to LPS resulting in a decrease in the growth rate as compared to untreated cells, but similar to negative control CPT (Figure. 5.10). At 24 hours, cell viability significantly decreased to ~55% as compared to untreated reference group, whereas at 48 hour treatment, cell growth of treated cells rapidly decreased to ~20% as compared to untreated cells, thus the same growth pattern was followed as CPT treated cells (Figure 5.10). Therefore, time dependent LPS effect appeared to cause very significant damage to trophoblast cell survival.

Dose dependent effect of LPS treatments on JEG-3 cells are presented in figure 5.11. Treated JEG-3 cells were incubated with 1, 10 and 20 μg/ml LPS for 24 hours. The results indicated that at 24 hours of treatment with 1 μg/ml LPS, JEG-3 cells did not show significant difference on cell viability as compared to control. Whereas, 10, and 20 μg/ml LPS showed a steady decrease (85% and 75% respectively) in cell viability as compared untreated group. Thus, results of proliferation assay indicate that LPS presence can activate some signalling pathway in the JEG-3 cells that can lead to cell death.
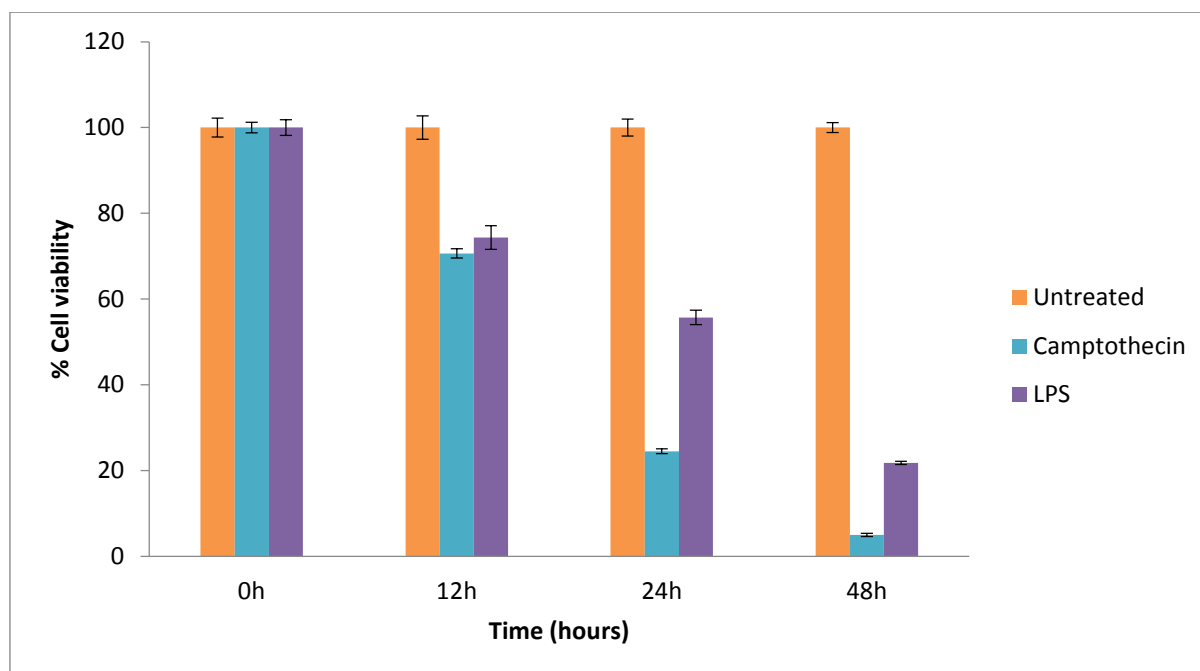
Figure 5.10: Cell proliferation assay of JEG-3 cells in response to time dependent bacterial LPS.

JEG-3 cells were seeded in 96 well-plates and treated with indicated concentrations of LPS. The values on ordinate represent corrected percentage cell viability ± SD of quadruplicate samples. Abscissa illustrates time points of each observation taken for cell growth under specified conditions. Untreated cells were used as a positive control while CPT-camptothecin was served as a negative control. LPS- lipopolysaccharide treated sample.
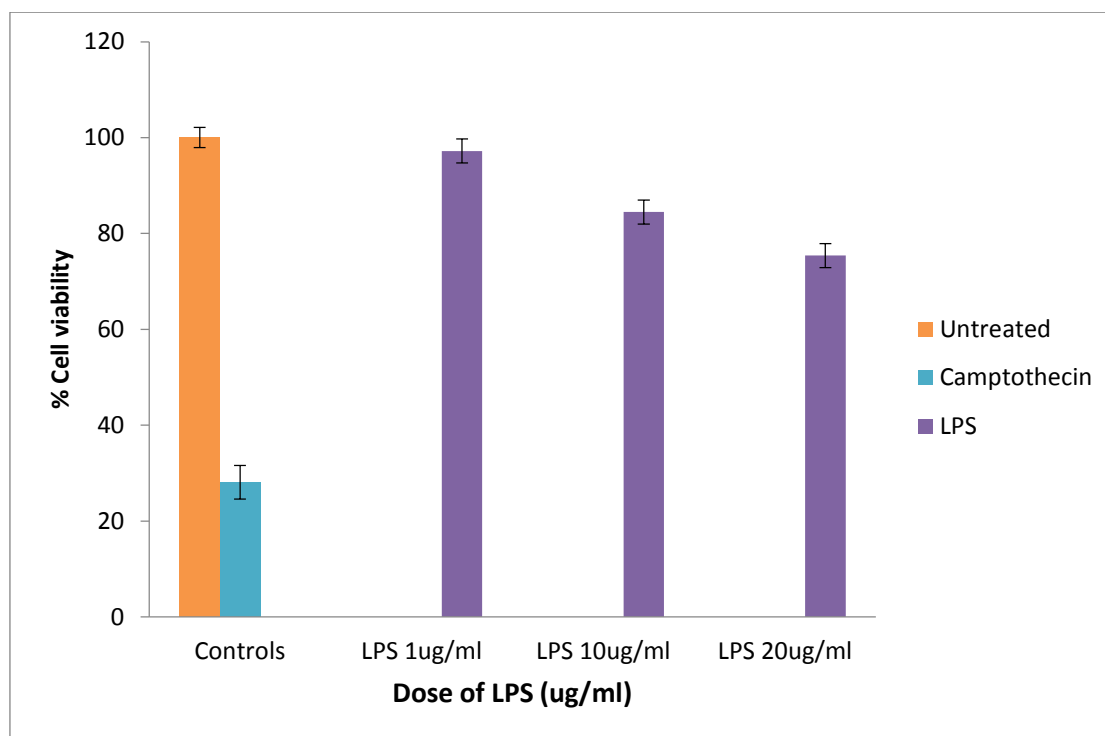
Figure 5.11: Cell proliferation assay of JEG-3 cells in response to dose dependent LPS treatments.

JEG-3 cells were seeded in 96 well-plates and treated with indicated concentrations of LPS. The values on ordinate represent corrected mean percentage cell viability ± SD of quadruplicate samples. Abscissa illustrates time points of each observation taken for cell growth under specified conditions. Untreated cells were used as a positive control while CPT-camptothecin was served as a negative control. LPS- lipopolysaccharide treated sample.

5.2.7 Effect of LPS on NF-κB activation in trophoblast JEG-3 cells

Effect of LPS was examined on NF-κB activation in JEG-3 cell when cells were incubated with 20 µg/ml LPS for 12, 24 and 48 hours. NF- κB activation was investigated by microscopy followed by colocalisation analysis for localisation of NF-κB p65 in trophoblast cell nucleus in response to LPS (Fig. 5.12).

Micrographs of JEG-3 cells show distribution of NF-κB in the cytoplasm (red colour) of all untreated and treated cells but no detectable amount of NF-κB can be seen inside the nucleus (blue colour) in the control and 12h LPS treated cells (Fig. 5.12). However, the distribution of NF-κB (red colour) in the nucleus (blue colour) in 24h treated cells increased. The same pattern was followed resulting in a significant increase in the distribution of NF-κB (red colour) in the nucleus (blue colour) of 48hr h LPS treated cells Thus suggesting that NF-κB activation in trophoblast cells occur after the first 24 hours of LPS incubation.

In order to further investigate the localisation of NF-κB inside the nucleus, colocalisation of NF-κB and nuclear DNA was performed by using colocalisation threshold plugin in ImageJ software (Fig 5.12 right column). The 2D colocalisation scatter plot shows a linear regression fit of the intensities of red and blue channels, in the scatter plot. The diagonal white line in the scatter plot is the best fit, the gradient of which is the ratio of the intensities of both channels. The colocalisation of nuclear DNA and NF-κB represents that NF-κB is activated upon LPS treatment and translocated in to the nucleus from the cytoplasm of the cell at 24 hours onwards.

The mean Pearson Correlation Coefficient (PCC) values for control and each LPS treatment group are represented in the bar graph (Figure 5.13). The data represents that the localization of NF-κB in the nucleus significantly increased with the LPS incubation times, as compared with the control untreated group. Therefore, NF-κB is activated and translocated from cytoplasm to the nucleus with the effect of LPS treatment and this activation is significantly apparent at 24

hours of LPS incubation with trophoblast cells.

Time (hours) LPS 20µg/ml	Composite of Red and Blue	2D Colocalisation Scatter Plot
Control		
12 h		
24 h		
48 h		
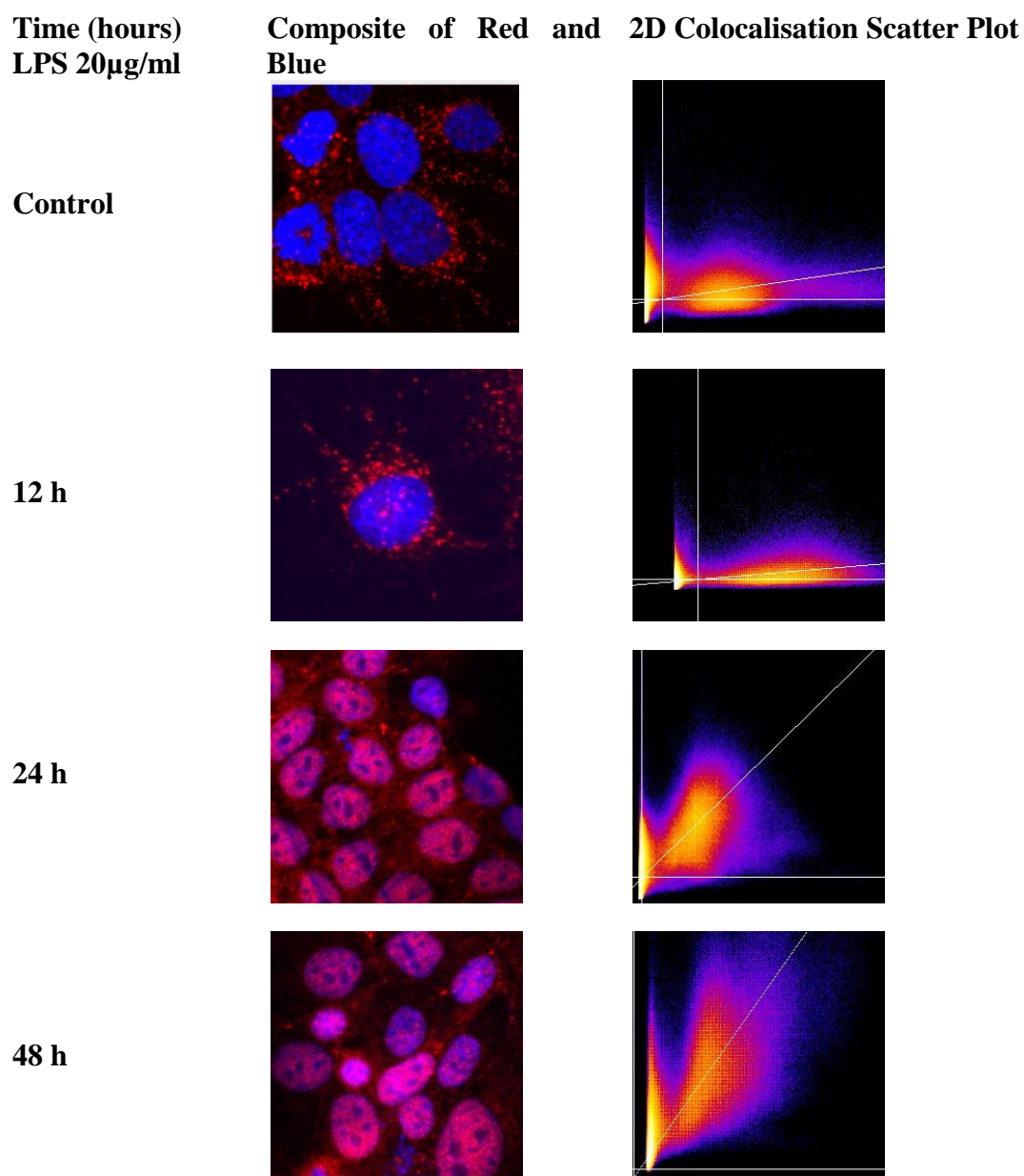
Figure 5.12: Indirect immunofluorescence and confocal microscopy analysis demonstrating the effect of LPS infectious agents on localisation of NF-κB p65 in trophoblast cells.

JEG-3 cells were cultured in LabTek 8-well chambers at a density of 3 x 10³ cells per well overnight in the presence of the indicated concentration of LPS (1, 10 and 20 ug/ml) for 24 hrs. Cells were stained with NFkB labelled with Alexa Fluor® 555 (red), cell nuclei were stained with 4', 6-diamidino-2-phenylindole (DAPI), which is shown in blue. Fluorochromes were acquired separately to evaluate the expression of NFkB using the Fiji software. Photomicrographs are representative of three independent experiments.
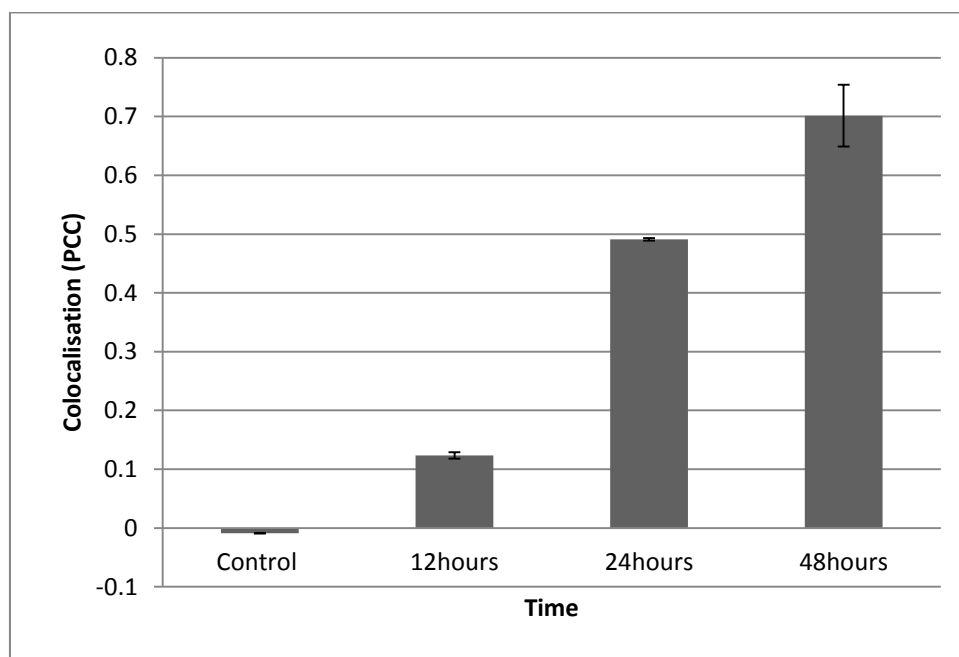
Figure 5.13. Quantitative analysis of colocalisation between nuclear proteins and NF-κB in JEG-3 cells, plotted against LPS treatment at different time points.

JEG-3 cells treated with LPS (20 ug/ml) for 12 hrs, 24 hrs and 48 hrs. Cells were stained with NF-κB antibody followed by staining with FITC-conjugated goat anti-mouse antibody. NF-κB expression levels were analysed by the use of Image J software. Grey bars represent expression of NF-κB in untreated and LPS treated JEG-3 cells. Bar graphs represent the level of nuclear proteins and NF-κB in mean values ± SD. Pearson Correlation Coefficient values were used to evaluate the colocalisation of NF-κB on JEG-3 cells. Data are representative of three independent experiments.

5.3 Conclusions

In this study, detection and quantification of Myoferlin on JEG-3 cell line was performed upon treatment with LPS. Myoferlin and VEGF quantification estimated by flow cytometry and confocal microscopy showed significant decrease in LPS treated JEG-3 cells in dose and time dependent manner. Similar observation was detected using western blot analysis. Cell proliferation analysis revealed a significant decrease in trophoblast cell growth in 48 hours of LPS treatment. NF-κB analysis following LPS treatment of JEG-3 cells revealed activation of NF-κB pathway in trophoblast JEG-3 cells.

Chapter 6

Discussion

This study was designed to explore the role of trophoblast in the maintenance of utero-placental tolerance during infection. Pregnancy involves a major involvement of both the adaptive and innate immune system. During pregnancy, the maternal immune system changes dramatically; it provides protection to the mother as well as the embryo in early stages or the fetus following implantation. A fundamental question not yet fully understood is whether the adaptive and innate recognition system changes equally during pregnancy. Several observations indicate that parts of the immune system are enhanced while others are suppressed. It has also been shown that pregnant females are susceptible to intracellular pathogens and are biased towards humoral rather than cell-mediated immunity. In this context, based on the pattern of cytokines released by the maternal immune system, it has been suggested that pregnancy is a Th2 non-inflammatory cytokine (e.g. interleukin-10 (IL-10), granulocyte–macrophage colony-stimulating factor (GM-CSF) and IL-3, in feto–placental growth, as opposed to a Th1 cytokine (e.g. interferon-γ (IFN-γ) and tumour necrosis factor-α (TNF-α phenomenon (Athanassakis, 2002; Wegmann et al., 1993). In a separate study it was shown that abortion prone women who proceed to have a successful pregnancy are more Th2 biased than abortion-prone women who abort. It was also shown that recurrent aborters who undergo spontaneous abortions have a stronger Th1 bias than aborters who have normal pregnancy (Makhseed et al., 2001). These studies highlight the importance of cytokines in pregnancy development.

Since cytokines controlled a variety of immunological phenomenon including cell surface receptors involved in signalling and immune responsiveness it can be argued that the Th2 pregnancy associated pattern of cytokines have a profound influence in immunity as a whole during pregnancy. Overall, the Th2 cytokine pattern during pregnancy creates a balance of

soluble factors that can prevent infections without compromising maternal immunity.

The state of mild immunosuppression is that the Th2 pregnancy pattern implies that the mother undergoes a period of 'mild immunosuppression'. This would explain that fact during pregnancy the mother is susceptible to otherwise benign infections from pathogens such as bacteria and viruses. A recent example is the outbreak of Zika virus, this pathogen can cause intrauterine growth restriction and spread from an infected mother to her fetus during pregnancy or at delivery (Larocca et al., 2016).

Bacterial infections can on the other hand affect pregnant women from the time of fertilization, implantation of the fertilized ovum through the time of delivery and peri-partum period. These infections can also affect the development of the fetus and the new born. Bacterial infections can include *E. coli, Group B Streptococcus, Listeria monocytogenes, Chlamydia trachomatis* and *bacterial vaginosis* among others (Watt et al., 2003). Many of these infections can trigger the innate recognition system as a first line of protective immunity. Similar to the cells of the immune system like lymphocytes and macrophages, trophoblast cells can express receptors of innate recognition system. These receptors include pattern recognition receptors (PRR) (Shaikly et al., 2008).

In this study, emphasis was placed on the pattern recognition receptors designated CD14 and MARCO. Their potential role in the immunology of trophoblast cells remains to be deciphered.

Pattern recognition receptors play a primary role in innate recognition through surveillance of invading pathogens (Rallabhandi et al., 2006). PRR can recognise the pathogen associated molecular patterns (PAMPs) from pathogens such as bacteria, viruses and fungi. Upon recognition of PAMPs by PRR, a cascade of signalling reactions is initiated to provide the first line of defence to the infected host. The human placental choriocarcinoma cell line, JEG-3 was used as a model system since many of their biological and biochemical characteristics are similar

with syncytiotrophoblast and cytotropoblast cells of the placenta (Matsuo and Strauss, 1994; Hiden et al., 2007). A combination of techniques including cellular, biochemical and bioimaging were employed to examine expression and immunomodulation of receptors CD14, MARCO, Myoferlin and VEGF in response to LPS. The potential involvement of NF-κB as a non-specific transcriptional regulator in response to LPS was also examined.

Intrauterine infection has been associated with preterm labour in up to 40% of cases (Lamont, 2003). Furthermore, evidence of infection have been reported in almost 80% of preterm deliveries at <30 weeks of gestation (Goldenberg et al., 2000). Intrauterine infections may be caused by bacterial agents. In order to investigate the effect of bacterial infections on various cellular biological functions, bacterial endotoxin LPS have been used for in vitro studies of various cellular systems. Therefore, LPS was applied to the in vitro trophoblast model system to investigate the trophoblast responses to infection conditions.

LPS is an important component of the outer membrane of Gram-negative bacteria which is an effective activator of immune responses upon bacterial infection and is likely to affect the maternal immune response during pregnancy (Sankala et al., 2002). In fact, Lipopolysaccharide (LPS) is recognised by TLR-4 and is a major cause of septic shock in intrauterine infection.

Previous studies have reported that CD14 and MARCO receptors have a key role in the pathogenesis of septic shock (Oliver et al., 1999). Secretion of pro-inflammatory cytokines and the activation of NF-κB upon stimulation of human monocytes/ macrophages with LPS have been found to involve CD14 and MARCO receptors.

In this study, surface expression of CD14 was observed on the JEG-3 cell surface. Regulation of CD14 in response to LPS in dose and time dependent manner revealed that CD14 expression increased with incubation times and with increasing concentration of LPS, where 20 μg/ml LPS treatment significantly induced the CD14 expression at all time points (12, 24 and 48 hours).

Immunofluorescence imaging by confocal microscopy and immunoblotting analysis further confirmed the expression and regulation of CD14 on JEG-3 cells. The expression of CD14 and MARCO on JEG-3 cells haven not been previously reported. Experiments have shown that CD14 is one of the components of a receptor complex which mediates the LPS-induced signal transduction. CD14 plays a significant role in this potent immune response through the transfer of LPS to the TLR-4:MD2 complex (Gangloff et al., 2005). However a study with CD14-deficient murine macrophages has shown evidence of a CD14-independent pathway of signal transduction by different LPS chemotypes. The majority of Gram-negative bacteria synthesize 'smooth LPS' (Gangloff et al., 2005). The smooth LPS are composed of the lipid moiety, a core polysaccharide and a variable O-polysaccharide whereas the failure to attach either of the components other than lipid A moiety results in the formation of 'rough LPS'. In both the chemotypes of LPS, the lipid A moiety is the bioactive element which has pathogenic functions in infections caused by Gram-negative bacteria. Subsequent to induction with rough LPS, equal quantities of TNF was secreted by both the CD14-deficient murine macrophages and the CD14-expressed macrophages and no secretion of TNF to smooth LPS was observed. This signifies the necessity of CD14 for only the smooth LPS for the activation of TLR-4:MyD88 pathway. Furthermore no IFN-α/β was secreted upon stimulation with smooth or rough LPS which indicates that CD14 is required for TLR-4: TRIF pathway activation by both the LPS chemotypes.

 (Anas et al., 2010). Therefore this suggests that the possibility of CD14 been expressed on trophoblast cells due its necessity for the activation of TLR-4: MyD88 and the TLR-4: TRIF pathway as TLR-4 is expressed on trophoblast cells and the results of this study supports this hypothesis (Klaffenbach et al, 2005).

Surface expression of MARCO receptors on JEG-3 cells has been observed in this study. The fluorescence intensity of MARCO decreased as the concentration of LPS increased. It was

observed that the surface expression of MARCO is down-regulated upon treatment as the concentration of LPS increases over time, where most significant differences were observed at 48 hours. This was confirmed with confocal microscopy and immunoblotting results where the expression followed the same pattern.

In mice, the majority of MARCO is expressed on the marginal zone macrophages in the spleen, on macrophages of the medullary cord in lymph nodes and on peritoneal macrophages (Granucci et al., 2003). The expression of human MARCO is detected to be most robust in the liver, lymph nodes, monocytes and alveolar macrophages which are involved in the filtration of blood and lymph fluids (Jozefowski et al., 2005). However the expression of MARCO on trophoblast cells appears to be elusive. As its expression is widely studied on monocytes it's used as a positive control for our study we initially examined the expression pattern of MARCO on THP-1 which is a monocytic cell line. MARCO is found to have a variety of functions such as relegation of

TLR-4 mediated responses (Mukhopadhyay et al. 2011). As the expression of MARCO appears to be associated with TLR-4 mediated responses which is expressed on trophoblast cells and its role as a major immune cell the expression pattern was examined and the results obtained of expression of MARCO on JEG-3 cells reinforces this hypothesis of the study.

The effect of LPS on CD14 and MARCO on JEG-3 cells was the other key focus of this study.

In order to investigate this effect, JEG-3 cells were stimulated with 1μg/ml, 10μg/ml and 20μg/ml of LPS for a period of 12, 24, and 48 hours for each receptor. The interesting observation was that surface expression and total protein concentration detected by immunoblotting significantly increased for CD14 in contrary to MARCO which significantly decreased. MARCO has the capability of binding both Gram-positive and Gram-negative bacteria (Granucci et al., 2003). It has been suggested that MARCO plays a role in antimicrobial defence system and the up-regulation of its expression during bacterial infections in macrophages of the liver and spleen provides evidence for this concept (Arredouani et al., 2004).

Thelen et al., (2010) reported that the degrees of MARCO transcription and cell surface expression are increased after bacterial binding which further supports its significance in phagocytosis of bacteria. Moreover the expression of MARCO can be stimulated upon bacterial infection or LPS injection as LPS present on the Gram-negative bacteria acts as a ligand of MARCO (Sankala et al., 2002).

In addition to CD14 and MARCO the expression profile of Myoferlin and VEGF antigens were also examined on JEG-3 as well as cell proliferation following challenge with LPS. Myoferlin, one of the members of the Ferlin family and is a membrane protein encoded by the MYOF gene and found in cell membranes, nuclear membranes and cytoplasmic vesicles (Bernatchez, et al., 2007). A high expression of myoferlin has been observed in skeletal and cardiac muscles and weak expression in the brain, kidney and placenta. Myoferlin is necessary for membrane repairing and regulation of VEGF signal transduction. There is data suggesting that successful implantation of the developing embryo in the maternal uterus is associated with EVT proliferation and invasion of the uterine wall. Decreased EVT proliferation and trophoblast cell death has been associated with pregnancy complications such as preeclampsia and intrauterine growth restriction thus resulting in inadequate trophoblast invasion (Smith et al., 1997; Allaire et al., 2000; Crocker et al., 2003; Kakinuma et al., 1997;). We have hypothesized that there is a correlation between the down-regulation of Myoferlin and the decreased cell proliferation of trophoblast cells upon bacterial infection. Detection of Myoferlin on JEG-3 cell line was carried out upon treatment of JEG-3 cells with LPS. It was observed that this treatment reduces Myoferlin expression.

VEGF expression has come to light in the recent years in the context of angiogenesis and tumour metastasis. Both processes have a parallel with trophoblast physiology during embryonic development and placentation. VEGF function requires the interaction with specific receptors; in addition several VEGFRs isoforms have been identified. Whether there is a role for VEGF in

embryo development is unclear, although apparent lack of VEGF at the feto-maternal interface has been observed. Whether VEGF is modulated during bacterial infection or other factors is still not clear. There seems to be a scarcity of studies in this regard. It is possible that VEGF is modulated at different stages of pregnancy or in pregnancy abnormalities. An in vitro model was developed to test the effect of LPS on the expression of VEGF in JEG-3cells. Western blot analysis of LPS stimulated trophoblast cells revealed that as the LPS exposure time increases the amount of VEGF protein present decreased. Considering that the control samples gave the same results in each condition and the only factor that has been changed is the LPS dosage and time treated, it is reasonable to assume that the change in VEGF expression is a direct consequence of the LPS treatment.

Previous studies have used serum of pregnant women in order to gain an understanding of hormone levels and detect potential abnormalities in VEGF concentrations. Evan et al. used the serum of women in their first trimester of normal pregnancy. They detected that VEGF serum concentration increases up until 10 weeks of gestation. However in pre-clamptic pregnancies, women had a reduced VEGF levels (Lyall et al., 1997; Reuvekamp et al., 1999). This is direct evidence of how VEGF can cause trophoblast dysfunction, which could result in feto-maternal dysfunction. A typical consequence is preeclampsia, a disorder of pregnancy characterized by high blood pressure. The underlying mechanism of pre-eclampsia involves abnormal formation of blood vessels in the placenta. VEGF is likely to be involved but its exact mechanism is not yet understood. Simmons et al. studies VEGF expression by immunostaining the decidua and villi from pre-eclamptic women; the results showed an increase in VEGF concentration (Simmons et al., 2000).

In an attempt to approach the molecular basis of infections, the study was then focused on trophoblast cell proliferation and activation of NFκB. In this part of study, JEG-3 cell line was used for the in vitro study model. Cell proliferation is a crucial factor for extravillous trophoblast

(EVT) cells for proper embryo implantation, invasion into maternal uterine wall and a successful pregnancy. The study results show that trophoblast JEG-3 cells' propagation is significantly affected in case of LPS infection, with a rapid decrease in cell proliferation.

The data in this study shows that in JEG-3 cells, treatment of NF-κB is involved in cellular responses to stimuli such as stress, cytokines, bacterial or viral antigens (Gilmore, 2006). Incorrect regulation of NF-κB has been linked to inflammatory and autoimmune diseases, viral infection, septic shock, and improper immune development (Perkins, 2007). Therefore, the activation of NF-κB mediated by trophoblast cell infection has been investigated here. Microscopic data shows significant increase of translocation of NF-κB from cytoplasm to nucleus after 24 and 48 hours of LPS treatment. This indicates that NF-κB has been activated in response to LPS at 24 and 48 hours of treatment. It has been previously reported that NF-κB is activated in JEG-3 cells after 48 hours of LPS treatment (Lappas et al., 2006). Activation of NF-κB in response to treatment of. LPS ligation to TLR-4 can signal via both MyD88-dependent and -independent pathways (Akira and Hoshino, 2003). As a result, NF-κB can signal first trimester trophoblast cells to produce high levels of cytokines, includingIL-2, IL-6, TNF-α and

IFN-γ (Abrahams et al., 2004). Trophoblast cells are highly sensitive to these cytokines, such as, placental expression of IFN-γ and TNF-α has been associated with trophoblast cell death consequence of the activation of NF-κB is the production of various pro-inflammatory mediators. Lipopolysaccharide induces a dose dependent increase of cytokines, interleukin (IL)-8 and IL-6 and a decrease in EVT invasion. (Aschkenazi et al., 2002; Yui et al., 1994). It was observed that LPS exposure lead to an increase in signalling pathways and phosphorylation.

In summary, trophoblast cells are the only embryo derived cells which are present at the feto-maternal interface and present a repertoire of selectively expressed receptors at the cell surface and thus function as a sensory system. Trophoblast recognises and responds to bacterial antigens (Guleria and Pollard, 2000) at utero-placental interface Receptors expressed at the cell surface

and their quantitative modulation play a vital role in achieving immune recognition and self-tolerance needed for pregnancy to develop. Thus it can be suggested that trophoblast has the capability to respond as a pregnancy specific immune system.

Conclusion

Trophoblast cells and their membrane bound receptors and ligands function including CD14, MARCO and Myoferlin and VEGF act as a sensory system. Their quantitative modulation play a vital role in achieving the immune recognition and self-tolerance needed for pregnancy to develop. Furthermore, effect of bacterial agents on NF-κB activation has also been investigated. This data can help in future studies to investigate the TLR responses and associated signalling pathways involved in human pregnancy in cells isolated from normal pregnancy or patients suffering from pregnancy associated diseases like pre-eclampsia.

References

Abrahams, V. M., Bole-Aldo, P., Kim, Y. M., Straszewski-Chavez, S. L., Chaiworapongsa, Romero, R., and Mor, G. (2004). Divergent trophoblast responses to bacterial products mediated by TLRs. *J Immunol,* **173**, p4286-96.

Abrahams, V.M. and Mor G. (2005) Toll-like receptors and their role in the trophoblast, *Placenta*, **26**, p540-547.

Abrahams, V. M., Visintin, I., Aldo, P. B., Guller, S., Romero, R., and Mor, G. (2005). A role for TLRs in the regulation of immune cell migration by first trimester trophoblast cells. *J Immunol,* **175**, p8096-104.

Agrawal, V., and Hirsch, E. (2012). Intrauterine infection and preterm labor. *Semin Fetal Neonatal Med,* **17**, p12-9.

Akira, S., and Hoshino, K. (2003). Myeloid differentiation factor 88-dependent and -independent pathways in toll-like receptor signaling. *J Infect Dis,* **187 Suppl 2**, S356-63.

Akira, S., and Takeda, K. 2004.Toll-like receptor signalling. *Nat Rev Immunol.* **4(7):** p499–511.

Allaire, A. D., Ballenger, K. A., Wells, S. R., McMahon, M. J., and Lessey, B. A. (2000). Placental apoptosis in preeclampsia. *Obstet Gynecol,* **96**, p271-6.

Anas, A ; Van der Poll , T and de Vos, A.F. (2010), Role of CD14 in lung inflammation and infection, *Critical Care*, p1-8

Anton, L., Brown, A. G., Parry, S., and Elovitz, M. A. (2012). Lipopolysaccharide induces cytokine production and decreases extravillous trophoblast invasion through a mitogen-activated protein kinase-mediated pathway: possible mechanisms of first trimester placental dysfunction. *Hum Reprod,* **27**, p61-72.

Arck, P. C., and Hecher, K. (2013). Fetomaternal immune cross-talk and its consequences for maternal and offspring's health. *Nat Med,* **19**, p548-56.

Arredouani, M ; Yang, Z ; Imrich, A ; Ning, Y. Y ; Qin, G ; and Kobzik, L. (2006) The Macrophage Scavenger Receptor SR-AI/II and Lung Defense against Pneumococci and Particles., *American Journal of Respiratory Cell and Mollecular Biology*, **35**,p474-4781

Arredouani, M ; Yang, Z ; Ning, Y. Y ; Qin, G ; Soininen, R ; Tryggvason, K and Kobzik, L. (2004) The Scavenger Receptor MARCO Is Required for Lung Defence against Pneumococcal Pneumonia and Inhaled Particles. *The Journal of Experimental Medicine*, **200**, p267-272

Athanassakis, I. (2002) Interplay between T helper type 1 and type 2 cytokines and soluble major histocompatibility complex molecules: a paradigm in pregnancy. Immunology, **107**, p281-287.

Bernatchez, P. N., Acevedo, L., Fernandez-Hernando, C., Murata, T., Chalouni, C., Kim, J., Erdjument-Bromage, H., Shah, V., Gratton, J. P., McNally, E. M., Tempst, P., and Sessa, W. C. (2007). Myoferlin regulates vascular endothelial growth factor receptor-2 stability and function. *J Biol Chem,* **282**, p30745-53.

Crocker, I. P., Cooper, S., Ong, S. C., and Baker, P. N. (2003). Differences in apoptotic susceptibility of cytotrophoblasts and syncytiotrophoblasts in normal pregnancy to those complicated with preeclampsia and intrauterine growth restriction. *Am J Pathol,* **162**, p637-43.

Burrough, E.R.; DiVerde, K. D.;Sahin, O;Plummer,P. J.;Zhang,Q and Yaeger, M.J. (2011). Expression of Toll-like Receptors 2 and 4 in Subplacental Trophoblasts From Guinea Pigs (Caviaporcellus) Following Infection With Campylobacter jejuni. *Veterinary Pathology,* **48**, p381-388.

Davis, D. B., Doherty, K. R., Delmonte, A. J., and McNally, E. M. (2002). Calcium-sensitive phospholipid binding properties of normal and mutant ferlin C2 domains. *J Biol Chem,* **277**, p22883-8.

de la Torre, Y. M., Buracchi, C., Borroni, E. M., Dupor, J., Bonecchi, R., Nebuloni, M., Pasqualini, F., Doni, A., Lauri, E. and Agostinis, C. (2007) Protection against inflammation-and autoantibody-caused fetal loss by the chemokine decoy receptor D6. *Proceedings of the National Academy of Sciences,* **104**, p2319-2324.

Dimitriadis, E., Nie, G., Hannan, N. J., Paiva, P., and Salamonsen, L. A. (2010). Local regulation of implantation at the human fetal-maternal interface. *Int J Dev Biol***54**, p313-22.

Drake, P. M., Gunn, M. D., Charo, I. F., Tsou, C.-L., Zhou, Y., Huang, L. and Fisher, S. J. (2001) Human placental cytotrophoblasts attract monocytes and CD56bright natural killer cells via the actions of monocyte inflammatory protein 1α*. The Journal of experimental medicine,* **193**, p1199-1212.

Fernandez, N., Cooper, J., Sprinks, M., AbdElrahman, M., Fiszer, D., Kurpisz, M., and Dealtry, G. (1999). A critical review of the role of the major histocompatibility complex in fertilization, preimplantation development and feto-maternal interactions. *Hum Reprod Update,* **5**, p234-48.

Gangloff, S. C; Zahringer. U; Blondin, C; Guenounou, M; Silver, J; Goyert, S. M. (2005) Influence of CD14 on ligand interactions between Lipopolysaccaride and its receptor complex, *The Journal of Immunology*, **175**, p3940-3945

Gegner, J.A.; Ulevitch, R.J. and Tobias, P.S. (1995).Lipopolysaccharide (LPS) Signal Transduction and Clearance Dual roles for LPS binding protein and membrane CD14. *Journal of Biological Chemistry*. **270**, p5320-5325.

Gilmore, T. D. (2006). Introduction to NF-kappaB: players, pathways, perspectives. *Oncogene,***25**, p6680-4.

Goldenberg, R. L., Hauth, J. C. and Andrews, W. W. (2000) Intrauterine infection and preterm delivery. N Engl J Med, **342**, p1500-7.

Granucci, F ; Petralia, F; Urbano, M; Citterio, S ; Di Tota, F ; Santambrogio, L . (2003) The scavenger receptor MARCO mediates cytoskeleton rearrangements in dendritic cells and microglia, *Blood*, **102**, p2940-2947

Guleria, I., and Pollard, J. W. (2000). The trophoblast is a component of the innate immune system during pregnancy. *Nat Med,* **6**, p589-93.

Hanna, J., Goldman-Wohl, D., Hamani, Y., Avraham, I., Greenfield, C., Natanson-Yaron, S., Prus, D., Cohen-Daniel, L., Arnon, T. I. and Manaster, I. (2006) Decidual NK cells regulate key developmental processes at the human fetal-maternal interface. *Nature medicine,* **12**, 1065-1074.

Hanna, J., Wald, O., Goldman-Wohl, D., Prus, D., Markel, G., Gazit, R., Katz, G., Haimov-Kochman, R., Fujii, N. and Yagel, S. (2003) CXCL12 expression by invasive trophoblasts induces the specific migration of CD16–human natural killer cells. *Blood,* **102**, 1569-1577.

Heidenreich, S (1999) Monocyte CD14: a multifunctional receptor engaged in apoptosis from both sides, *Journal of Leukocyte Biology*, **65,** p737-743

Hemberger, M. (2012). Health during pregnancy and beyond: Fetal trophoblast cells as chief co-ordinators of intrauterine growth and reproductive success. *Ann Med,* **44**, p325-37.

Holmlund, U., Cebers, G., Dahlfors, A. R., Sandstedt, B., Bremme, K., Ekstrom, E. S., and Scheynius, A. (2002). Expression and regulation of the pattern recognition receptors Toll-like receptor-2 and Toll-like receptor-4 in the human placenta. *Immunology,* **107**, p145-51.

Horne, A.W.; Stock, S.J. and King, A.E. (2008).Innate immunity and disorders of the female reproductive tract.*Reproduction*.**135**, p739-749.

Hunt, J. S., Langat, D. K., McIntire, R. H. and Morales, P. J. (2006) The role of HLA-G in human pregnancy. *Reproductive Biology and Endocrinology,* **4**, p1.

Jabeen, A., Miranda-Sayago, J. M., Obara, B., Spencer, P. S., Dealtry, G. B., Hayrabedyan, S., Shaikly, V., Laissue, P. P., and Fernandez, N. (2013). Quantified Colocalization Reveals Heterotypic Histocompatibility Class I Antigen Associations on Trophoblast Cell Membranes: Relevance for Human Pregnancy. *Biol Reprod* .

Kanellopoulos-Langevin, C., Caucheteux, S. M., Verbeke, P. and Ojcius, D. M. (2003) Tolerance of the fetus by the maternal immune system: role of inflammatory mediators at the feto-maternal interface. *Reproductive Biology and Endocrinology,* **1**, p1.

Kawai, T., and Akira, S. (2007). Signaling to NF-kappaB by Toll-like receptors. *Trends Mol Med,* **13**, p460-9.

Klaffenbach, D., Rascher W., Rollinghoff, M., Dotsch J., Meibner, U., Schnare (2005) Regulation and signal transduction of Toll like receptors in human choriocarcinoma cell line.*AJRI*, **53**: p77-84

Knofler, M. (2010). Critical growth factors and signalling pathways controlling human trophoblast invasion. *Int J Dev Biol* **54**, p269-80.

Knofler, M., Vasicek, R., and Schreiber, M. (2001). Key regulatory transcription factors involved in placental trophoblast development--a review. *Placenta,,* **22 Suppl A**, S83-92.

Koga, K., and Mor, G. (2008). Expression and function of toll-like receptors at the maternal-fetal interface. *Reprod Sci,* **15**, p231-42.

Koga, K., Aldo, P. B., and Mor, G. (2009). Toll-like receptors and pregnancy: trophoblast as modulators of the immune response. *J Obstet Gynaecol Res,* **35**, p191-202.

Koga, K. And Mor, G. (2010) Toll-Like Receptors at the Maternal-Fetal Interface in Normal Pregnancy and Pregnancy disorders, *Am J Reproductive Immunology***, 63(6)**, p587-600

Kusumoto, Y., Fukase, K., Kusumoto, S., Adachi, Y., Kosugi, A., Miyake, K. 2003.Lipopolysaccharide interaction with cell surface toll-like receptor 4-MD-2: higher affinity than that with MD-2 or CD14. *J Exp Med.* **198(7): p**1035-1042

Labeta, M.O.; Durieux, J.J.; Fernandez, N; Herrmann, R and Ferrara, P. (1993). Release from a human monocyte-like cell line of two different soluble forms of the lipopolysaccharide receptor, CD14. *European Journal of Immunology*.**23**, p2144-2151.

Lamont, R. F. (2003) Infection in the prediction and antibiotics in the prevention of spontaneous preterm labour and preterm birth. *BJOG*,110 Suppl **20**, p71-5.

Larocca, R. A., Abbink, P., Peron, J. P. S., Paolo, M. d. A., Iampietro, M. J., Badamchi-Zadeh, A., Boyd, M., Kirilova, M., Nityanandam, R. and Mercado, N. B. (2016) Vaccine protection against Zika virus from Brazil. *Nature*.

Levy, O. (2005). Innate immunity of the human newborn: distinct cytokine responses to LPS and other Toll-like receptor agonists. *Journal of Endotoxin Research*.**11, p113**-116.

Lotz, S., Aga, E., Wilde, I., Zandbergen, G., Hartung, T., Solbach, W., and Laskay, T. (2004). Highly purified lipoteichoic acid activates neutrophil granulocytes and delays their spontaneous apoptosis via CD14 and TLR2. *Journal of Leukocyte Biology*, **75(3)**: 467-477

Lorne, E; Dupont, H and Abraham, E. (2010). Toll-like receptors 2 and 4: initiators of non-septic inflammation in critical care medicine. *Intensive Care Medicine*, **36**, p1826-1835.

Ma, Y; Krikun, G; Abrahams, V.M.; Mor, G and Guller, S. (2007). Cell Type-Specific Expression and Function of Toll-Like Receptors 2 and 4 in Human Placenta: Implications in Fetal Infection. *Placenta*, **28**, p1024-1035.

Makhseed, M., Raghupathy, R., Azizieh, F., Omu, A., Al-Shamali, E. and Ashkanani, L. (2001) Th1 and Th2 cytokine profiles in recurrent aborters with successful pregnancy and with subsequent abortions. Human Reproduction, **16**, p2219-2226.

Mantovani, A., Bonecchi, R. and Locati, M. (2006) Tuning inflammation and immunity by chemokine sequestration: decoys and more. *Nature Reviews Immunology,* **6**, p907-918.

Marty, N. J., Holman, C. L., Abdullah, N., and Johnson, C. P. (2013). The c2 domains of otoferlin, dysferlin, and myoferlin alter the packing of lipid bilayers. *Biochemistry,* **52**, p5585-92.

Matsuo, H. and Strauss, J.F. 3rd (1994) Perixome proliferators and retinoids affect JEG-3 choriocarcinoma cell function. *Endocrinology*, **135**, p1135-1145

Mor, G. (2008). The Role of Toll-like Receptors in Trophoblast–Immune Interaction. *Annals of New York Academy of Sciences*, **1127**, p221-128

Moynagh, P. N. (2005). TLR signalling and activation of IRFs: revisiting old friends from the NF-kappaB pathway. *Trends Immunol,* **26**, p469-76.

Mukhopadhyay, S., Varin, A., Chen, Y., Liu, B., Tryggvason, K., and Gordon., S. (2011) SR-A/MARCO−mediated ligand delivery enhances intracellular TLR and NLR function, but ligand scavenging from cell surface limits TLR4 response to pathogens, **117**: p1319-1328

Obara, B., Jabeen, A., Fernandez, N., and Laissue, P. P. (2013). A novel method for quantified, superresolved, three-dimensional colocalisation of isotropic, fluorescent particles. *Histochem Cell Biol,* **139**, p391-402.

Panigel, M. (1986). The human placenta. Anatomy and morphology. *Clin Obstet Gynaecol,* **13**, p421-445.

Rallabhandi, P; Bell, J; Boukhvalova, M.S.; Medvedev,A; Lorenz, E; Arditi, M; Hemming,V.G; Blanco, J.C.G.; Segal D.M. and Vogel, S.N. (2006) Analysis of TLR4 Polymorphic Variants: New Insights into TLR4/MD-2/CD14 Stoichiometry, Structure, and Signalling, *Journal of Immunology*, **177**, p322-332.

Riley, J. K. (2008). Trophoblast immune receptors in maternal-fetal tolerance. *Immunol Invest,* **37**, p395-426.

Robinson, J. M., Ackerman, W. E. t., Behrendt, N. J., and Vandre, D. D. (2009). While dysferlin and myoferlin are coexpressed in the human placenta, only dysferlin expression is responsive to trophoblast fusion in model systems. *Biol Reprod,* **81**, p33-9.

Romero, R., Espinoza, J., Goncalves, L. F., Kusanovic, J. P., Friel, L., and Hassan, S. (2007). The role of inflammation and infection in preterm birth. *Semin Reprod Med,* **25**, p21-39.

Roy, D.L.; Padova, F.D.; Adachi, Y;Glauser, M.P.; Calandra, T and Heumann, D. (2001). Critical Role of Lipopolysaccharide-Binding Protein and CD14 in Immune Responses against Gram-Negative Bacteria. *Journal of Immunology*, **167**, p2759-276

Sankala, S; Brannstrom, A; Schulthess,T; Bergmann, U; Morgunova, E; Engel, J; Tryggvason, K. And Pikkarainen, T. (2002) Characterization of Recombinant Soluble Macrophage Scavenger Receptor MARCO, *The Journal of Biological Chemistry, 277,* p33378-33385

Schumann, R.R. (2011) Old and new findings on lipopolysaccharide-binding protein: a soluble patten-recognition molecule, *Biochemical Society Transactions*, **39**, p989- 993

Shaikly, V. R., Morrison, I. E., Taranissi, M., Noble, C. V., Withey, A. D., Cherry, R. J., Blois, S. M. and Fernández, N. (2008) Analysis of HLA-G in maternal plasma, follicular fluid, and preimplantation embryos reveal an asymmetric pattern of expression. *The Journal of Immunology*, 180, p4330-4337.

Thelen,T; Hao,Y; Medeiros,A.I ; Curtis, J.L ; Serezani, C.H ; Kobzik, L ; Harris, L.H ; Aronoff, D.M. (2010) The Class A Scavenger Receptor , Macrophage Receptor with Collagenous Structure, Is the Major Phagocytic Receptor *Clostridium Sordellii* Expressed by Human Decidual Macrophages, *The Journal of Immunology*, **185**, p 4328-4335

Tobias, P.S; Soldau, K; Gegner, J.A.; Mintz, D and Ulevitch, R.J. (1995). Lipopolysaccharide Binding Protein-mediated Complexation of Lipopolysaccharide with Soluble CD14. *Journal of Biological Chemistry*, **270**, p10482-10488.

Tran, P. B. and Miller, R. J. (2003) Chemokine receptors: signposts to brain development and disease. *Nature Reviews Neuroscience,* **4**, p444-455.

Watt, S., Lanotte, P., Mereghetti, L., Moulin-Schouleur, M., Picard, B. and Quentin, R. (2003) Escherichia coli strains from pregnant women and neonates: intraspecies genetic distribution and prevalence of virulence factors. Journal of clinical microbiology, **41**, p1929-1935.

Wegmann, T. G., Lin, H., Guilbert, L. and Mosmann, T. R. (1993) Bidirectional cytokine interactions in the maternal-fetal relationship: is successful pregnancy a T H 2 phenomenon? Immunology today, 14,p353-356.

White, A. F. B., and Demchenko, A. V. (2014). Modulating LPS signal transduction at the LPS receptor complex with synthetic lipid a analogues. *Advances in Carbohydrate Chemistry and Biochemistry*, **71**: p339–389.

Wright, S. D. (1995) CD14 and Innate recognition of bacteria, *Journal of Immunology: Commentary*, **0022,** p1767-95

Yang, R.B.; Mark, M.R.; Gurney, A.L. and Godowski, P.J. (1999) Signalling Events Induced by Lipopolysaccharide-Activated Toll-Like Receptor 2, *Journal of Immunology*, **163**, p639 – 643.

Youn, J.H.; Oh, Y.J.; Kim, E.S.; Choi, J.E. and Shin, J.S. (2008). High Mobility Group Box 1 Protein Binding to Lipopolysaccharide Facilitates Transfer of Lipopolysaccharide to CD14 and Enhances Lipopolysaccharide-Mediated TNF-α Production in Human Monocytes. *Journal of Immunology*, **180**, p5067 -5074.

Zanoni, I., Ostuni, R., Marek, L. R., Barresi, S., Barbalat, R., Barton, G. M., Granucci, F. and Kagan, J. C. (2011) CD14 controls the LPS-induced endocytosis of Toll-like receptor 4. Cell, 147, p868-880.

Zhang, Y., Blattman, J. N., Kennedy, J., Duong, J., Nguyen, T., Wang, Y., Davis, R. J., Greenberg, P. D., Flavell, R. A., Dong, C. 2004. Regulation of innate and adaptive immune responses by MAP kinase phosphatase 5.*Nature,* **430:p**793–797.

Appendix

BACTERIAL LPS DIFFERENTIALLY MODULATES THE EXPRESSION OF MYOFERLIN IN TROPHOBLAST CELLS

Niwedhie Muhandiram[1], Asma Jabeen[1], Nelson Fernàndez[1]

[1]School of Biological Sciences, University of Essex, Colchester, United Kingdom

Myoferlin, one of the members of the Ferlin family is a membrane protein encoded by the MYOF gene and found in cell membranes, nuclear membranes and cytoplasmic vesicles. A high expression of myoferlin is observed in skeletal and cardiac muscles and weak expression in the brain, kidney and placenta. Myoferlin has been found to be necessary for membrane repairing and regulation of VEGF signal transduction. VEGF is not restricted to the vascular system and contributes to wound healing, cell division and proliferation. Successful implantation of the developing embryo in the maternal uterus is associated with Extravillous Trophoblast (EVT) cell proliferation and invasion of the uterine wall. Decreased EVT proliferation and trophoblast cell death has been associated with pregnancy complications such as preeclampsia and intrauterine growth restriction thus resulting in inadequate trophoblast invasion. We have hypothesized that there is a correlation between the down-regulation of Myoferlin and the decreased cell proliferation of trophoblast cells upon bacterial infection. In this study, detection and quantification of Myoferlin on JEG-3 cell line was performed upon treatment with Lipopolysaccharide (LPS). Proteomics quantitative data, revealed that LPS treatment induced a significant (p=0.0002) decrease in the expression level of Myoferlin in trophoblast cell line. Myoferlin quantification estimated by flow cytometry also showed significant decrease in LPS treated JEG-3 cells in dose dependent manner. Whereas, fluorescence microscopic imaging results confirmed the same. The cell proliferation assay revealed a significant decrease (62%) in trophoblast cell growth in 48 hours of LPS treatment. In conclusion, decreased Myoferlin expression is associated with the decreased cell proliferation of trophoblast cells upon bacterial LPS treatment.

Appendix I

Chemical reagents used in this study

A. Cell culture

Fetal bovine serum (FBS)

Ham's F-12 with stable glutamine

Dulbecco's Modified Eagle's Medium/ Ham's F-12

Dimethyl sulfoxide (DMSO)

Phosphate Buffer Saline (PBS)

Accutase

B. Immunofluorescent labelling

Bovine serum albumin (BSA)

Paraformaldehyde (PFA)

Phosphate Buffer Saline (PBS)

Triton-X100

Vectashield mounting medium

C. Proteomics

Accutase

Acrylamide/bis 30% (37.5 : 1)

Ammonium per sulphate (APS)

Bromophenol blue

CelLytic MT reagent

Coo Assay reagent

Dithiothreitol (DTT)

Ethylene diamine tetra acetic acid (EDTA)

Formaldehyde

Glycerol

Isopropanol

Methanol

Non-fat dry milk

Protease inhibitor cocktail

Protease and phosphatase inhibitors

Proteo-JET Cytoplasmic and Nuclear protein extraction kit

Polyvinylidene fluoride (PVDF) membrane

Sodium dodecyl sulphate (SDS)

Sodium thio sulphate

N, N, N′, N′-Tetra methyl ethylene diamine (TEMED)

Tris-base

D. Cell proliferation assay

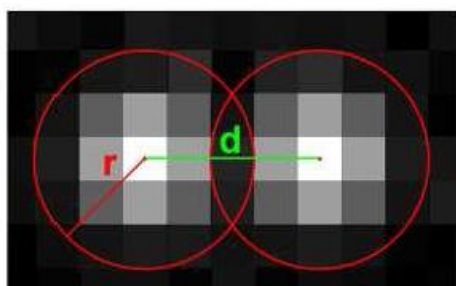Fetal bovine serum (FBS)

Phosphate Buffer Saline (PBS)

Lipopolysaccharide (LPS) O5:B55

Camptothecin

CellTiter 96 AQueous one cell proliferation assay kit

Appendix II

A) Illustration of parameters used for colocalisation analysis.

$r_{(default)} = 138$ nm
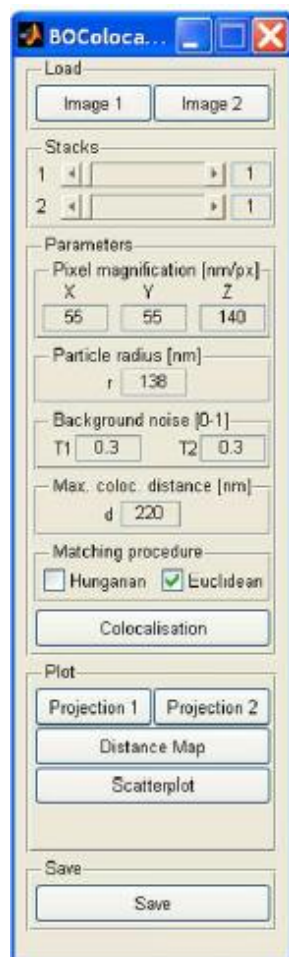
$d_{(default)} = 220$ nm

$T_{1,2\ (default)} = 0.3$

where,   r-radius,   d-distance   between   two   centroids,   and   T-noise   level

B) Colocalisation analysis flow

Screen shot of Graphical User Interface showing flow of colocalisation analysis algorithm from top to bottom.

Appendix III

Proteomics

A) Sample buffer 5X (Store at -20°C)

Reagents	Amount in 10 ml
0.5 M Tris HCl pH 6.8	1.2 ml
50% Glycerol	5 ml
10% SDS	2 ml
1% Bromophenol blue	1 ml
DI water	0.7 ml
DTT	0.386 g

B) SDS-PAGE One Dimensional

Resolving gel 12%

Reagents	Amount in 10 ml
DI water	3.35 ml
1.5 M Tris HCl pH 8.8	2.5 ml
Acrylamide/bis 30% (37.5 : 1)	4.0 ml
Ammonium persulphate (APS) 10%	50 µl
SDS 20%	100 µl
TEMED	5 µl

Stacking gel 4%

Reagents	Amount in 10 ml
DI water	6.1 ml
0.5 M Tris HCl pH 6.8	2.5 ml
Acrylamide/bis 30% (37.5 : 1)	1.3 ml
Ammonium persulphate (APS) 10%	50 µl
SDS 20%	100 µl
TEMED	10 µl

C) Protein extraction / Rehydration Buffer

Recipe taken from Biorad protein extraction kit; (Catalog # 163-2087)

Reagents	Final concentration	Amount in 25 ml
Urea (FW 60.06)	7 M	10.52 g
Thiourea (FW 76.12)	2 M	3.81 g
CHAPS	4% w/v	0.5 g

Make it up without Protease inhibitor, DTT and Ampholyte.

Distribute into 980 µl aliquots and store at -80°C until use (avoid re-freezing)

On the day of protein extraction

Thaw the protein extraction / rehydration buffer aliquot and follow as below;

Reagents	Final concentration	Amount in 1 ml
Protease inhibitor cocktail (100X)	1X	10 µl
DTT (FW 154.25)	20 mM	0.003g (3 mg)
Ampholyte or IPFG buffer	1% v/v	10 µl
Benzonase	--	1 µl

The amount 1 ml of protein extraction buffer is added to 10×10^6 cells.

D) Bradford Assay, colorimetric method for total protein quantitation

Bradford assay is based on the principal that when coomassie dye binds the protein in an acidic medium, a shift in absorption occurs from 465 nm- 595 nm resulting in a colour change from brown to blue. Protein standards, test samples and blank cell lysis buffer were deposited onto microplate wells as 5 µl aliquots. Bradford assay reagent equilibrated to room temperature, 250 µl was added to each well. Microplate was mixed for 30 sec and incubated for 1 min at RT. Samples were then read at 595 nm within 15 min of preparation. Protein concentrations of the samples were estimated from the absorbance of the standards. All the samples and standards were corrected for background absorbance.

E) Stock solutions

10X Phosphate Buffer Saline (PBS)

NaCl   80 g

KCl   2 g

KH_2PO_4 (anhydrous) 2 g

Na_2HPO_4 (anhydrous) 2 g

Purite water   1000 ml

1.5 M HCl pH 8.8

27.23 g Tris-base

80 ml   DI water

   Add conc HCl to adjust pH 8.8 and add DI water to make final volume 150 ml. Store at 4^oC.

0.5 M HCl pH 6.8

6 g   Tris-base

60 ml   DI water

Add conc HCl to adjust pH 6.8 and add DI water to make final volume 100 ml. Store at 4^oC.

10% APS (make fresh)

100 mg APS

1 ml   DI water

10% SDS (Store at RT)

10 g   SDS

100 ml DI water

1% Bromophenol Blue

10 ml preparation and store at room temperature (RT).

0.1 g   Bromophenol blue

10 ml   DI water

10X Electrophoresis buffer/ Running Buffer

30 g   Tris-base

144 g   Glycine

10 g   SDS

1 L DI water

Transfer buffer for western blotting

1L preparation. Store at 4°C. It is used as cold and improves heat dissipation during transfer.

Tris-base   3.03 g

Glycine   14.4 g

DI water   500 ml

Methanol   200 ml

pH will be between 8.1 to 8.5 depending on the quality of Tris-base, methanol and DI water. Make the final volume 1L with DI water.

Wash buffer (PBS-T 0.1%)

PBS   999ml

Tween-20   1 ml

Store at RT.

Blocking Buffer (Freshly made)

Non-fat dry milk-Marvel 5 g

PBS-T 0.1%   1